European Commission Grant Agreement Number: 869300

Call identifier: H2020-LC-CLA-2018-2019-2020 Topic: LC-CLA-06-2019

Type of action: RIA, Research and Innovation action

Starting date: 01.09.2020 Duration: 48 months

Project website: futuremares.eu

# Project Deliverable Report D3.2
# *Local adaptation potential of key coastal species*

Dissemination level: **Public**

Type of deliverable: Report

Due date: Project month 34 [30.06.2023]

Project Milestone(s) achieved:

*None of relevant*

## FutureMARES Project

*FutureMARES* - Climate Change and Future Marine Ecosystem Services and Biodiversity is an EU-funded research project examining the relations between climate change, marine biodiversity and ecosystem services. Our activities are designed around two Nature-based Solutions (NBS) and Nature-inclusive Harvesting (NIH):

Effective Restoration (NBS1)

Effective Conservation (NBS2)

Nature-inclusive (sustainable) Harvesting (NIH)

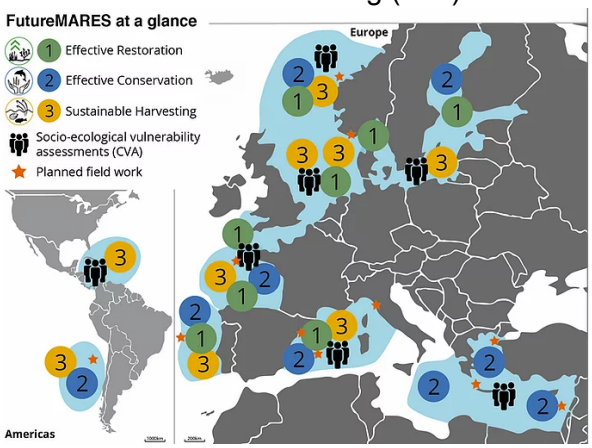


We are conducting our research and cooperating with marine organisations and the public in Case Study Regions across Europe and Central and South America. Our goal is to provide science-based policy advice on how best to use NBS and NIH to protect future biodiversity and ecosystem services in a future climate.

*FutureMARES* provides socially and economically viable actions and strategies in support of NBS for climate change adaptation and mitigation. We develop these solutions to safeguard future biodiversity and ecosystem functions to maximise natural capital and its delivery of services from marine and transitional ecosystems. To achieve this, the objectives of *FutureMARES* defined following goals:

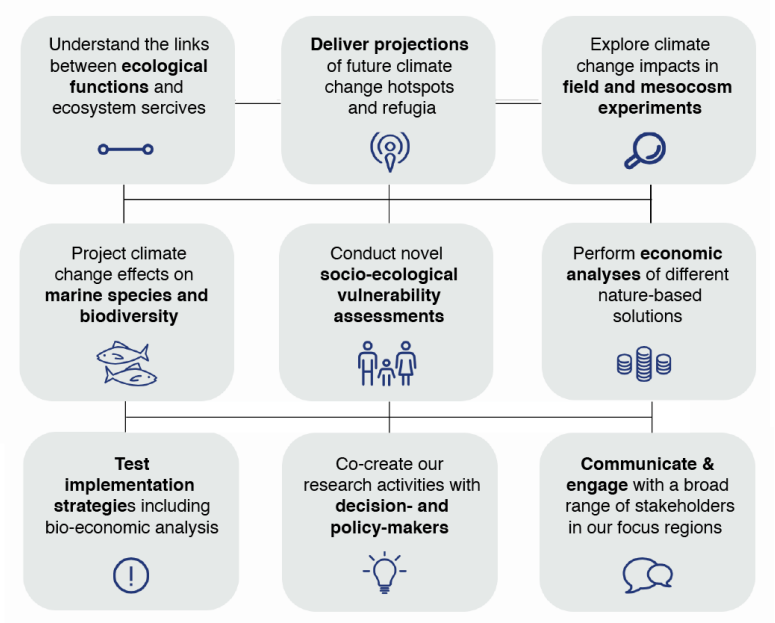

| **Deliverable data** | |
|---|---|
| **Work Package(s) / Task(s):** | WP3/Task 3.2 – Local adaptation potential of key coastal species through within-population physiological plasticity |
| **Lead beneficiary:** | CIIMAR - Interdisciplinary Centre of Marine and Environmental Research |
| **Responsible author:** | Francisco Arenas |
| **Contact:** | farenas@ciimar.up.pt |
| **Co-authors:** | Pauline Kamermans, Brenda Walles, Axel Chabrerie, Luis F. Pereira, Fernando Lima, Rui Seabra, Sandra Ramirez-Calero, Jean Batiste Ledoux, Aldo Barreiro, Marta Pagès-Escola, Alba Medrano, Angel Lopez, Laura Figuerola, Cristina Linares, Joaquim Garrabou. Fabio Bulleri, Chiara Ravaglioli, Ludovica Pedicini, Sofía Hernández-Chan, Ana Queiros, Jana Verdura, Jorge Santamaría, Raül Golo, Cèlia Sitjà, Cristina Galobart, Emma Cebrian and Gil Rilov. |
| **Date of delivery:** | 28/08/2023 |
| **Deliverable type:** | Report |
| **Date of internal approval (for the submission to EC)** | 28/08/2023 |

**Involved partners**

| Project partner (affiliation) | First name | Last name | E-mail |
|---|---|---|---|
| CIIMAR | Francisco | Arenas | farenas@ciimar.up.pt |
| WUR | Pauline | Kamermans | pauline.kamermans@wur.nl |
| CIBIO | Fernando | Lima | fplima@gmail.com |
| UniPI | Fabio | Bulleri | fabio.bulleri@unipi.it |
| CSIC | Joaquim | Garrabou | garrabou@icm.csic.es |
| PML | Ana | Queiros | anqu@pml.ac.uk |
| IORL | Gil | Rilov | rilovg@ocean.org.il |

**Document history**

| Version | Date | Description |
|---|---|---|
| **01** | 22/06/23 | V1.0 – Initial version, by Francisco Arenas |
| **02** | 29/06/23 | V2.0 – Second draft by Francisco Arenas |
| **03** | 24/08/23 | V3.0 – Updated version from the Scientific Coordinator (M. Peck -NIOZ) |
| **04** | 28/08/23 | V4.0 – Final version approved by Francisco Arenas |

Suggested citation for this report: Arenas F. Kamermans P., Walles B., Chabrerie A., Pereira L.F., Lima F., Seabra R., Ramirez-Calero S., Ledoux J.B., Barreiro A., Pagès-Escola M., Medrano A., Lopez A., Figuerola L., Linares, C., Garrabou J., Bulleri F., Ravaglioli C., Pedicini L., Hernández-Chan S., Queiros, A., Verdura J., Santamaría J., Golo R., Sitjà C., Galobart C., Cebrian E. and Rilov G. (2023) – *Local adaptation potential of key coastal species through within-population physiological plasticity*. FutureMARES Project Deliverable 3.2 report

FutureMARES receives funding from the European Union's Horizon 2020 research and innovation programme under grant agreement No 869300 "Climate Change and Future Marine Ecosystem Services and Biodiversity"

*Table of content*

## List of symbols, abbreviations and a glossary

| | |
|---|---|
| CC | Climate change |
| CHS | Cumulative heat stress |
| CTmax | Critical thermal maximum |
| DoA | Description of Action, a part of the project Grant Agreement describing the project work plan |
| DW | Dry weight |
| EC GA | European Commission Grant Agreement – a contract between the European Commission and FutureMARES consortium |
| EC | European Commission |
| GA | Grant Agreement |
| NBS | Nature-based Solutions |
| PAM | Pulse Amplitude Modulated fluorescence |
| RCP | IPCC Representative Concentration Pathway (greenhouse gas scenario) |
| Tn.x | Task – an sub-component of a work package where “n” is a number of the work package and “x” is a number of the task within this work package |
| Topt | Temperature at optimal performance / optimum temperature |
| TPC | Thermal Performance Curve |
| WP | Work Package |

**Executive summary**

Deliverable 3.2 reports on the outcome of experiments conducted by various FutureMARES partners to evaluate the environmental sensitivity of coastal species with emphasis on thermal physiology and tolerance. One of the primary goal was to significantly improve our understanding of the potential for population-specific changes in tolerance to climate-driven stressors such as rising temperatures. Laboratory and field measurements were performed using a standard framework to examine changes in key physiological rates of habitat-forming plants and animals. The work elucidates important sources of variability in responses among and within (populations of) species such as changes in thermal tolerance across latitudes or environments with different mean and/or variance of temperature. Task 3.2 contributes new empirical data important for i) improving ecological projections of climate impacts, ii) guiding habitat restoration efforts of coastal habitats supporting marine biodiversity, and iii) reveals current knowledge gaps and future research needs regarding the acclimatization or adaptive capacity of habitat forming species to climate change on ecological timeframes.

In total, work was performed on regional differences in tolerance to climate-driven stressors in habitat-forming species within six Storylines. This includes intertidal species such as European flat oyster (*Ostea edulis*) in Storyline 10 and the brown macroalgal seaweed *Ascophyllum nodosum* in Storylines 21-23, and shallow water species such as the red gorgonian *Paramuricea clavate* in Storyline 29, the perennial caespitose macroalgae *Ericaria crinite in Storyline 29 and the seagrass Posidonia oceanica* in Storyline 28. The report also provides details on a new apparatus created to perform heatwave experiments on plants and animals exposed to periodic flooding and drying in the intertidal zone and an r-package for estimating the Critical Thermal maximum (CTmax) from standard temperature ramping experiments.

The empirical data collected on thermal stress responses suggested, across all Storylines, the capacity for species to adapt to prevailing, local temperature conditions. For example, a latitudinal gradient in thermal sensitivity to heatwaves was clear from differences in survival, growth or other performance across nine populations of *Ascophyllum nodosum* with the highest and lowest temperature tolerance and optimum in this seaweed from Portugal and Norway, respectively. Similarly, comparisons of eight populations of E. crinite indicated increased thermal tolerance in populations from habitats at the warm edge of the distribution in the Mediterranean Sea. Strong heatwave impacts on the growth of oysters was observed although patterns suggested stronger

performance oysters from Norway compared to The Netherlands. Spatial and temporal variability was observed across three, genetically different, local populations of the red gorgonian that help identify candidates with better thermal tolerance for restoration activities. Similarly, work on *Posidonia oceanica* highlighted how historical differences in exposure to heat waves can, even at small spatial scales (e.g. across the Tuscan Archipelago and mainland Tuscany), be related to different physiological and biochemical properties of their leaf tissues suggesting locally adapted phenotypes to heat stress. Work on *Posidonia oceanica* also highlighted how multiple environmental factors can interact to cause stress in habitat-forming species. Deep or shallow water plants of this seagrass were not sensitive to ocean acidification (OA) when exposed to normal (average) temperatures but OA had negative impacts on growth performance of both shallow and deep plants during a heatwave year (2022).

## Introduction

Shifts in aquatic and terrestrial animals due to climate change have been documented for decades (e.g. Root et al. 2003). The impacts of climate change on key abiotic factors such as temperature and pH are already surpassing the physiological tolerance levels of organisms, especially at the low latitudinal limit of historical distributions, posing a threat to the resilience and functioning of ecosystems (Connell et al., 2018; Wang et al., 2021). Species that have limited capacity for adaptive responses, such as phenotypic plasticity or genotypic adaptation, face the risk of local extinction if they cannot disperse and establish themselves in new regions (Carpenter et al., 2008; Hoffmann and Sgro 2011). Consequently, the distributional limits of species at lower latitudes are contracting (Parmesan, 2006) and, for those species that can redistribute themselves, are expanding poleward (Antão et al., 2022). Such shifts are evident throughout European regional seas where analyses of changes in cumulative temperature indices (CTIs) conducted in FutureMARES suggested tropicalization and deboralization in 70% of the taxa / regions tested (Chust et al. submitted).

To make more robust projections of climate impacts, it is important to understand the variation in physiological thresholds for temperature change that exist and how this variation in thermal sensitivity changes among populations at different latitudes. At the present time, such knowledge is largely lacking for marine plant and animal species. Together with phenotypic plasticity, genetic variability is the second immediate mechanism that allows a population to persist when its local environment changes. Identifying the degree to which organisms are able to acclimatize or adjust their sensitivity to regional environmental change will provide crucial knowledge to anticipate climate change impacts on biological systems. By identifying the among-regions variation in thermal tolerance thresholds, we can gain insight on the current environmental safety margins and how these change across the distribution of species (Stuart-Smith et al. 2015). This knowledge is crucial for projecting potential shifts in species' distributions and assessing the resulting impacts on associated communities under current and future climate change scenarios (Sunday et al. 2011).

Thus, the objectives of Task 3.2 were to:

1. Search for evidence on local adaptation on marine organisms by investigating variation in physiological responses across space (macro-physiological approach - King et al. 2018).
2. Provide new relevant information to feed mechanistic models able to improve our accuracy in projecting the impact of climate change (CC) on target species.

**Defining the Challenge**

In order to effectively project future changes in biodiversity in the face of climate change, it is necessary to move beyond simple correlative approaches and develop new process-based models. To enhance the accuracy of our projections, it is important to deepen our understanding of various aspects of species' biology that contribute to their ability to persist in rapidly changing environments and increase the likelihood of evolutionary rescue (Morley et al. 2019). One crucial step towards achieving this is to define the physical tolerance of species, including their environmental niche breadth, plasticity, and adaptive capacity across the geographical distribution of species. In fact, relying solely on thermal performance estimates from a single population at a single location can lead to incorrect estimates on the response of species to future ocean warming. This limited approach frequently underestimates the risk of climate change to central or cold-edge populations, while simultaneously overestimating the sensitivity of warm-edge populations, especially when taking into account local adaptation (Bennett et al., 2015). Empirical studies on local adaption use reciprocal transplant or “common garden” experiments. In Task 3.2, FutureMARES aimed to design experiments using common protocols applied by several partner institutions across European regional seas in order to quantify current variability in thermal sensitivity of target marine species at the population level.

**Approach**

The work in Task 3.2 is based on laboratory experiments that essentially focused on temperature as the most relevant climate change driver. Experimental designs play a fundamental role in understanding the intricate relationship between temperature and the various physiological responses exhibited by marine organisms. This is particularly crucial because these responses are based on processes operating at different temporal scales. When it comes to combating thermal stress, marine organisms employ one or several different physiological mechanisms, which are not mutually exclusive. These include:

- Resistance (enduring limited or no damage) is a mechanism providing protection to short-term events (min to days).
- Acclimation, aka plasticity (changes in biochemical pathways and molecules that allow for a new stable physiological state in response to new conditions) is a mid-term process and provides protection from days to weeks.
- Adaptation (process involving genetic alterations better fit to deal with changed environments) is a long-term process that increases physiological fit over generations.

In addition, migration and behavioural alterations (the underpinning of which can also be due to resistance, plasticity or adaptation mechanisms) affect the ability of (mostly faunal) species to cope with increasing temperature as discussed by Bates and Morley (2020) and King et al. (2018).

Thermal experiments can be challenging due to many potential issues related to the selection of adequate species, temperatures and environmental parameters. Replication and independence also need to be thoroughly considered and included in the experimental planning to allow statistically robust inferences. Another issue is the balance between realism and simplification. Some amount of realism is important to link laboratory results to the real-world situation, but some simplification is always necessary to make experiments feasible. The simulation of heat waves in experiments is a case and point. Heat waves are, by definition, natural events that are exceptional in nature. That means that, in order to correctly simulate heat waves in the laboratory, one has to have some realistic information (from observations or from models) on the statistical distribution of temperatures experienced by the species being studied. Only with this information is it possible to plan treatments in experiments that mimic potential situations in the field now and in the future. Gaining information on the statistical distribution of temperatures for study organisms is not always easy or possible.

We briefly review some common experimental approaches used in CC studies.

a) Ramping experiments

Ramping experiments are used to identify CTmax (critical thermal maximum). CTmax is defined as the arithmetic mean of the collective thermal points at which the end-point is reached (Figure 1). Depending on the species, different end-point measures have been used including death, loss of adhesion, balance and loss of heart function (e.g. Moyano et al. 2017). This is a quick approach with some advantages but also major drawbacks.

Procedure

Temperature increases at a certain rate, and end-point events are recorded as they happen.

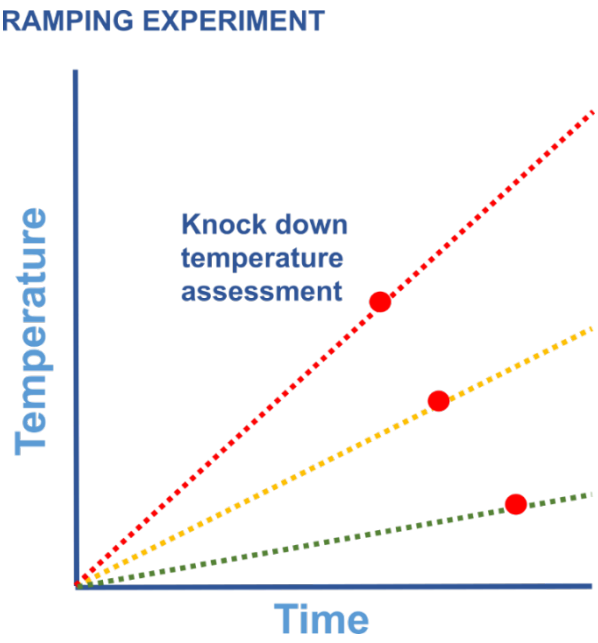


*Figure 1: Ramping experiment basic design with three different ramping speeds*

Pros:

- One of the quickest ways to obtain data linked to upper thermal threshold for species;
- One of the easiest methods. Experimental apparatuses are usually cheap and easy to assemble.
- For some species (mostly animals), end-points are easy to identify;
- Yields consistent measures across populations or species if the same protocol is used.

Cons:

- Not that suitable for primary producers due to difficulty in when end-point response occurs (particularly death since living and dead plants look similar);
- The rate of increase usually affects CTmax estimates, as organisms that can cope with high heating rates tend to tolerate higher temperatures (Rezende et al. 2014);
- The protocol is not designed to identify thermal optimum;
- Estimates of CTmax are sensitive to seasonal effects;
- Ramping of temperatures is frequently done at unrealistically high rates such that the maximum temperatures are seldomly observed in the real world, and the

duration of ramping does not correspond with rates of increase in temperatures in situ;

- For intertidal animals, the timing of tides or whether heat treatments should be applied while organisms are submerged in water or exposed to air are issues frequently neglected, but likely important to real-world impacts;

Therefore, while it is relatively easy to compile CTmax values, the direct usefulness of CTmax estimates for biogeographic studies or as inputs in projection models is debatable. Values of CTmax provide context when compared across species (or populations) from different latitudes (e.g. Pörtner & Peck 2010) and seasons (to shed light on acclimation potential) but additional types of physiological experiments need to be conducted and different measurements made to increase the robustness of models making projections of climate-driven changes in distributions.

b) Static gradient experiments

These experiments are typically performed to estimate the reaction norm of an organism to its environment. Reaction norms describe the relationship between the phenotype of an individual genotype and its environment. In the context of temperature, the term commonly used in literature is "thermal performance curve" (TPC). These TPCs define the performance of individuals (measured through growth, reproduction, movement velocity, cardiac performance, feeding rate, etc.) as a function of temperature. These TPCs have three regions: i) an ascending phase within which performance increases (often exponentially) with temperature, ii) a performance peak, which indicates the optimal temperature for the bodily function under study (growth, running speed), and iii) a descending phase within which increasing temperature leads to decrements in performance (waters are too warm for the organism). There are also some dynamic treatments such as those used by Anton et al. (2020), but the temperature cycle of each treatment is nonetheless kept constant throughout the experiment.

Procedure

Static gradient experiments involve several treatments, each of which is constant throughout the entire experiment. Each study subject experiences the same environment from start to end. Only by combining different treatments (some at colder temperatures, some at warmer temperatures) one can assemble the TPC of a population or species (Figure 2).

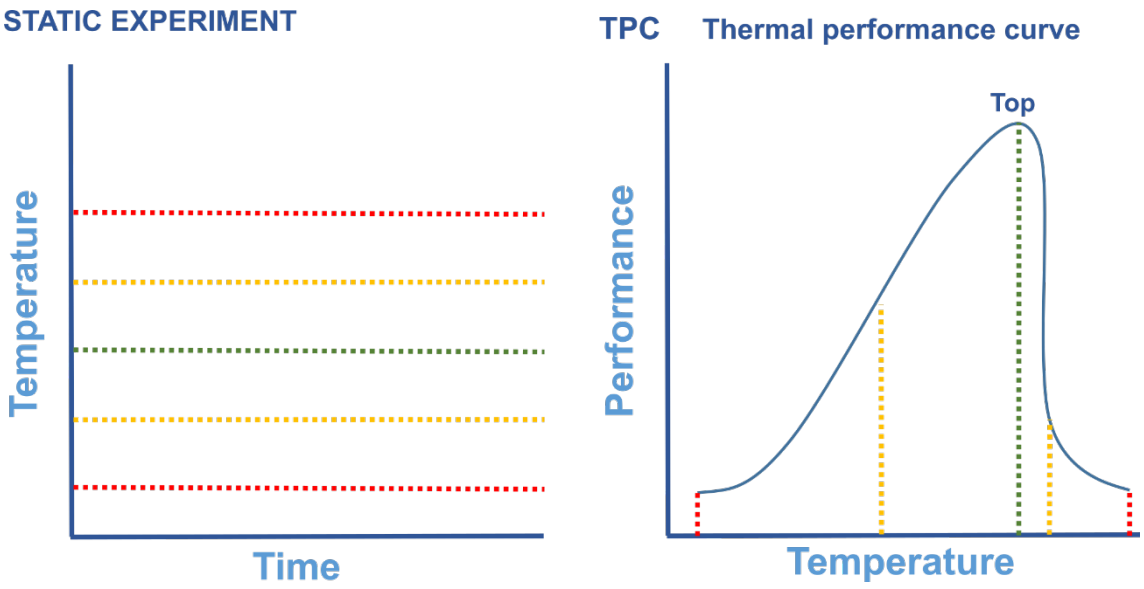


*Figure 2: Static experiment and resulting thermal performance curve*

TPCs can be measured using different fitness proxies, such as growth or feeding rates, reproductive allocation, running speed, etc. For these traits, peaks indicate the thermal optima. TPC can also be measured using metabolic traits such as respiration or photosynthetic activity. These can be quicker to measure but not necessarily better, as peak rates of the metabolic proxies typically occur at warmer temperatures than peaks of performance traits (Shah et al. 2021).

Pros:

- They are useful to examine species thermal optima and critical thresholds;
- The design of experiments are still fairly simple and experiments are relatively inexpensive to conduct;
- Fewer decisions need to be made when considering the potential experimental design compared to other sorts of experiments.

Cons:

- Due to practical issues, the number of treatment levels is often restricted and thus the performance data are not continuous, instead being inferred from a relatively small set of different temperature treatments. If treatment levels differ by multiple °C, determining the temperature of peak performance may need to be done by interpolation;
- Responses may depend on the duration of the experiment. Experiments should be long enough to get steady responses (for example in mortality or growth rates), but that comes with its own conceptual and technical challenges;

- Constant temperatures in a laboratorial setting do not necessarily reflect natural temperature fluctuations, particularly in dynamic coastal or shallow-water habitats. The incorporation of natural variability has been shown to dramatically change the results (Lugo et al., 2020; Marshall et al., 2021);
- It may be difficult to keep consistence (while not jeopardizing independence) across experimental units;
- As with CTmax, data are relatively easy to collect but their usefulness for biogeographic studies or to be directly used in projection models will depend on the match between laboratory and field conditions.

c) Heat wave and “delta” experiments

Research on marine heatwaves is a rapidly emerging within the field of climate change research. Heat wave experiments are designed to simulate the realistic impacts of increases of temperature. This approach can be tied to climatic data and used to infer the impact to a given population of facing realistic heatwaves (the frequency and magnitude of which have been increasing over the last decades and are projected to become even more severe if climate change continues unabated). Heat waves can be defined based on their duration, intensity and overall profile, but always in comparison to the “norm” (Hobday et al. 2016). A similar approach to heat wave simulation is to add constant offsets to the observed temperature profiles for a given study location. This type of methodology is also known as “delta increase” because it increases observed temperatures by a particular amount (the difference is called “delta”). The amount of temperature that is added (+2 ºC, +3 ºC) is arbitrary but may be informed, for example, by IPPC scenarios. This approach is significantly simpler than a true heatwave simulation but the results are also more artificial. Still, “delta increase” experiments offer an improvement over the previously-discussed methodologies because they incorporate natural variability in the temperatures experienced during the laboratory experiment.

Procedure

Climatology is gathered. Natural temperature variability is kept. Controls replicate the natural variability while treatments add a constant (delta) or varying (heat wave) positive offsets (Figure 3).

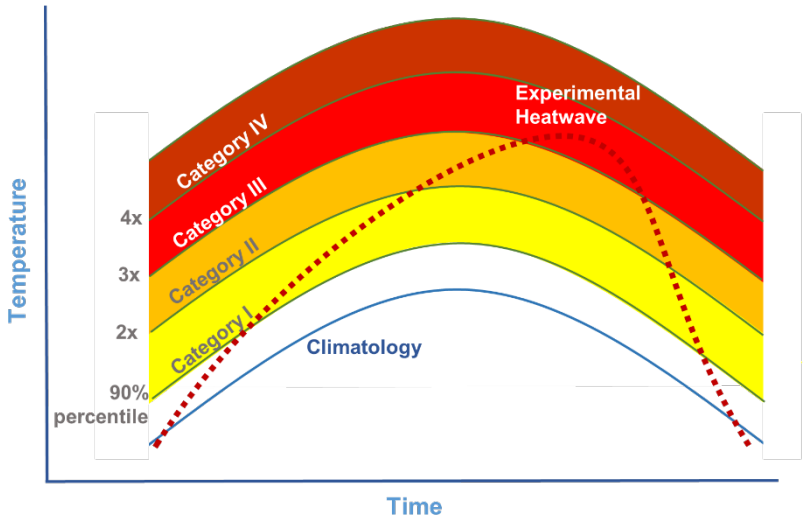


*Figure 3: Heatwave characterization with an experimental heatwave, adapted from Hobday et al. (2018).*

Pros:

- Reflects the realistic and variable nature of temperature;
- Because the temporal variance in temperature could reduce CC stress experienced by organisms (Benedetti-Cecchi et al. 2006), conclusions are much more realistic;
- If correctly performed, these experiments can be truly informative and predictive, and are much more useful for subsequent modelling.

Cons:

- Climatology data for the target site must be known beforehand in order to calculate heatwaves. Climatology data is tied to a particular location (in other words what is normal at one site may be abnormally hot or cold at another). This means that a great deal of thought has to be put into experiments that span large geographical areas in order to draw correct conclusions.
- Experiments are typically longer than the simpler experiments discussed earlier, and that comes with its own challenges;
- The deleterious effects of temperature are harder to find because the natural variability reduces stress, meaning that the methods to evaluate the physiology must be able to detect subtler changes;
- Experimental designs are markedly more complex.

### Variable responses to be assessed

Experiments on the effects of climate change can measure many different fitness proxies from survival, growth or feeding rates to reproductive allocation or fertility. Metabolic traits, such as primary productivity or respiration rates, or physiological responses, such as oxidative stress or photosynthetic activity (such as pulse amplitude modulated fluorescence, PAM), are also often used. Behavioural responses are also feasible in mobile species. Organism structural responses can also be used in calcifying organisms such as corals. The most advanced "*Omics*" (from genomics to gene expression, metabolomics, etc.) are becoming widely available.

Given the diverse backgrounds of the research teams engaged in Task 3.2 and the differences among focal species, a decision was made to concentrate on fitness proxies that provided data of the utmost ecological relevance while being straightforward to measure. These proxies include rates of survival, growth, and feeding. Research teams with the ability to assess other responses have used other proxies. For example, work on plants could include PAM, and heart rate or valve gap were used in bivalves. Nevertheless, in order to facilitate large-scale coordinated experiments, the partners reached a consensus on a standardized set of responses. Therefore, Task 3.2 focused primarily on responses directly linked to species fitness such as growth and survival, considering them as the central responses.

**One step forward: FutureMARES experimental chamber & protocol**

The partners in Task 3.2 have effectively collaborated to conduct experiments involving various marine species. Initially, a protocol was developed to transport live subtidal kelp species and, although efforts were made to ensure prompt delivery within short time frames (2-3 days), the health of fronds was found to be unsatisfactory. Consequently, it was determined that in situ experiments with subtidal species should be conducted at each respective partner institution.

To ensure standardized experiments across different institutions, one partner in Task 3.2 has actively engaged in designing an experimental chamber. This chamber enables the precise control of temperature profiles, essential for climate change (CC) experiments. Additionally, the chamber allows an automated simulation of tides including solar heating during low tides, as depicted in Figure 4. By implementing this experimental chamber, Task 3.2 aimed to achieve consistent experimental conditions to facilitate comparisons among different research sites in the future.

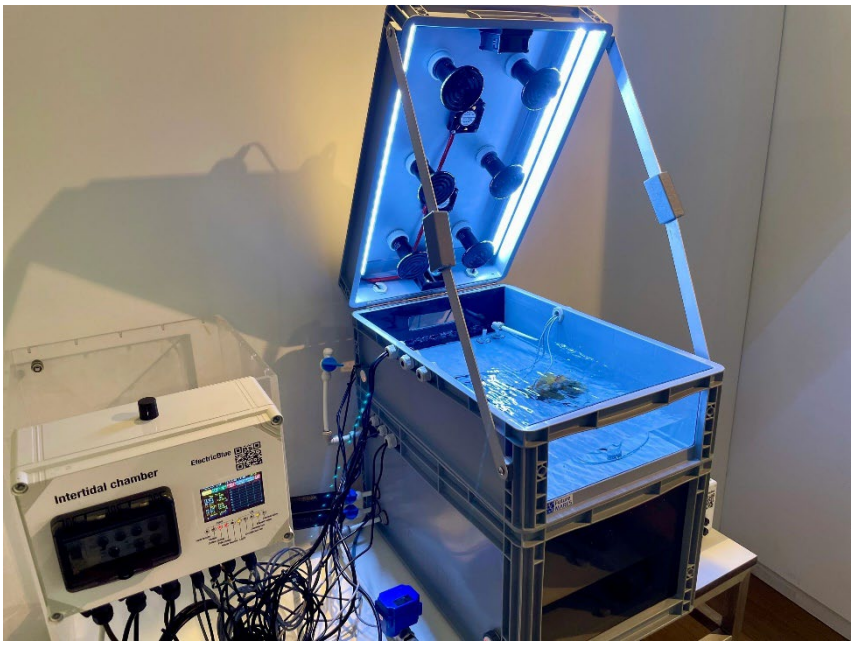


*Figure 4: Intertidal chamber designed and partially funded within the WP3 -FutureMARES.*

ElectricBlue (a non-profit technology transfer startup and spin-off company from the FutureMARES partner CIBIO-Biopolis) is the company in charge of the manufacturing of the chamber. At the time of writing this report, the chamber has been manufactured and has been delivered to several different marine laboratories.

Precise information regarding this chamber can be obtained in this link:

https://electricblue.eu/intertidal-chamber

Furthermore, a protocol adapted to the chamber has been formulated and tested using several intertidal species. The protocol was discussed in the Workshop celebrated in Haifa in May 2023 and will be implemented by laboratories in Mediterranean and Atlantic basins with common species using the intertidal chamber and common target species. Details of the protocol are presented in the last chapter of this Deliverable 3.2

**Contribution to the project**

Projections of regional physical and biogeochemical CC impacts delivered from statistically downscaled IPCC model runs in WP2 (Tasks 2.1 & 2.2) were used to guide experimental conditions aimed at defining lethal and sub-lethal responses at population level in Task 3.2 experiments. Results from these experiments help to identify which populations are more resilient to global change and which ones will be most at risk of extinction. This includes identifying how climate safety margins change across the geographical distribut of species. Results from Task 3.2 will feed Deliverable 2.3 on historical and future CC hotspots and refugia and impacts on connectivity patterns (NIVA). Task 3.2 also links to the modelling of connectivity produced in Task 3.3. The outputs generated in Task 3.2 will also provide valuable support for the mechanistic modeling produced in WP4, particularly in Task 4.1, by assessing the potential of local adaptation to enhance resilience against CC and decrease potential species-specific responses such as distribution shifts.

**Dissemination and Exploitation**

The present report includes several chapters that will be published in the upcoming months once data analyses and integration of results is completed. Results will be also integrated in the corresponding Storyline reports (to date SL10, SL21, SL23, SL28 & SL29 have been involved in experimental work within Task 3.2)

# Chapter 1 - Effect of marine heat waves on the physiological responses of the European flat oyster *Ostrea edulis*: regional differences

SL10 – Contributors Pauline Kamermans & Brenda Walles

## *1.1 Introduction*

Heatwaves have become increasingly frequent and intense in recent years due to climate change, posing substantial challenges to marine ecosystems worldwide. Shallow coastal habitats are particularly susceptible to marine heatwaves. Among the affected organisms, bivalves such as the flat oyster *Ostrea edulis* Linnaeus 1758 play a critical ecological and economic role in European coastal regions. In The Netherlands, efforts are underway to restore flat oysters in the North Sea area to form biogenic habitat that increases biodiversity. For this, disease-free oysters are imported from other locations such as Norway. As heatwaves intensify, it is crucial to understand thermal impacts on oyster populations and evaluate potential regional variation in response to these extreme thermal events.

Storyline 10 compared the effects of heatwaves on three distinct European populations of *Ostrea edulis*. By examining these populations in different geographic regions, it was hoped to gain valuable insights into the adaptive capacity, vulnerability, and potential management strategies of this species under changing climatic conditions. The chosen populations for this comparative study were located in three key regions: Mediterranean Sea, the North Sea, and the Baltic Sea. These regions have distinct differences in water temperature, salinity, and other climate-driven factors.

Through a controlled laboratory experiment, this study investigated several metabolic aspects of oyster populations across an environmental gradient during and after heatwave events. Proxies measured were related to fitness responses such as changes in growth, mortality rates and health condition, as well as metabolic rates such as respiration and clearance rates.

The overall objective was to determine the effect of marine heat waves, which are likely to occur as a result of CC, on the physiological responses that can indicate stress for the European flat oyster.

### *1.2 Material & Methods*

*Experimental set-up*

Responses of *Ostrea edulis* to heat stress were measured during a six-week laboratory experiment. Oysters purchased from three different origins (Norway, Netherlands – in 2021 and 2022, and Croatia in 2022) were used to cover a latitudinal gradient. They were kept in separate 10-L containers within three larger 500-L tanks simulating different temperature regimes (Figure 5). Each container housed 5 oysters and three containers per origin were placed in each of three temperature regimes. Temperature regimes were maintained au Bain-Marie with heaters and thermostats: continuously 20° C, continuously 25 °C, or a heat wave treatment, in which the temperature alternated between 25 °C and 20 °C on a weekly basis (Figure 5, Figure 6).

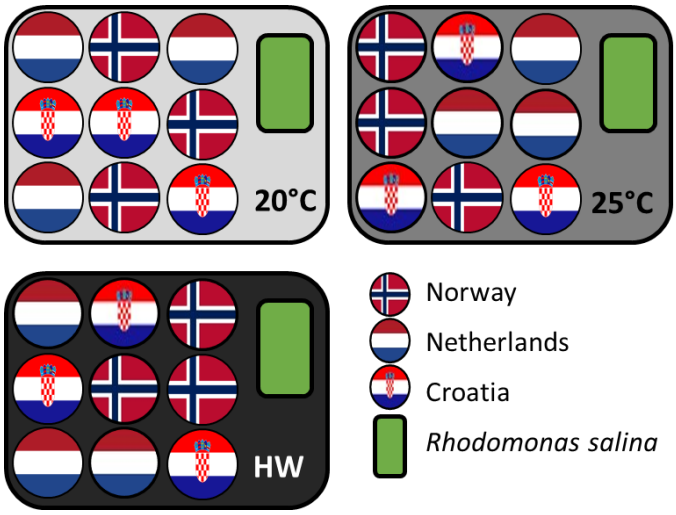


*Figure 5: Experimental set-up for heatwave experiments in Storyline 10.*

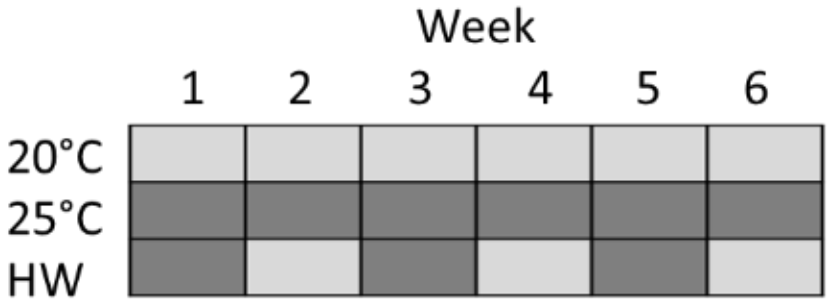


*Figure 6: Heatwave treatments used in this experiment. Grey cells 20 °C condition, Dark grey cells 25 °C condition.*

The containers and tanks were filled with 1 µm filtered seawater. Aeration was provided to each container. Flat oysters from Norway were collected in Hafrsfjord, flat oysters from the Netherlands were collected in the Oosterschelde estuary and flat oysters from Croatia were collected in Maliston Bay. After arrival in the laboratory, an acclimation period started in which the temperature in the containers was raised from the temperature of the collection area to 20 ºC at a rate of 1 ºC per day. Oysters were continuously fed at a rate of 0.77 ml $min^{-1}$ with live *Rhodomonas salina* algae (800.000 cells $ml^{-1}$) bought from a local hatchery (Roem van Yerseke). Three times a week, seawater in the tanks was replaced by new water that had been acclimated to the temperature regime in the tank functioning as the Bain Marie. Temperature was monitored every 10 minutes with HOBO MX2201 temperature loggers in each container. Parameters indicative of water quality were monitored three times a week just before refreshing of the water: salinity, $O_2$ concentration and pH were measured using a Hach HQd Field case Cat. No. 58357-000. The $NO_2$ and $NH_4$ concentrations were determined using Salifert Profi-test for NH3/NH4 and Salifert Profi-test for $NO_2$.

*Survival, growth and condition*

Survival was determined by counting the oysters alive at each cleaning event (i.e. 3 times per week).

To investigate the impact of temperature on growth and condition, shell length and wet weight was measured at the beginning of the experiment and 6 weeks later at the end of the experiment. Shell length was measured with callipers to the nearest 0.01 mm along the axis perpendicular to the hinge to shell edge. Wet weight was determined with scales to the nearest 0.01 g. Each oyster was numbered with a FPN glue-on shellfish tag of Hallprint. Growth rates were calculated per individual as an increase in wet weight (equation 1) and in shell length (equation 2) per unit time.

1. $\frac{\ln W_f - \ln W_i}{t} * 100$
2. $\frac{L_f - L_i}{t}$

with $W_f$ the final and $W_i$ the initial wet weight in g, $L_f$ the final and $L_i$ the initial shell length in mm and $t$ the time in days.

Subsamples of oysters of all three origins were stored at -20 °C at the beginning of the experiment. And at the end of the experiment, all remaining oysters were stored at -20 $^0$C. Condition index ($CI$) was calculated per individual as ash-free dry weight per gram shell weight (equation 3)

3. $\frac{AFDW}{DW_{shell}} * 100$

To determine ash-free dry weight ($AFDW = DW - AW$) flesh was separated from the shell and dried at 70 °C until a constant weight to determine dry weight ($DW$) in g, followed by combusting at 540°C until weight constancy to determine the ash-weight ($AW$) in g. Dry shell weight $DW_{shell}$ in g was measured after drying at 70 °C until weight constancy.

*Respiration rate*

The respiration rate of one randomly selected oyster per container was measured once a week for the entire 6-week experimental period. Plastic cylindrical containers with a volume of 512 ml were first filled with aerated and filtered sea water which was taken from the tanks. To aerate the water, water from the tanks was filled into a 20-L bucket and then manually aerated by repeatedly pouring it back and forth into another 20-L bucket. This process allowed the water to reach 100% oxygen saturation. Once the water was saturated, the initial oxygen concentration in water (in % and in mg $L^{-1}$) was measured using an oxygen logger and recorded. The oxygen consumption chambers were then submerged in the 20-L buckets and filed with the oxygen saturated water. Once all air bubbles had been removed, an oyster was placed inside the chamber and the chamber was sealed shut. As soon as the chamber was sealed a timer was started. In 2021, chambers containing 20 ˚C water were sealed for 1.5 h. Chambers at 25 ˚C were sealed for 1.5 h, 1.0 and 0.75 hrs at weeks 1, 2-3, and 4-6, respectively.. In 2022 chambers containing 25 ˚C were sealed for 1 hour. These times wereadjusted to avoid having the final oxygen concentration drop below 70%, a threshold at which oysters begin to transition to anaerobic metabolism (Schade et al., 2019). After the timer ended, oxygen concentration (in % and in mg $L^{-1}$) was measured and recorded.

$Respiration\ rate$ was calculated in mg $h^{-1}$ $g^{-1}$ (equation 4)

4. $$Respiration\ rate = \left(\Delta O_2 - \Delta O_{2,\,blanco}\right) * \left(\frac{1}{DW_{flesh}}\right)^b$$

In which $\Delta O_2$ is the oxygen depletion in mg $L^{-1}$ $h^{-1}$ for a container with ($\Delta O_2$) and without an oyster ($\Delta O_{2,\,blanco}$) to correct for exchange with the surrounding; $DW_{flesh}$ is the dry tissue weight in mg after drying at 70°C untill weight constanty; and $b$ a temperature dependent constant with a value of 0.825 at 20°C and 0.886 at 25 °C (Haure et al. 1998).

*Clearance rate*

Clearance rate (CR) is the rate at which a certain volume of water is cleared from all particles. For this, the particles need to be 100% efficiently retained by the bivalve gills (Smaal, 1997). The range in cell sizes of the algal species used was 4 to 10 µm, which is 100% retained by flat oysters (Cranford et al., 2011). Once a week, clearance rates were measured in an experimental flow-through system. The same oysters as for the respiration rate determination were placed in 850-ml chambers through which water was pumped with a peristaltic pump from a tank with filtered seawater and *Rhodomonas* kept at the same temperature as the treatment of that week. The system consisted of 21 chambers for oysters and 4 chambers without oysters. Flow rates were adjusted such that a significant difference in particle concentration (approx. 30%) was detected between the water flowing into the chambers and the water flowing out of the chambers (Pascoe et al., 2009). Flow rates varied between 12-16 l $h^{-1}$. The oysters were given time to adapt (approx. 1 h), after which the clearance rates were measured. For this, the outflowing water was sampled for each chamber and the concentration of particles ranging between 4 and 10 µm was measured using an Accuri Flow Cytometer. To correct for particle settlement inside the chambers we measured the particle concentration in the water flowing out of a control treatment, a chamber without an oyster. The CR was determined by measuring the number of particles in the outflow and comparing these data with the outflow of the control. For the calculation of the CR the following formula (Widdows, 1985) was used (equation 5):

5. $CR = ((Cin - Cout)/Cin) * Q$

where:

CR = clearance rate in l/h per individual

$C_{in}$ = particle concentration of the outflow of the control (number/l)

$C_{out}$ = particle concentration of the outflow (number/l)

Q = flow rate in l $h^{-1}$.

CR was weight standardized using the following equation (equation 6):

6. $CRs = CR/DWb$

in which DW is the dry weight of the individual and $b$ a temperature dependent constant of 0.791 and 0.747 for 20°C and 25°C, respectively (Haure et al., 1998).

*Valve gape*

The valve gape of individual oysters was determined using a Biophys sensor. This sensor was developed by the Royal Netherlands Institute for Sea Research (NIOZ) and can be used to measure a number of different variables, such as pressure and temperature. (Bertolini et al., 2021) describe the sensor. For this experiment, the sensors "hall function" was primarily used. The sensor detects the distance of a magnet from a sensor. After all oysters had been distributed to their containers, one of the five oysters was randomly selected to be used for the valve gape measurements. This resulted in 9 oysters per temperature treatment, 3 for each origin. The shells of these oysters were blotted dry and a small magnet was attached using a waterproof glue. These oysters were then kept in a fridge at around ~7 ˚C overnight to allow the glue to harden. They were then ready to be attached to the sensors. Prior to attaching the individual oysters to their sensors, the sensors were programmed. This was done using the program Tera Term, where the specific functions of the sensor could be set. All functions except for the hall function were disabled (to save battery). The hall function was set for 10 second intervals. Oysters were then attached to the sensor with a clamp, and the clamps were then secured to the wall of their container. After the completion of the experiment, the sensors were disabled, and the data were downloaded for analyses..

*Heart rate*

The heart rate of oysters was measured with the PULSE sensor developed by Electric Blue. Following Olabarria et al., (2016) the sensor was glued to the shell above the heart. The technique combines an IR emitter and an IR detector. IR light passes through the shell and illuminates the heart and nearby circulatory vessels. Changes in shape or volume of the circulatory structures during a heartbeat, cause a change in the amount of IR light reflected from the oyster back to the IR detector. These changes in reflected IR light, transduced to changes in electrical current, are then electronically amplified and filtered, and the signal is logged into a memory card by a microprocessor. Data were recorded continuously for 1 min every 15 min throughout the experimental period. In total, 10 oysters were logged this way (in the heat wave treatment three oysters from Norway, two from The Netherlands and two from Croatia and in the 25 ºC treatment three oysters from Norway). The heart rate was computed automatically using a custom-made R (R citation) script. In 2021 the sensor was not functioning properly, but a new version (PULSE V2) was used in 2022 which gave good results, although the oysters turned out to be very sensitive to disturbance (Figure 7). Thus, data analysis will focus on night recordings when no personnel was near the oysters.

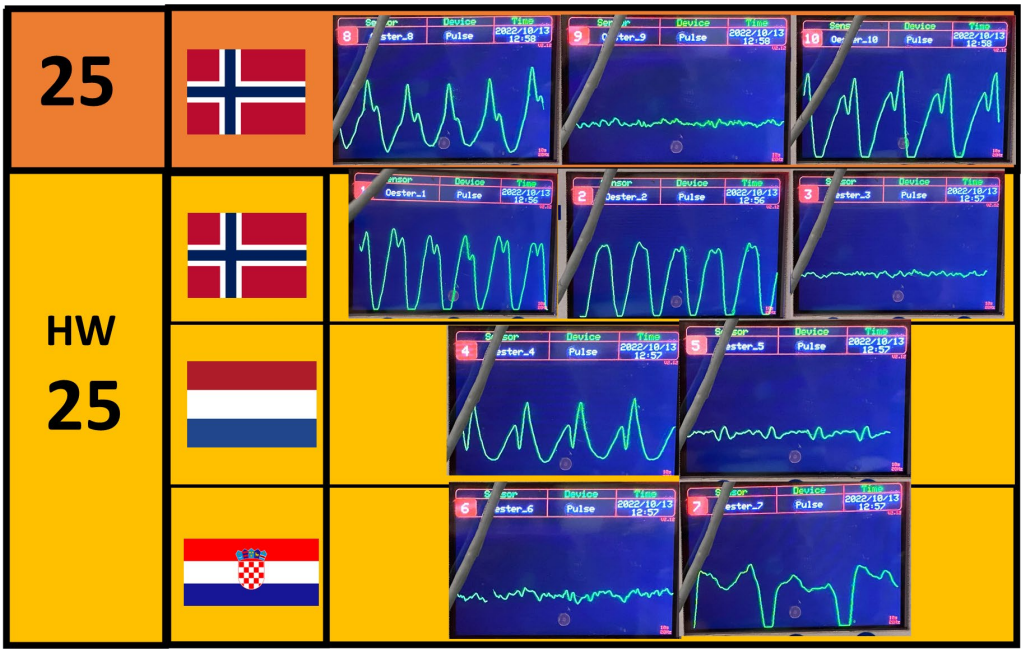


*Figure 7: Snapshot of recordings with PULSE V2 sensors attached to three oysters from Norway, two oysters from The Netherlands and two from Croatia in the heat wave treatment and to three oysters from Norway in the 25 $^{o}$C treatment.*

*Genetics*

The abductor muscles of each of the oysters used in the 2021 experiment was removed after the experiment was completed and sentfor DNA sequencing. A sample of initial oysters (not used in the experiment) was also sent (30 from The Netherlands and 30 from Norway for a total of 60). The aim was to understand which sections of DNA were responsible for heat resistance and whether the experiment resulted in any changes/differences between oysters in the different temperature treatments. Once the experiment was completed and all the oyster growth measurements had been taken, oysters were shucked open. The abductor muscle was carefully removed and placed into a labelled vial. These vials were then filled with ethanol and placed in the freezer. Every two days for a total of three times, the ethanol was removed and replaced with fresh ethanol. The samples were then packaged and sent to the University of Southampton, United Kingdom, for DNA processing and data analysis.

### *1.3 Results and conclusions*

Data analysis is ongoing and some preliminary results are available in Table 1. Survival was 100% except for the oysters from Croatia where survival ranged from 66 to 93 % and was best in the 25 ºC treatment. In both years, oysters from Norway showed the best growth, followed by oysters from The Netherlands and lowest growth was observed in oysters from Croatia. The oysters from Croatia arrived in poor condition with low meat content and were not able to compensate for that during the six-week experiment. In general, growth was highest in the 20 ºC treatment. In 2021, oysters grew least in the heat wave treatment, while in 2022 the lowest growth was found in the 25 ºC treatment. As expected, respiration rate was higher at 25 ºC than at 20 ºC. However, respiration rates gradually declined in oysters in the heat wave treatment. Clearance rate was highly variable among individuals and no clear treatment effect was observed. Statistical analysis of the growth, respiration and clearance rate data is in progress. Analysis of valve gape and heart rate data is in progress.

*Table 1: Summary of physiological measurements madeon O. edulis exposed to different temperature regimes. 20 = continuously 20°C, 25 = continuously 25°C and HW= heat wave treatment, in which the temperature alternated between 25°C and 20°C on a weekly basis. NO = O. edulis from Norway, NE = O. edulis from The Netherlands, CR = O. edulis from Croatia. 10 is best performance, 1 is worst performance. Nd = no data, Ap = analysis in progress.*

| Response | Treatment | Origin + year | | | | |
|---|---|---|---|---|---|---|
| | | NO 2021 | NE 2021 | NO 2022 | NE 2022 | CR 2022 |
| Survival | 20 | 10 | 10 | 10 | 10 | 7 |
| | 25 | 10 | 10 | 10 | 10 | 9 |
| | HW | 10 | 10 | 10 | 10 | 8 |
| Growth | 20 | 10 | 6 | 10 | 7 | 2/3 |
| | 25 | 10 | 4 | 8 | 5 | 1 |
| | HW | 8 | 2 | 9 | 6 | 2/3 |
| Condition | 20 | ? | ? | 7 | 10/9/8 | 1/2 |
| | 25 | ? | ? | 5 | 10/9/8 | 1/2 |
| | HW | ? | ? | 6 | 10/9/8 | 3 |
| Respiration | 20 | 10 | 10 | 10 | 10 | 10 |
| | 25 | 7 | 7 | 7 | 7 | 7 |
| | HW | 4 | 4 | 4 | 4 | 4 |
| Clearance | 20 | Nd | Nd | 5 | 5 | 5 |
| | 25 | Nd | Nd | 5 | 5 | 5 |
| | HW | Nd | Nd | 5 | 5 | 5 |
| Valve gape | 20 | Ap | Ap | Ap | Ap | Ap |
| | 25 | Ap | Ap | Ap | Ap | Ap |
| | HW | Ap | Ap | Ap | Ap | Ap |
| Heart rate | 20 | Nd | Nd | Ap | Ap | Ap |
| | 25 | Nd | Nd | Ap | Ap | Ap |
| | HW | Nd | Nd | Ap | Ap | Ap |

Based on the results obtained so far, the physiological responses growth and respiration rate are indicative of stress in flat oysters as a result of exposure to marine heat waves. Results on valve gape and heart rate may provide more information.

### *1.4. Acknowledgements*

We thank Ainhoa Blanco, Emiel Brummelhuis, Jennifer Chin, Suzanne Cornelisse, Pim van Dalen, Ad van Gool, Jack Perdon, Diedrich Vahrenkamp and Wouter Suykerbuyk of Wageningen Marine Research for their contribution to the experiments.

## Chapter 2 – Seawater thermal tolerance of an intertidal canopy species across its European range of distribution

SL21-23 Contributors: Axel Chabrerie, Luis F. Pereira, Francisco Arenas, Fernando P. Lima, R. Seabra.

### *2.1 Introduction*

*Ascophyllum nodosum* Linnaeus (Le Jolis) is a common, fucoid seaweed that forms complex habitats in the upper intertidal zone and displays a broad distribution range within the North Atlantic region from Svalbard to Portugal. Like other macroalgae, this species forms a large and stable canopy throughout the year as its frond can reach up to 5 m length and individuals can leave up to 15 years (Jenkins et al., 2004). The complex structure of these algal forests harbours a highly diverse assemblage, offering refuge from predators and protection against wave action, desiccation, etc. (Wernberg and Filbee-dexter 2019), (Jenkins et al., 2004). Additionally, *A. nodosum* plays a key role in coastal ecosystem processes, such as nutrient cycling and primary production (Schiel & Foster, 2015; Thomsen et al., 2015). Consequently, it is regarded as a foundation species within coastal ecosystems, holding significant ecological and economic value (Buschmann et al., 2006; Schiel & Foster, 2015).

The recent rise in sea surface temperature (SST) caused by human activity poses an increasing threat to marine ecosystems, particularly impacting coastal communities. According to the Intergovernmental Panel on Climate Change (IPCC, 2018), it is projected that the SST in the North Atlantic region will potentially increase by up to +4°C by the end of the century. This increase has been associated with shifts in intertidal community (Fernández, 2016, (Díez et al. 2012), (Pineiro-Corbeira et al. 2016). The response of marine community is not even as the size and intensity of the effect depends on locations facing different degree of warming. In the case of the north Portuguese coast, the local North West Iberian upwelling creates a cold pocket that represents a climate refugee for many boreal species, which ultimately results in one of the most diverse marine algae assemblages of Europe (Salois et al. 2022). However, the increase of global temperature has been responsible for changes in oceanic circulation and wind pattern affecting the NW Iberian upwelling, and this oceanic phenomenon is expected to decrease in intensity the following years (Sydeman 2014), (Sousa et al. 2020). These changes could have significant implications for local marine communities, particularly for boreal species like A. nodosum. These species reach their southern distribution limit in Portugal and thrive there due to the favourable conditions created by the NW Iberian upwelling (Assis et al., 2018; Salois et al., 2022; Monteiro et al., 2022)

A commonly held perspective regarding the sensitivity of this species to global warming suggests that trailing range populations may face higher risks. This assumption stems from the tendency to consider species as single, homogeneous units with consistent thermal limits throughout their distribution range (Bennett et al., 2015). However, the response to temperature does not always exhibit consistent patterns among populations within a species. Moreover, there is evidence indicating the existence of potential phenotypic variation within several species of macroalgae (King et al., 2019, Wernberg et al., 2016a). A study by Gerard and Dubois (1988) reported that *Saccharina latissima* populations from warmer regions had higher heat tolerance than populations from colder regions suggesting adaptation to local conditions. Another study from *Wernberg* et al. (2016) reported intra-specific differences to increasing temperature from samples of three species taken along a latitudinal (2-4°C) gradient with greater temperature dependence of metabolism for algae from warmer locations (increased Q10) although temperature optima were similar (Wernberg et al., 2016a). On the other hand, Liesner et al. (2020) reported nearly identical responses to temperature among populations sampled across a latitudinal gradient despite marked difference in genotypes.

Given this results of previous measurements, the extent of intra-specific variation of thermal tolerance is expected to vary from one species to the other, and the overall response to increasing temperature of a species might be mediated by the expression of temperature resistant phenotypes. With the intensity and speed at which global warming is occurring, it becomes crucial to identify such phenotypes that could be key to successful and effective restoration (Coleman et al., 2020).

In this set of experiments, we tested whether different populations collected across a large latitudinal gradient would display different eco-physiological responses to atmospheric and oceanic temperatures. The present study aims to identify potential variation in different population of the specie *Ascophyllum nodosum*. We hypothesized that variation of *in situ* temperature across the large distribution range of *A. nodosum* would produce locally adapted phenotypes.

### *2.2. Material & Methods*

Specimen collection

Individuals of *Ascophyllum nodosum* were collected across a latitudinal gradient, from Straumøyna, Norway (60°55'N 4°48'E) to Viana do Castello, Portugal (41°42N

8°50'). All sites were selected for their extensive rocky intertidal zone, and display a large gradient of annual average SST (5 °C, see Figure 8)

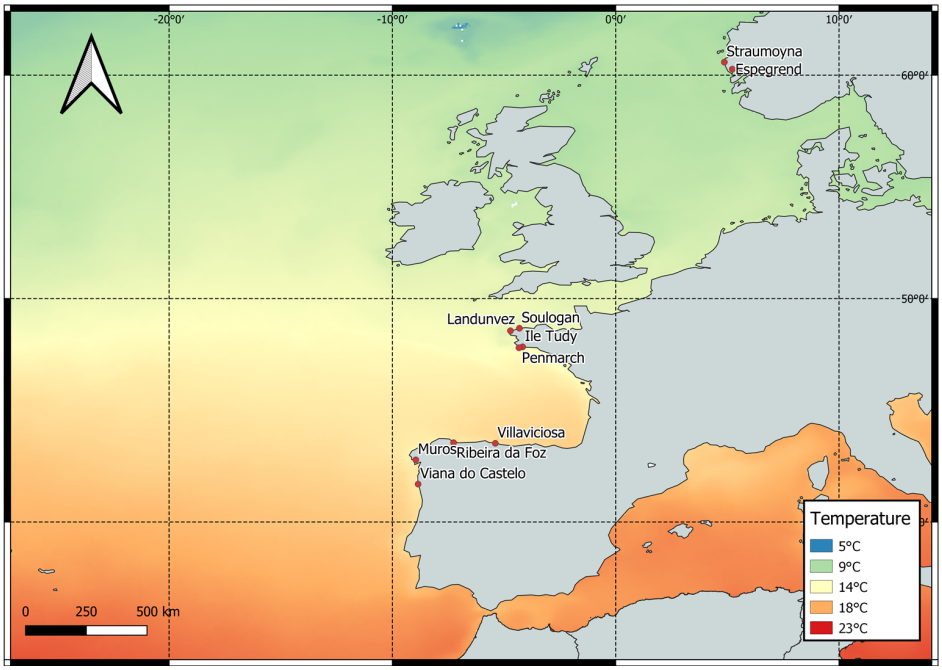


*Figure 8. Collection sites of the different populations of Ascophyllum nodosum. In situ average temperatures range from 7.8°C (Espegrend) To 14.5 °C (Ribeira da Foz)*

Young individuals showing absence of air bladders were selected in the upper intertidal and collected by gently cutting the base as closed as possible to the holdfast. Fronds were then transported by plane in cool boxes within 2 days. Upon arrival, algae were distributed in 60-l tanks with circulating natural seawater insuring good water motion and sufficient nutrient concentration for optimal growth. The system was equipped with full spectrum lamps (Cube 50, Aquamedic®) and with a tidal cycle of 5 h activated by micro controllers associated to motorized valves and pumps.

Fronds were utilized in two separate experiments. The initial experiment focused on examining the effects of atmospheric heatwaves, whereas the second aimed to clarify the relationship between temperature, primary productivity, and respiration rates of the species along a latitudinal gradient.

Experimental design for intertidal heatwaves

We designed the experiment as a mechanistic, short-term exposure to heat stress during low tides, simulating aerial exposure (Figure 9). Immersion duration was fixed to 5 hours, as observed in the field for this species. Therefore, a tide cycle of 7:5h (high:low) was applied to all treatments during the 20 days of experiment. Regarding low tide temperatures, a previous pilot study evaluated the low tide temperature stress on *A. nodosum*. Here, the peak temperatures was based on a 10-year-long temperature

dataset from robot-limpets, i.e., temperature sensors embedded in a limpet shell (Lima and Wethey 2012) deployed in Moledo do Minho (Portugal - 41°50'23.83″N; 8°52'26.37″W - 18Km from sampling site) to determine climatology and following heatwaves categories. Temperatures analysis for this site showed an average maximum temperature of 28.5 ºC in the 9-yr period between 2007 to 2016. Additionally, previous trials indicated that 38.5 ºC is a critical peak for atmospheric temperature exposure. Hence, two peak temperature treatments were included (36.5 and 40.5 ºC) to capture population-specific differences in thermal performance. To evaluate a possible recovery after a 10-d heat wave, another 10 days under control conditions (28.5 ºC peak temperature at low tide) was conducted.

Water temperature at the southern limit varies significantly (14 to 20.5 ºC) according to the action of the Canary Current upwelling. Such variation can cause a cumulative effect over the heatwave impact. Therefore, the previous 4 treatments were duplicated. Under high tide, all 4 heatwave treatments (28.5, 36.5, 38.5 and 40.5 ºC) were exposed when submerged to a normal upwelling temperature at the southern limit (14.5 ºC) or to a temperature experienced during lower upwelling (20.5 ºC).

Tide control was achieved via automatization of 1/2 inch ball valves (U.S. Solid, United States of America) which discarded all water from each tank, while high tide was achieved via a water pump that filled the experimental units with fresh seawater at the acclimated temperature. A total water replacement occurred at every high-low tide cycle, all tanks represent independent systems. Water temperature during high tide was maintained via 500-l tanks that contained all experimental tanks in a 15 ºC water bath system, and water cooling was achieved via recirculation with a water chiller (TECO TR15).

Air temperature during low tide was achieved through a fine control of two 125 W infrared lamps per experimental tank. Heat lamps were turned on/off according to a customized PID algorithm (Proportional-Integral-Derivative) that employed a variable time window of action every 10 seconds. A fan with 43,9 $m^3\ h^{-1}$ air flow (60mm wide) was turned on during all low tide to avoid temperature stratification. using a microprocessor to regulate the output. Two robolimpets (temperature sensors embedded in a limped shell) deployed inside each tank provided temperature feedback to the microcontroller (ATMEGA2560), which coordinated all electrical functions.

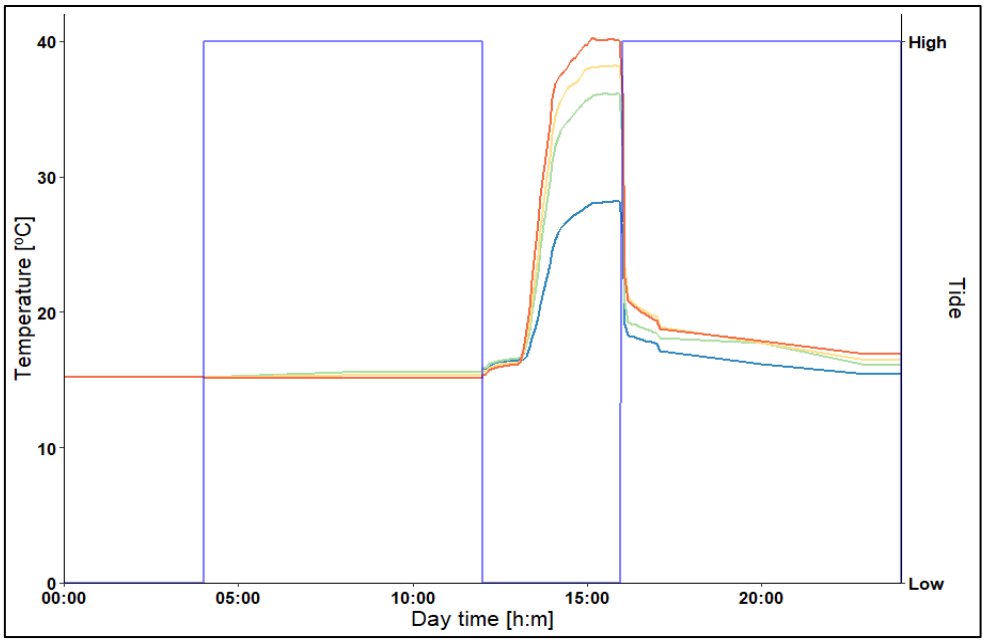


*Figure 9. Experiment tide and temperature profiles for the 20-day experiment.*

Therefore, specimens from the 10 populations (n= 10 pre population) were exposed to tidal cycles encompassing 2 low tides a day, for 20 days. However, the atmospheric heatwave occurred only during the first 10 days with low tide temperatures raised gradually with realistic rates. Peak temperatures of each treatment (28.5, 36.5, 38.5 and 40.5 ºC) were achieved for only 1 hour. During the following 10-d recovery period, all treatments were maintained at 15 ºC.

Assessment of temperature effects on respiration and primary productivity rates

A second set of young fronds was kept in the mesocosms for three months with sea water temperature at 17 °C and with tidal regime as in the previous experiment. The extended acclimation period was implemented to eliminate any legacy effects from previous temperature conditions and to ensure that the observed response in the experiment was solely attributed to the temperatures applied during the experiment.

For each set of incubation, four individual replicates per population were randomly distributed onto plastic racks and labelled using numbered plastic rings for a total of 40 algae per set. Due to replicate limitations, each set was then exposed to 3 levels of temperature separated by 3° C increments (i.e., 7, 10, 13 °C) and the overall temperatures for all the sets ranged from 7 to 33 °C (i.e. incubations were performed at 10 different temperatures: 7, 10,13,16,19, 22, 24, 27, 30 and 33 C). Prior to the incubation, algae were gradually acclimated to the next experimental temperature at a rate of 1 °C $d^{-1}$ to minimize stress due to abrupt exposure to higher temperature.

In order to assess the eco-physiological response to increasing temperature of each population, we measured metabolic rates (primary productivity and respiration rate) through photosynthesis-irradiance (P-I) curves where oxygen evolution was recorded inside incubation chambers at successive increasing irradiance levels. Incubation chambers consisted of 20 cl sealed acrylic chambers partially submersed inside of a water bath maintaining constant temperature. Water motion inside the incubation chambers was maintained using magnetic stirrers. Each incubation chamber was filled with 5-µm filtered sterilized (UV) seawater. Each chamber was equipped with optical oxygen sensors (OxyPro®, PreSens). We simultaneously used 4 chambers with 4 optical sensors placed inside a light controlled cabinet able to perform six different light intensity levels: 0, 25, 85, 140, 390, 690 µE $m^{-2}$ $s^{-1}$. The light source inside the chamber was composed of LED sources and light intensity inside the chamber was monitored using a PAR light sensor (Walz). In each run, an empty chamber was used as blank control to correct for seawater respiration

P-I curves from productivity data were fitted using the R package phytotools using the model of Eilers and Peters (1988) following the equation:

$$GPP = \frac{GPmax2(1+\beta)(E/Eopt)}{(E/Eopt)^2 + 2\,\beta E/Eopt + 1}$$

where GPmax is the maximum productivity at selected irradiance and temperature, Eopt is the optimum light intensity and β the slope of photo-inhibition. Our analysis focused on the maximum gross productivity estimated from the PI curve (µmol $O^2$ g $DW^{-1}$ $min^{-1}$) as it appeared to be the most responsive parameter to our treatments. Each individual algal frond was dried at 60 °C for 48 h to obtain estimation of dry weight (DW) and correct values of P-I curves.

Fitting thermal performance curves and statistical analyses

Analyses of the data from both experiments are still undergoing. We present some initial plots and preliminary statistical analyses.

In the case of the first experiment, the effects of region, seawater temperature and heatwave intensity (air temperature) on the growth of the fronds were analysed using linear mixed models (LMMs). The factors region (South, Center and North), seawater temperature (warm vs. cold) and heatwave intensity (Control (28.5), Mid (36.5), High (38.5) and Extreme (40.5)) were included in the fixed part of the model as predictor variables, while population (nested in Region) and tank (nested in the interaction Seawater temperature x Heatwave intensity) were included as random effects. We used

linear models not to find a single ‘‘best’’ model describing the relationship between predictors and dependent variables but to analyse causality between them. Therefore, once each full multiple model was set, we proceeded to select those predictors with a truly significant effect on the response variable using a stepwise model selection procedure applying AIC as the selection criteria. Models were run using lmerTest package. Residuals were checked with Q-Q plots and plots of standardized residuals versus expected values, using DHARMa package. The same package was used to assess heteroscedasticity and checked for over-dispersion.

For the second experiment investigating the impact of temperature on the metabolic rates of *Ascophyllum nodosum*, we constructed thermal performance curves to better comprehend the reaction norm of photosynthesis of Ascophyllum nodosum to temperature. These curves were built based on the responses measured during the experiments. We fitted TPCs using the nls.multstart and rTPC packages following the methodology described by Padfield et al. (2021). This method consists in fitting non-linear models using the package nls.multstart which estimate best fit for non-linear regression by comparing AIC scores over several iterations. The Gauss-Newton fit commonly used to describe metabolic processes is highly sensitive to the choice of starting values and is often source of errors when estimating physiological response of an organism. This package addresses this problem by allowing the determination of starting value which make the estimation of best fit more reliable. A Sharp-Schoolfield was fitted and rTPC package was then used to calculate derived parameters from the fits describing the temperature dependence of productivity. Our models included Topt the optimum temperature at which maximum rate was reached, thermal safety margin defined as the difference between Topt and Ctmax (critical thermal maxima at which productivity drops to 5% of its maximum value), as well as the energy of deactivation for the process at temperature beyond Topt.

Lastly, we used parametric bootstrapping in order to compare descriptors extracted from the TPCs using the boot package (version 1.3-27, (Canty and Ripley 2022). The method estimates 95% CI of each descriptor based on 1,000 bootstrap replicates of the model using resampling method. We then considered descriptor to be significantly different if their 95% CIs were not overlapping.

### *2.3. Results*

Analyses of results from both experiments are still undergoing. We present some plots and preliminary statistical analyses.

<u>Atmospheric heatwaves experiments</u>

Figure 10 and Figure 11 illustrate the growth rates of the fronds both at the end of the 10-d atmospheric heatwave and at the end of the subsequent 10-d recovery period (day 20).

*RGR% - After 10 of heat stress*

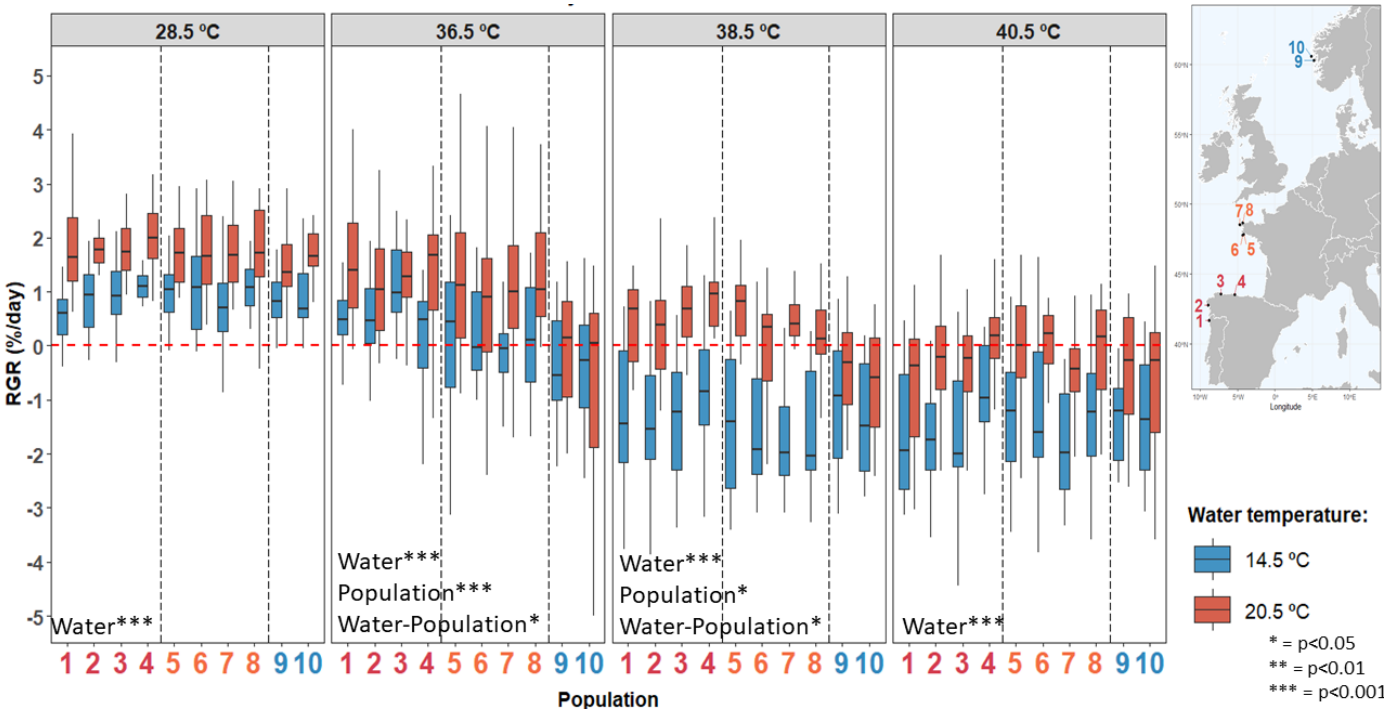


*Figure 10. Residual Growth Rate (RGR) in percent per day (% / day) for the 10-d heatwave stress (n=10). Populations are numbered by growing latitude (1-Viana do Castelo, 2- Ria de Muros, 3- Ria da Foz, 4- Ria de Villaviciosa, 5- Landunvez, 6- Île-Tudy, 7-Penmarch, 8- Soulogan, 9- Espegrend and 10- Straumoyna). The location of the 10 populations is provided in the insert map.*

*RGR – After 10 days of recovery*

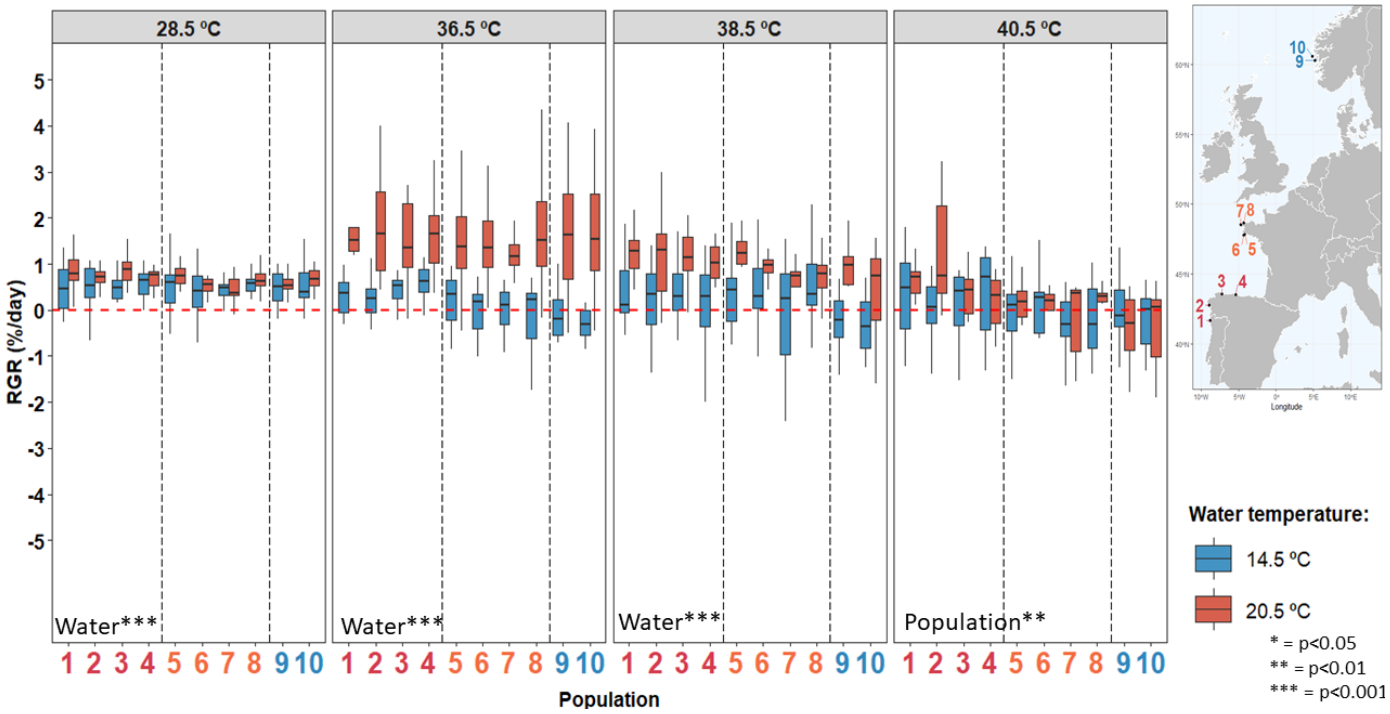


*Figure 11. Residual Growth Rate (RGR) in percentage per day (%/day) during the 10-d recovery period (n=10). Populations are numbered by growing latitude with the location shown in the insert map.*

Results from these analyses show a significant effect of Region both at the end of the heatwave and at the end of the recovery period. Temperature of the water is also significant during the heatwave and the intensity of the heatwave is always significant even when the heatwave was not active, suggesting a legacy effect in the recovery rates.

*Table 2 Summary of results for the linear mixed models on the RGR (relative growth rates) after the first 10 days (heatwave period) and the second 20 days (recovery period).*

| Effect | 10 days RGR | 20 days RGR |
|---|---|---|
| ***Fixed effects*** | ***Estimate (SE)*** | ***Estimate (SE)*** |
| Intercept | 7.149(1.09)*** | 6.657(2.77)* |
| Region North | -0.3836(0.115)** | -1.099 (0.28)** |
| Region Centre | -0.1385(0.094) | -0.586 (0.23)* |
| Water temp | -0.7757(0.272)* | - |
| Air temp | -0.2067(0.028)*** | -0.191 (0.06)* |
| ***Random effects*** | ***$\sigma^2$ (SD)*** | ***$\sigma^2$ (SD)*** |
| Population | 0.0028(0.052) | 0.049(0.22) |
| Tank | 0.272(0.552) | 1.390(1.17) |
| Residual | 2.379(1.542) | 9.01 (3.00) |
| ***Post-hoc contrasts for Region effect*** | | |
| Region North<Region South | | |
| Region Centre=Region South | | |
| Region Centre=Region North | | |

Seawater effects were strong and highly conspicuous in the final mortality rates (see Figure 12). Results of this response and other are still under analyses.

*Mortality – After 20 days*

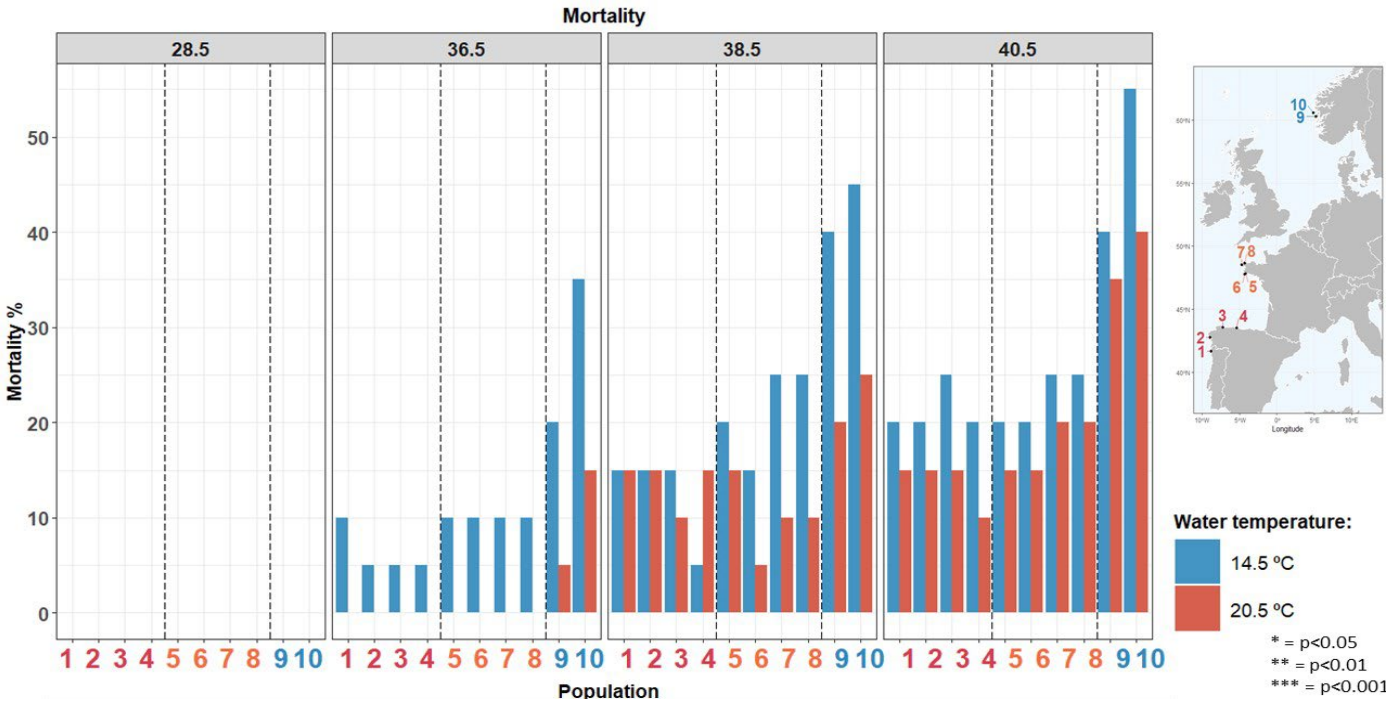


*Figure 12. Observed mortality after 20 days of trial (n=10). Populations are m«numbered by growing latitude (1-Viana do Castelo, 2- Ria de Muros, 3- Ria da Foz, 4- Ria de Villaviciosa, 5- Landunvez, 6- Île-Tudy, 7-Penmarch, 8- Soulogan, 9- Espegrend and 10- Straumoyna).*

Assessment of temperature effects on respiration and primary productivity rates

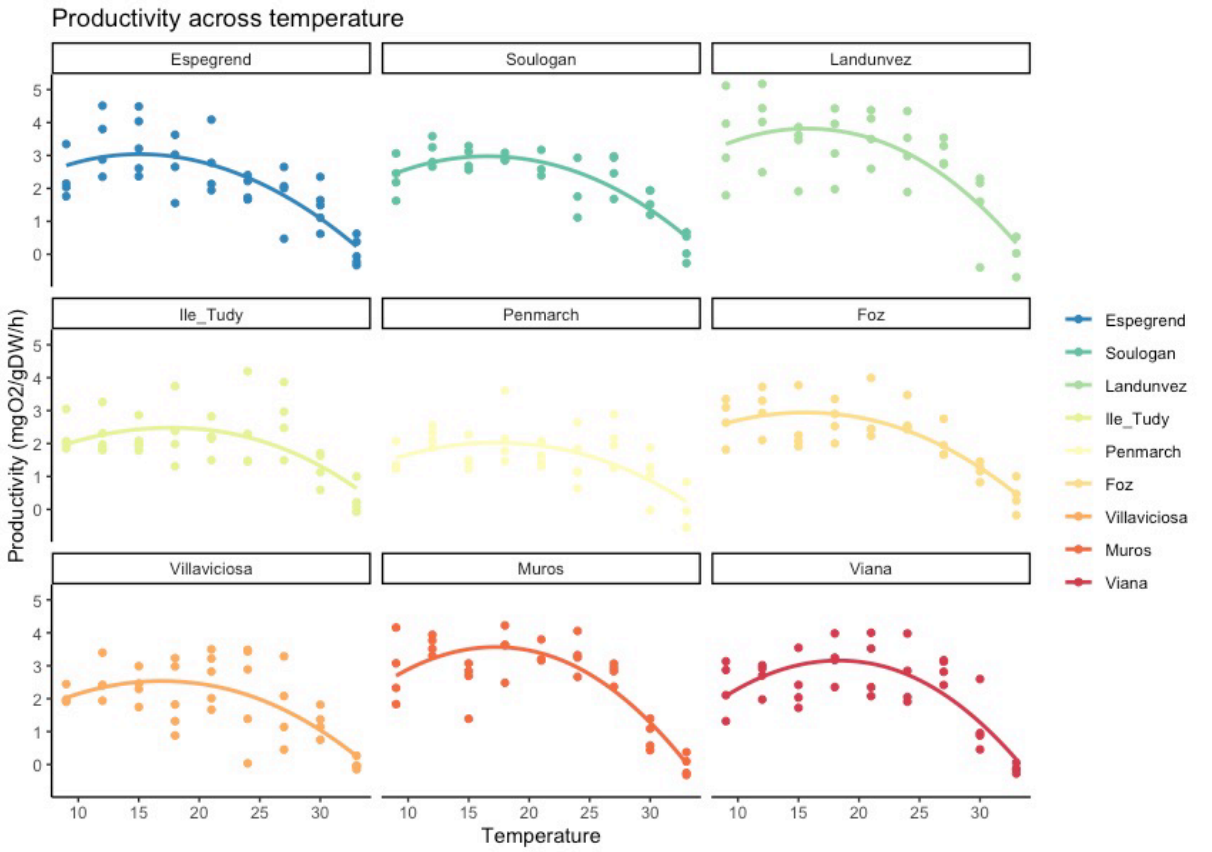


*Figure 12: Thermal performance curves of maximum primary productivity according to the method described in Padfield et al.( 2021) for the 9 populations of A. nodosum.*

*Thermal performance curves - optimal Temperature*

Figure 13 displays the thermal performance curves estimated for the nine populations examined in this experiment. Optimal temperature calculated from these TPCs ranged from 16.27 °C (Espegrend, Norway) to 25.26 °C (Penmarch, France), Figure 14. Significant differences were observed between populations collected in Espegrend (16.27 °C, ci (confidence interval):13.88-18.38) and several populations in France: Ile Tudy (24.41 °C, ci: 20.13, 27.50), Penmarch (25.26°C, ci: 22.14-28.35) and the Iberian Peninsula: Muros (22.09 ºC, ci: 17.91-22.29 °C) and Viana (22.9, ci: 19.57-26.75 °C).

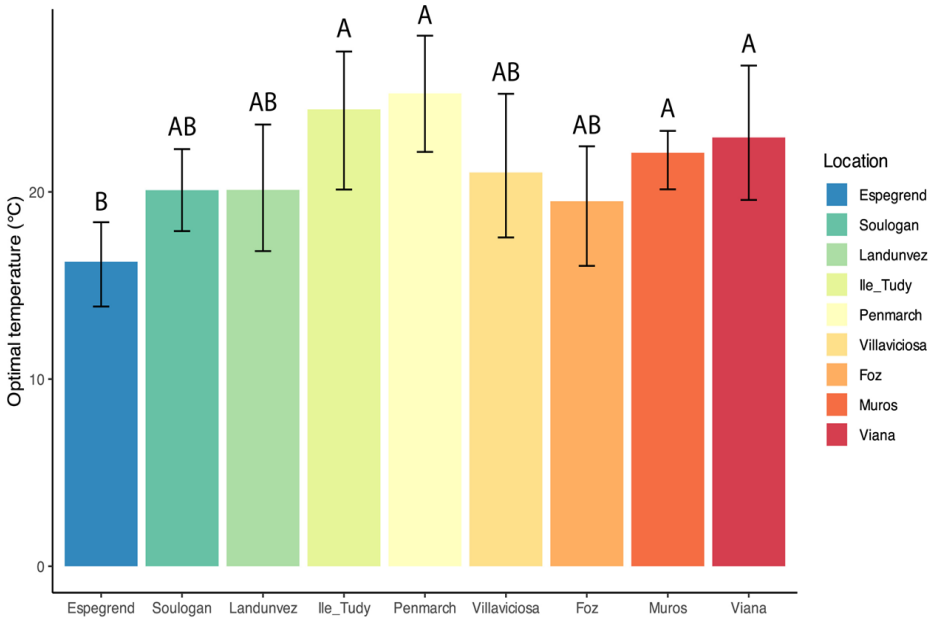


*Figure 13. Temperature optima estimates for populations of Ascophyllum nodosum collected along a latitudinal gradient. Values are presented as estimates ± 95% CI (n=40). Estimates were calculated from Thermal perfromance curves and compared by overlapping confidence intervals.*

*Temperature dependence of photosynthesis: Energy of activation and deactivation*

Values of activation energy (Ea) were between 0.023 eV (ci 0.015-0.032) in Foz, Spain, and 0.181 eV (0.023-0.300) in Muros, Spain (Figure 15). Fronds collected in Espegrend had lower values of Ea (0.043 eV, 0.031-0.053) than Villaviciosa (0.120 eV, 0.080-0.180) and Viana (0.180 eV, 0.110-0.250) populations. Values of Ea at Foz (0.023 eV, 0.015-0.032) were lower than those of other populations except Landunez, France (0.03eV, 0.015-0.041).

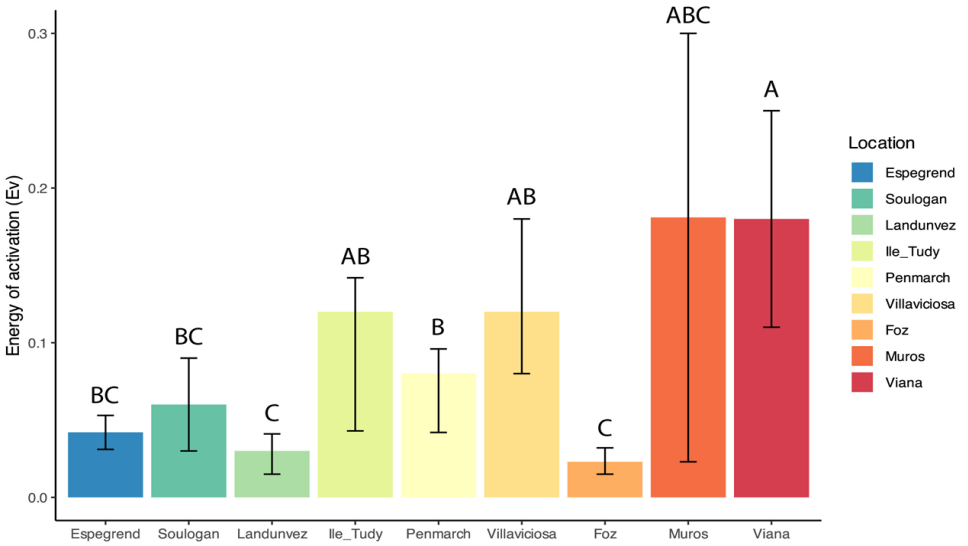


*Figure 14. Energy of activation (Ea) estimates for populations of Ascophyllum nodosum collected along a latitudinal gradient. Values are presented as estimates ± 95% CI (n=40). Estimates were calculated from Temperature-productivity curves and compared by overlapping confidence intervals (ci).*

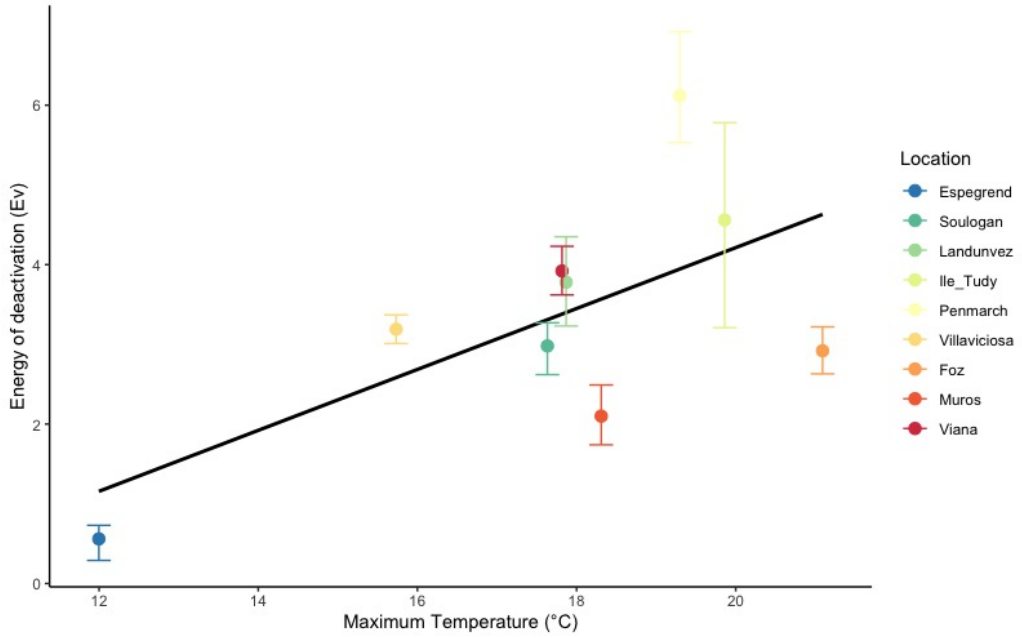


*Figure 15: Relation between energy of deactivation estimates and maximum in situ temperature for populations of Ascophyllum nodosum collected along a latitudinal gradient. Values are presented as estimates ± 95% CI (n=40). Estimates were calculated from TPCs.*

Differences in the Energy of deactivation (Eda) across populations (collection sites) followed a similar pattern as differences in the Ea. Values of Eda ranged from 0.56 (Espegrend, Norway) and 6.12 (Penmarch, France). Significant differences were found between the population collected in Penmarch (6.12 eV, ci: 5.53, 6.92) and all other populations apart from population of Landunvez (3.78 eV, ci: 3.23, 4.35) which is relatively close to Penmarch. The population of Espegrend (0.56 eV, ci: 0.29, 0.73) differed from all other populations. The populations of Viana and Landunvez had similar Eda (3.92 eV, ci: 3.62 to 4.23). Finally, the Pearson correlation coefficient between Energy of deactivation and maximum in situ temperature was estimated to be 0.64 (p = 0.059) with populations from Muros and Foz departing from the tendency of linear increase in Eda with maximum temperature (Figure 16).

### *2.4. Discussion*

The two experiments used in SL21-23 had distinct approaches and objectives. The atmospheric heatwave experiment was designed to simulate present and extreme future atmospheric conditions, making it a realistic representation of potential scenarios of CC. Notably, this study stands out as one of the pioneering investigations that examine the

interplay between seawater temperature and atmospheric heatwaves. The experimental design encompassed a gradient of atmospheric heatwave treatments which exerted significant impacts on the performance of *Ascophyllum* fronds. The presence of a latitudinal gradient in the responses was clear, implying that local conditions likely have an impact on thermal sensitivity. Fronds collected from Northern European sites suffered stronger deleterious effects from the intense atmospheric heatwave treatments used in the experiment. However, it is worth highlighting that the influence of seawater temperature was also clearly discernible, indicating its synergistic role in shaping the the ecophysiological response of this seaweed. The fronds in the treatments with colder water (14 ºC) exhibited poorer performance than those submerged at 20 ºC. Additional ongoing statistical analyses are expected to validate these findings.

The second experiment did not aim to predict the effects of realistic temperature increase scenarios on different populations of *Ascophyllum nodosum* across European waters. Instead, our goal was to assess the thermal dependence of metabolism of this intertidal species across it current range of European distribution. It has been assumed that populations of the same species experiencing different thermal regimes share a common thermal niche breadth. In this context, rear edge populations were thought to have a lower thermal safety margin compared to central edge populations, making the former more vulnerable to warming leading to range contraction. However, over the past decade, this view has changed with accumulating evidence of species-specific adaptation to local environmental conditions (Bennett et al., 2015; Wernberg et al., 2016). Our study demonstrated that different populations of *A. nodosum* sampled across its distribution range displayed differences in eco-physiological responses to increasing temperature. We found a tendency for increasing Topt at warmer compared to colder locations (i.e., significance difference between population from Espegrend and the population from Viana, as well as differences between French populations and the population at Espegrend). CTmax also increased with increasing Topt which led to rather subtle differences in thermal safety limits (the difference between CTmax and Topt). Thus, central and rear edge populations might be exposed to the same thermal risks as previously reported by Bennet et al. (2015) due the expression of thermal ecotypes.

Differences in sensitivity to temperature via Energy of activation (Ea) and energy of deactivation (Eda) may have important ecological implications for European seaweed assemblages, not only defining distribution edges but also abundance patterns (Piñeiro-Corbeira et al., 2018). In the limited number of experiments conducted to estimate the Ea in seaweeds, species that exhibited an upward trend in Ea with rising sea surface temperatures (SST) demonstrated a higher Ea compared to species that have suffered

historical range contraction (Piñeiro-Corbeira et al., 2018). Our study contributes to this emerging field by examining the variation in Ea and Eda, which are key parameters indicating the temperature-dependent nature of metabolism, across different populations. Our measurements indicated that the samples from Norway exhibited lower values for both Ea and Eda, suggesting a slower thermal response within this population. Unfortunately, we only examined one population from Norway and testing additional populations from this region might yield interesting results with relevance to local CC adaptation actions.

They are several known processes that could lead to local adaptation in response to changing environmental conditions. In areas of high gene flow, post settlement selection processes often lead to the survival of the fittest genotypes consequently shaping adapted phenotypes (Sanford and Kelly, 2011; Richardson et al., 2014). In the case of *A. nodosum* along the European coast, the highest intra-population difference in genotype occurs in Brittany (France) coincident with a strong difference in average temperature conditions across the transition between English Channel and the Bay of Biscay (Olsen et al. 2010). Adaptation to different local thermal conditions could be responsible for the observed differences in thermal traits among French populations despite the proximity of the collection sites.

These findings indicate that the ability to tolerate rising temperatures may have a substantial impact on the distribution of *A. nodosum* in the near future. Currently, species distribution models (e.g. Task 4.1) are widely utilized tools for projecting habitat distribution and identifying potential range shifts in a future climate. However, these models often fail to incorporate important factors such as plasticity and differences in ecotypes, resulting in less accurate predictions (Valladares et al., 2014). The work reported here presents a straightforward methodology and user-friendly tools for identifying thermal traits both between and within species. Furthermore, the identification of heat-resistant ecotypes has been demonstrated as a crucial factor for successful restoration efforts (Coleman et al., 2020). Future restoration efforts may encounter challenges due to limited knowledge about the thermal traits of different populations within a species.

We are performing genetic analyses of these nine populations that should be completed before the conclusion of FutureMARES. The methodologies described in this chapter of the Task 3.2 report, combined with the genetic characterization of different ecotypes, could serve as an important step towards implementing more effective restoration strategies. Temperature serves as a primary factor determining the distribution of

seaweeds. Despite uncertainty in the magnitude and scope of ocean warming, our projections of climate-driven changes in species distribution or restoration success using habitat-forming seaweeds (and other species) will be more robust if potential variations in thermal characteristics either among or within species are identified.

## Chapter 3 – Temporal variability in the response to thermal stress in the red gorgonian, *Paramuricea Clavata*: insights from common garden experiments

SL29 Contributors: Sandra Ramirez-Calero, Ledoux JB, Barreiro, A, Bensoussan N, López-Sendino P, Gómez-Gras D, Montero-Serra I, Pagès-Escolà M, Medrano A, López-Sanz A, Figuerola, L, Linares C, Garrabou J.

### *3.1 Introduction*

The Mediterranean Sea, considered as a hotspot of marine biodiversity and climate change (Cramer et al., 2018), has been affected by recurrent mass mortality events (MMEs) linked to marine heat waves (MHWs) with differential impacts among species, populations and individuals (Garrabou et al.. 2022). Habitat-forming octocorals such as *Paramuricea clavata* were strongly impacted with up to 80% of individuals affected in some localities (Cerrano et al.. 2000; Garrabou et al.. 2009; Garrabou et al., 2022). This Mediterranean octocoral is characterized by slow population dynamics and restricted dispersal abilities (Linares et al., 2008; Arizmendi-Mejía et al., 2015), thus, MMEs can have large impacts on the evolutionary trajectory of this species. Moreover, *P. clavata* has a key ecological role increasing habitat complexity in biogenic coralligenous communities. Thus, its decline owing to MMEs may have cascading effects on associated communities and related ecosystem functioning (Gomez-Gras et al., 2021) and related services.

Differential responses to MMEs among individuals and populations have been reported within both field and laboratory measurements applied to this species (Garrabou and Harmelin, 2002; Crisci et al., 2011), suggesting spatial variability in the response to thermal stress with differential impacts among individuals/populations. Yet, these studies have not included observations across consecutive years. Accordingly, the level of temporal variability in the response to thermal stress is totally unknown. This study aimed to analyze the differential response to thermal stress among individuals and populations of *Paramuricea clavata* across three consecutive years. We discuss our results in light of recent *in-situ* thermal history and of the genetic differences among individuals and populations.

### *3.2 Materials & Methods*

Individual samples of *P. clavata* were collected yearly from 2015 to 2017 in early September from three different locations around Medes Island (Spain, 42°02'60.00" N 3°12'60.00" E). Thirty healthy adult colonies (>50 cm) were initially tagged in 2014 at each location within a depth range of 15-20 m. From each marked colony, apical fragments were collected every year and allocated in the Aquarium Experimental Zone (ZAE) of the Institut de Ciències del Mar (ICM-CSIC) in Barcelona. After one week of acclimation in an open aquarium system at 17-18 °C, each colony branch was divided into two and common garden experiments were conducted with one control (18 °C) and one stress treatment (25 °C).

For the control, the seawater temperature was maintained between 16-18 °C during the whole experiment. For the stress treatment, the temperature was increased stepwise from 18 to 25 °C over a period of 3 days. Once the temperature reached 25 °C, thermal conditions were maintained for 25 days following previous methodology (Crisci et al., 2017). Feeding was carried out three times per week in each tank.

***Thermal environments.*** Thermal environments experienced by the colonies during the summer season (June, July and August) were characterized every year. Temperature data for Medes islands were obtained from the T-MEDNet database https://t-mednet.org with local temperature conditions documented using a standard protocol of multi-year time series collected every hour in 5 m intervals between the surface and 40 m depth.Our analysis includes the average local thermal regime (calculated from an entire annual-series), and a recent thermal regime (calculated over the 3-months period prior to the experiment: June, July and August) to contrast with thermotolerance responses of *P. clavata* reflected during the experiment. We use the same classification from the database to consider the severity of impacts from MHW-induced MMEs to classify the observed effects in our colonies, as follows: Low impacts: populations/individuals exhibiting less than 30%, Intermediate: between 30 and 60%, and Severe: more than 60% of affected colonies (Garrabou et al., 2019).

***Common-garden experiments.*** The percentage of tissue necrosis (extent of injury) was used as a proxy of colony response to thermal stress. Each individual was monitored visually every day until the end of the experiment. Then, we estimated the mean (and SD) extent of injury for each population and each year by using the average amount of injured tissue across all individuals. Secondly, the survival probabilities for each colony

and population during the time of the experiment (*i.e.* having less than 100% of injured surface) were evaluated using a series of COX models under the *survival* R-package (Therneau, 2020). Finally, since we sampled the same individuals every year, we also reported the daily trajectory of tissue necrosis for each colony each year separately to look for temporal variability at the population and individual levels.

***Genetic structure:*** Gene diversity estimates for each individual and locality were assessed using the genomic DNA of 87 individuals genotyped with 17 polymorphic microsatellites. Hardy Weinberg Equilibrium (HWE) was tested for each population, and we computed the inbreeding coefficients ($F_{IS}$ (Slatkin, 1991) in *adegenet (Jombart 2008)* and *Genepop* (Rousset, 2008) R-packages. We estimated the genetic diversity ($H_e$ and $A_r$) for each population in *poppr (Kamvar et al., 2015)* and *hierfstat (Goudet, 2005)*. A Discriminant Analysis of Principal Components (DAPC) was used to describe the genetic differences across populations from Medes Islands, specifying a *max.n.clust* = 3, a maximum number of 100 PCs and the lowest value of BIC (Bayesian Information Criterion). We computed pairwise $F_{ST}$s between population pairs and tested for their significance with a Fisher's exact test using *Genepop*. Additional genetic differentiation was tested using local $F_{ST}$'s in GESTE v2.0 with default parameters.

***Heterozygosity-Fitness correlation:*** To obtain a proxy for individual response to necrosis, a Principal Component Analysis (PCA) was applied considering each individual and year, and the percentage of necrosis per day as variable using *FactoMineR* R-package. The scores of PCA1 were employed as a proxy for phenotypic response to test whether the individual heterozygosity (standardized multilocus heterozygosity (sMLH) estimates in the Rpackage *InbreedR()*) was associated with increased resistance to thermal stress using a linear model (*lm(necrosis ~ sMLH))*.

### *3.3 Results*

#### *Thermal environments.*

The average local thermal regime for Medes islands exhibited similar mean annual temperatures around 17.0ºC ± 3.3 SD in 2015, 17.1ºC ± 3.3 SD in 2016 and 16.9ºC ± 3.6 SD in 2017. During the summer season, mean temperatures were lower for 2016 (20.6ºC ± 1.7 SD) and 2015 (20.7ºC ± 2.2 SD) and higher for 2017 (21.3ºC ± 2.0 SD). Recent thermal histories indicated temperature anomalies (extreme heat days) with contrasting patterns between years (Figure 17). 2017 exhibited the largest number of temperature anomalies with two surpassing the thermal risk zone of *P. clavata* (23ºC).

Furthermore, 2015 presented three temperature anomalies with only one surpassing 23ºC, whereas 2016 had only one anomaly reaching 23 ºC as maximum temperature (Figure 17).

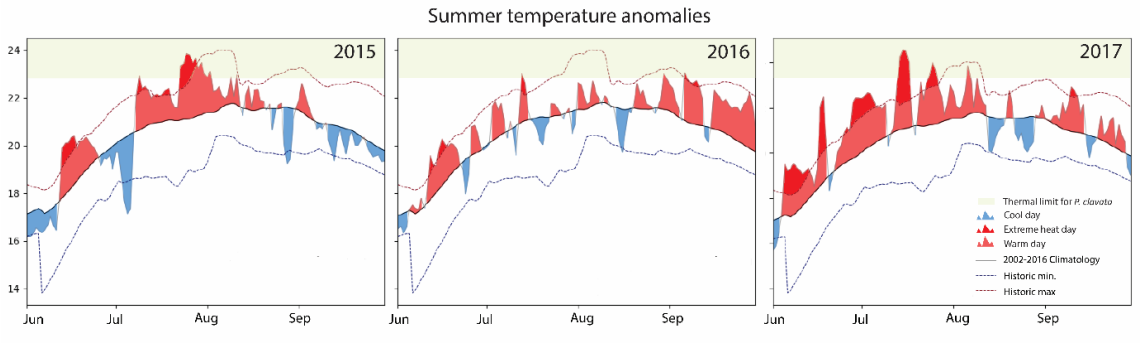


*Figure 16. Daily temperature values recorded during the three months prior to the experiment (Summer season) in the context of historic min and max recorded for this region. Days below climatology line were considered as "cool days", whereas days above were considered as "warm days". Temperature anomalies were recorded for each year and were considered as "Extreme heat days", highlighted in dark-red. The risk zone for P. clavata (>23 C) is represented in light-yellow.*

***Experiments:***

Tissue necrosis was observed for all populations in the three experiments. In 2015 and 2016, the extent of injury was below 40% at the end of the experiment (day 25). In contrast, all colonies were totally affected in 2017 (100% of tissue necrosis) by the 18$^{th}$ day, except for Pota del Llop where a 100% of tissue necrosis was reached at day 24. (Figure 18a). In addition, there were no significant differences in the survival probability when comparing between localities for any given year. Significant differences in the survival probability of colonies from the three localities were found across years ($p<0.001$). In 2015 and 2016, the probability of surviving slightly decreased only after day 15. In contrast, in 2017, the probability of survival sharply decreased after day 10. The probability of surviving in 2015 and 2016 was higher in comparison with 2017 (Figure 18b).

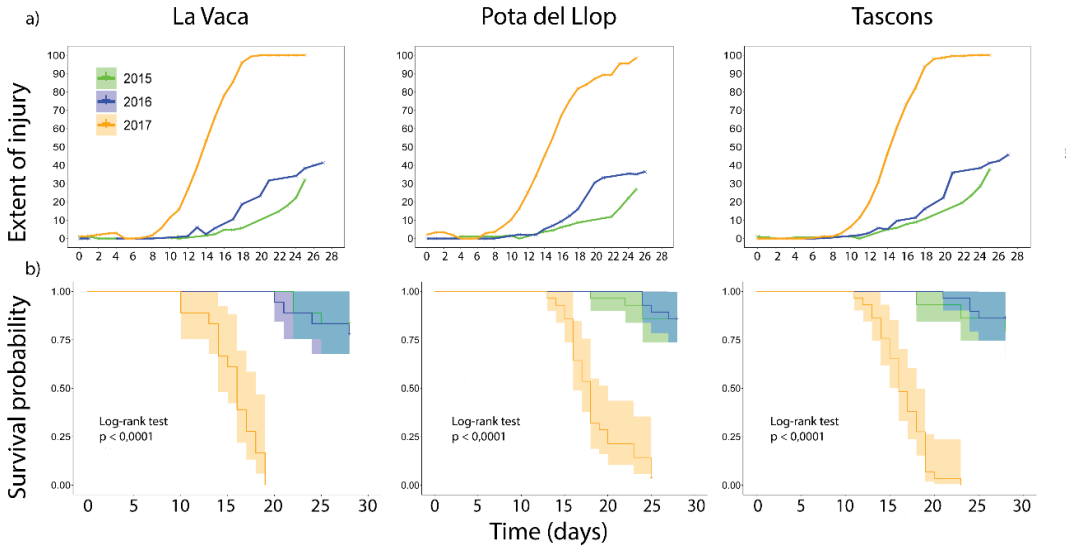


*Figure 17: a) Average tissue necrosis in common garden experiments in La Vaca, Pota del Llop and Tascons from 2015 to 2017. b) Differences in survival probability (i.e. mortality) across years in P. clavata when exposed to thermal stress Kaplan-Meier survival curve (p<0.001).*

The observed heterozygosity ($H_o$) in *P. clavata* varied from 0.609 to 0.664 among the three localities with a global Ho of 0.637, while the expected heterozygosity (*He*) ranged between 0.66 to 0.69 and a global value of 0.69. Pota del Llop displayed the highest number of alleles (8), while Tascons presented the lowest (7.27) (Table 2). Significant deviations from HWE were observed for all populations except Tascons (p>0.361, Table 3).

*Table 3: Genetic diversity statistics per population of* P. clavata. $H_o$ *(observed heterozygosity),* $H_e$ *(expected heterozygosity), local* $F_{ST}$*, observed* $F_{IS}$*, and HWE statistics. Significant values are highlighted in bold*

| | | | | | | **HWE** |
|---|---|---|---|---|---|---|
| | Ho | He | Allelic richness | Local $F_{ST}$ | $F_{IS}$ | *p-value* |
| **La Vaca** | 0.64 | 0.69 | 7.43 | 0.04 | 0.08 | **0.007** |
| **Pota del Llop** | 0.61 | 0.69 | 8.00 | 0.03 | 0.10 | **0.000** |
| **Tascons** | 0.66 | 0.66 | 7.27 | 0.05 | -0.15 | 0.361 |
| **Global** | 0.64 | 0.69 | 7.56 | **--** | **0.05** | **0.000** |

All pairwise comparisons of $F_{ST}$ were significant: La Vaca vs Pota del Llop (0.013, p<0.001), La Vaca vs Tascons (0.020, p<0.000), Pota del Llop vs Tascons (p<0.001 Table 4). The analysis of local $F_{ST}$ showed that the population from Tascons was the most differentiated from the others (0.051, 95% HPDI:[0.0304; 0.073]), followed by La

Vaca (0.040, 95%HPDI:[0.022; 0.059]) and Pota del Llop (0.036, 95%HPDI: [0.021; 0.051]).

*Table 4: Multilocus pairwise FST computed for three populations of P. clavata in the Mediterranean Sea based on 14 microsatellite loci are shown below the diagonal. Corresponding exact test p-values are shown above the diagonal.*

| | La Vaca | Pota del Llop | Tascons |
|---|---|---|---|
| **La Vaca** | -- | **0.001** | **6.44e-09** |
| **Pota del Llop** | 0.013 | -- | **4.82e-14** |
| **Tascons** | 0.020 | 0.035 | -- |

Multivariate analysis DAPC identified three genetic clusters (K=3) (Figure 19).

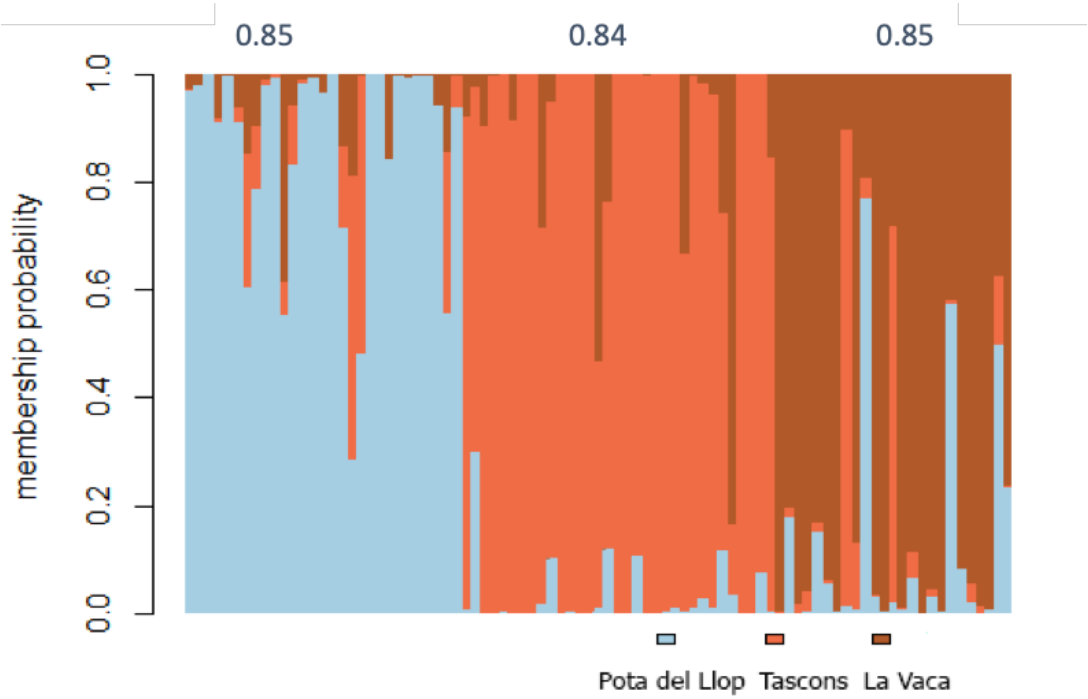


*Figure 18. Clustering analyses of P. clavata at Medes Islands. Each individual (n=87) is represented by a vertical line, where the different color segments indicate the proportion of membership to each genetic cluster (K=3): Pota del Llop (light-blue), Tascons (orange) and La Vaca (brown). The proportion of membership probabilities to each group (k=3) for the three populations are given above each cluster.*

sMLH values ranged from 0.294 to 0.882. The correlation between heterozygosity and fitness follows the expected negative trend with a decrease of fitness for low sMLH values. Yet, this trend was not significant (*p-value* = 0.66, Figure 20).

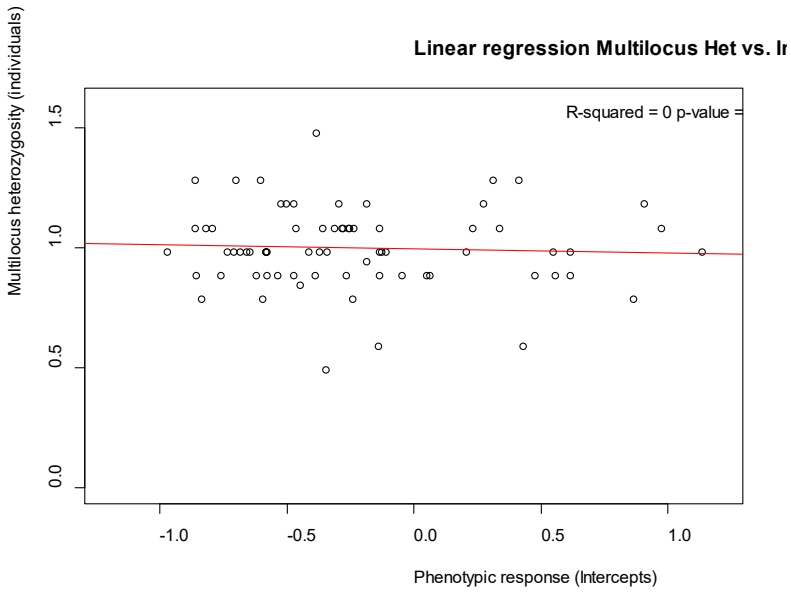


*Figure 19. Scatterplot of the sMLH values vs phenotypic responses with the regression line shown in red. R-squared value (r2=0) and p-value (p>0.66) are given at the top of the graph.*

### *3.4 Discussion*

In this work on SL29 characterized the spatial and temporal variability in the responses to thermal stress among individuals and populations of the red gorgonian *P. clavata*. We considered a local scale within 1 km$^2$ with three populations, while the temporal scale accounts for three consecutive years. We demonstrated a high variability in the percentage of tissue necrosis among the same individuals from the same population for a given year. This result is also in line with previous studies with *P. clavata* where necrosis values were variable across populations (Crisci et al., 2017) and individuals (Gomez-Gras et al., 2022) at different geographic scales.

We demonstrated a strong temporal variability in the response to thermal stress for all three populations. We found that the survival probability of colonies was strongly reduced in the 2017 experiment. Two non-exclusive hypotheses may potentially explain this result: i) impact of past thermal conditions (*i.e.* years before the experiment); ii) impact of recent thermal conditions (*i.e.* summer before the experiment). Preliminary results comparing 2017 with 2015 and 2016 thermal conditions at the depth where the populations dwell (15-20 m), point toward a stronger and longer thermal disturbance (>23°C) observed during June to September of 2017 in comparison with 2015 and 2016, supporting the high impact of recent thermal conditions on the response to thermal stress.

This study indicates that determining the thermal response of populations and individuals to marine heat waves may not be straightforward. Despite this, we also found some potential sensitivity/resistance patterns that may support climate adaptation conservation measures. Further studies focused on transcriptomic responses are needed to understand the potential adaptation of *P. clavata* populations in the Mediterranean Sea.

# Chapter 4 – Intraspecific variability in the response of *Ericaria crinita* to thermal stress

SL 29 Contributors: Jana Verdura, Jorge Santamaría, Raül Golo, Cèlia Sitjà, Cristina Galobart, Joaquim Garrabou & Emma Cebrian.

## *4.1 Introduction*

In marine ecosystems, the distribution patterns of species are mainly determined by temperature (Niell, 1977; Van den Hoek, 1982; Yarish et al., 1986; Van den Hoek et al., 1990), with marine organisms being particularly vulnerable to the effects of warming due to their temperature-constrained ecophysiology and geographical distribution (Sunday et al., 2012; Pinsky et al., 2019). At the present time, ample evidence exists for shifts in the distribution of marine species in response to warming stress (Wernberg et al., 2011; Somero, 2012; Poloczanska et al., 2013; Wiens, 2016). Species redistributions and local extinctions are of particular concern for habitat-forming species, because their disappearance can cause the collapse of the ecosystem they support (Smale & Wernberg, 2013; Wernberg et al., 2013, 2016; Hoegh-Guldberg et al., 2017; Hughes et al., 2017; Smale, 2020).

On intertidal and subtidal rocky shores in temperate and sub-polar regions, the main foundation species are brown macroalgae of the orders Fucales, Laminariales, Desmarestiales and Tyleptoridales (Feldmann, 1934; Giaccone, 1969). These canopy-forming macroalgae can create extensive and structurally complex assemblages that are similar to terrestrial forests (Steneck et al., 2002; Steneck & Johnson, 2013; Coleman & Wernberg, 2017), thus playing a fundamental role in the structure and functioning of shallow coastal habitats (Schiel & Foster, 2006; Wernberg & Filbee-Dexter, 2019).

Over the last years, many marine forest declines have been linked to the effects of chronic, gradual warming and to acute extreme warming events such as marine heatwaves (MHWs) (Wernberg et al., 2011; Tanaka et al., 2012; Smale, 2020; Wernberg, 2021). Additionally, future climate change scenarios project an increase in global warming and frequency of extreme events (Coumou & Rahmstorf, 2012; Perkins et al., 2012; Oliver et al., 2018, 2019). Despite this, the regional variability of macroalgae population responses to recent environmental change is larger than any global trend (Müller et al., 2009; Krumhansl et al., 2016), which highlights the need to consider local and regional-scale processes when aiming to understand the vulnerability of species across their distribution range. This is particularly relevant considering that many

macroalgae species are distributed across regions with different thermal characteristics, leading to the existence of intraspecific thermal divergence (King et al., 2018), something that should definitely be accounted for in the studies of species thermal-tolerance.

In the Mediterranean Sea, shallow rocky habitats are inhabited by canopy-forming macroalgae in the genus *Cystoseira*, *Ericaria* and *Gongolaria* (thereafter referred as *Cystoseira* sensu lato) (Feldmann, 1937; Giaccone & Bruni, 1973; Verlaque, 1987; Ballesteros, 1992) that create assemblages with similar functional properties to kelp forests and that represent the highest level of complexity in Mediterranean macroalgae-dominated assemblages (Ballesteros, 1988, 1990b, 1990a; Pinna et al., 2020). These species, similar to other canopy-forming species worldwide, are vulnerable to anthropogenic pressures and have experienced marked declines in recent years (Thibaut et al., 2005, 2015; Bianchi et al., 2014; Mariani et al., 2019), with climate warming emerging as an increasing threat for Mediterranean canopy-forming species (Capdevila et al., 2019; Verdura et al., 2021). However, our understanding of how these species respond to chronic thermal stress is still quite limited. For example, intraspecific differences in thermal performance or tolerance has never been assessed in these species. This information will be key to achieve an accurate understanding of the future trajectories that different populations might follow and to identify the most vulnerable and thermo-tolerant populations, which is fundamental for conservation and restoration prioritisation.

This experiment conducted as part of SL29 assessed the intraspecific variability in the thermal tolerance across a Mediterranean distribution range of the canopy-forming macroalgae *Ericaria crinita* (Duby) Molinari-Novoa & Guiry (= *Cystoseira crinita* Duby), thriving under different thermal regimes. We hypothesise that the populations from the coldest locations are less thermo-tolerant than those from the warmest edge of the distribution.

### *4.2 Material and Methods*

*Ericaria crinita* is a perennial caespitose macroalgae that mainly develops in the upper sublittoral zone, on shallow, well-illuminated and semi-exposed rocky reefs (Ballesteros, 1992; Gómez Garreta, 2000; Rodríguez-Prieto et al., 2013), where it forms marine forests. This species is widespread in the Mediterranean Sea, under a wide range of thermal regimes, although previous evidence shows that it is vulnerable to warming (Verdura et al., 2021).

In total, eight Mediterranean populations of *E. crinita*, separated by hundreds of kilometres were selected: Crete, Malta and Formentera represent areas in the warmer range of distribution; Menorca, and Sardinia represent mild thermal regimes; and Catalonia, Istria and French Riviera represent populations inhabiting the coldest range of the Mediterranean distribution.

Twenty individuals were collected at each locality between June and July 2018, cleaned from macro-epiphytes and/or organic matter and kept in plastic bags in cold and dark conditions for transport to the laboratory facilities at the Centre for Advanced Studies of Blanes (CEAB-CSIC, Spain). Once in the laboratory, individuals were examined to ensure their healthy status, gently washed, and placed in the acclimation tanks at 22°C with circulating natural seawater until the beginning of the experiment.

The experimental design was set to place the individuals at 4 different temperature conditions (26°C, 27°C, 28°C and 29°C). The two lowest temperatures are commonly reached at present during summer periods, while the highest temperatures were chosen to represent the extreme average conditions that the Mediterranean Sea might experience in the coming decades, especially in the warmer areas. An average increase in the Mediterranean SST of 3°C, and temperature anomalies (SST99Q) of 4°C are projected by 2100 under the RCP 8.5 scenario (Darmaraki et al., 2019). Each temperature treatment consisted of 3 independent sets of eight 12-L aquariums each (4 temperatures x 3 sets (replicates) x 8 aquariums) and each set was connected to a buffer tank. Temperature conditions were achieved by heating the seawater in the buffer tank by means of water temperature controllers (Teco TK 500). One individual of each population (8 populations) was randomly placed in an individual aquarium of each set. Initially, temperature was raised by 1°C per day from 22°C until the target temperature conditions were reached. That was the starting point of the experiment, which lasted 80 days. Photoperiod coincided with the natural light conditions.

To test the effects of thermal stress on individual performance, we assessed the variation in biomass through the experiment. Every specimen was weighted at day 0, 21, 38, 60 and 80. Prior to weighting, specimens were blotted dry using filter paper to standardise wet weight measurements and minimise weight variation due to seawater. Biomass variation at each sampled time (BVt), considered as a percentage of biomass lost, was calculated with the following formula:

$$BVt = ((Wt - Wb)/Wb) \times 100$$

where Wt is the weight of the specimen at the sampling time “t” and Wb is the weight of the specimen at the beginning of the experiment (time 0).

### *4.3 Results*

The different populations of *E. crinita* had a differential response to thermal stress in terms of biomass loss (%). As expected, populations from the colder regions were more impacted by the high temperatures than populations coming from warmer regions (Figure 21). Populations from the cold and core edges of distribution (Menorca, French Riviera, Istria and Catalonia) showed considerable higher biomass losses at 28 and 29°C (> 50% in Menorca and French Riviera and >75% in Istria and Catalonia; Figure 21). On the other side, populations from the warmer areas (Crete, Malta, Formentera and Sardinia) never exceeded 50% of biomass loss at any temperature condition (Figure 21).

The intraspecific differences were particularly evident at the higher temperatures. After 80 days at 29°C, individuals from populations from colder areas lost significantly more biomass than those from warmer populations, with Istria and Catalonia losing more than 75% of biomass, while Crete or Malta did not lose more than 35% of their biomass (Figure 21 and Figure 22). In contrast, at 26°C none of the populations lost more than 35% (Figure 21 and Figure 22).

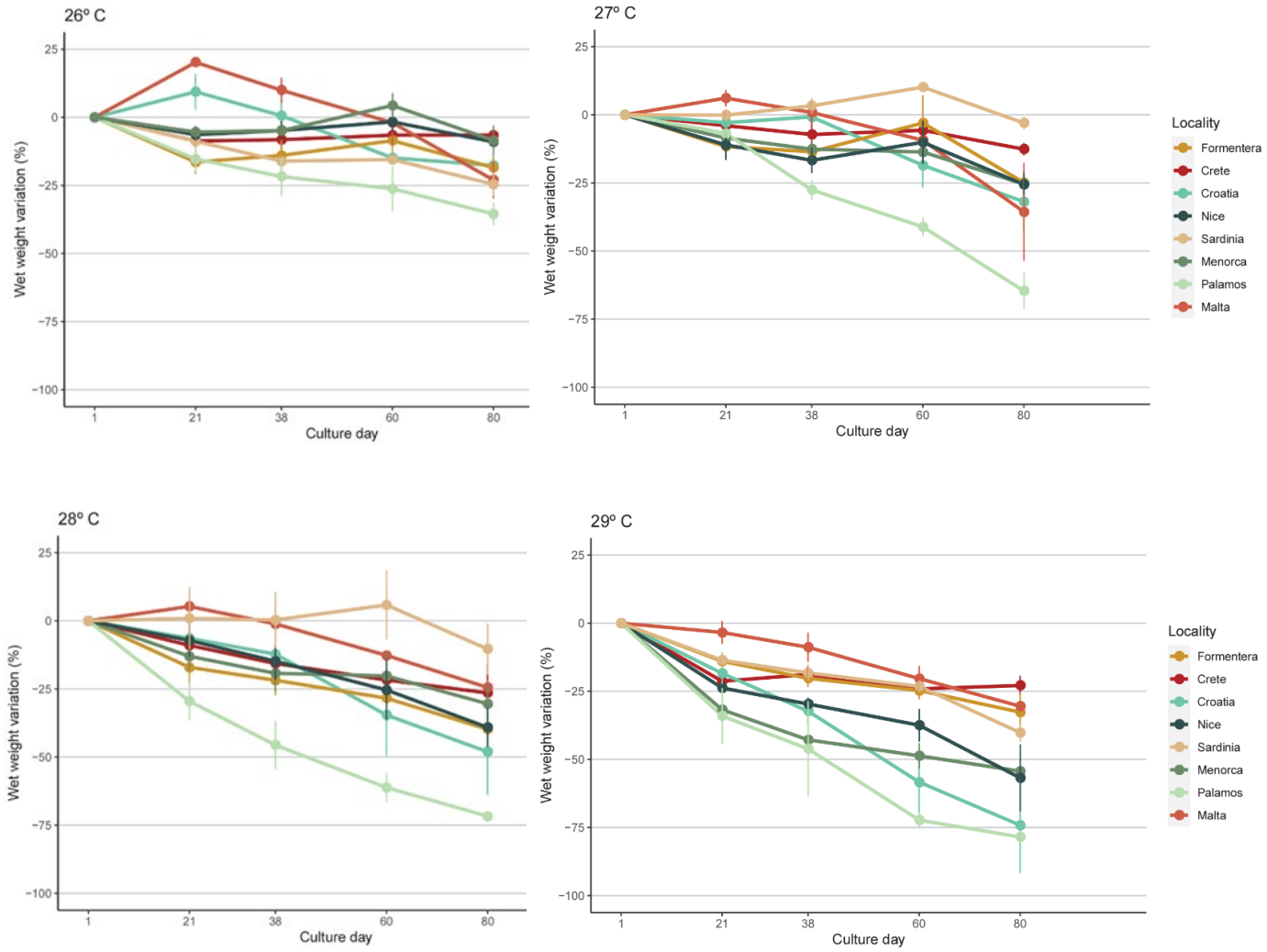


*Figure 20. Wet weight variation (mean ± SE) versus time (days) of Ericaria crinita individuals of the eight studied populations over the 80 days of exposure grouped by the different thermal experiment conditions.*

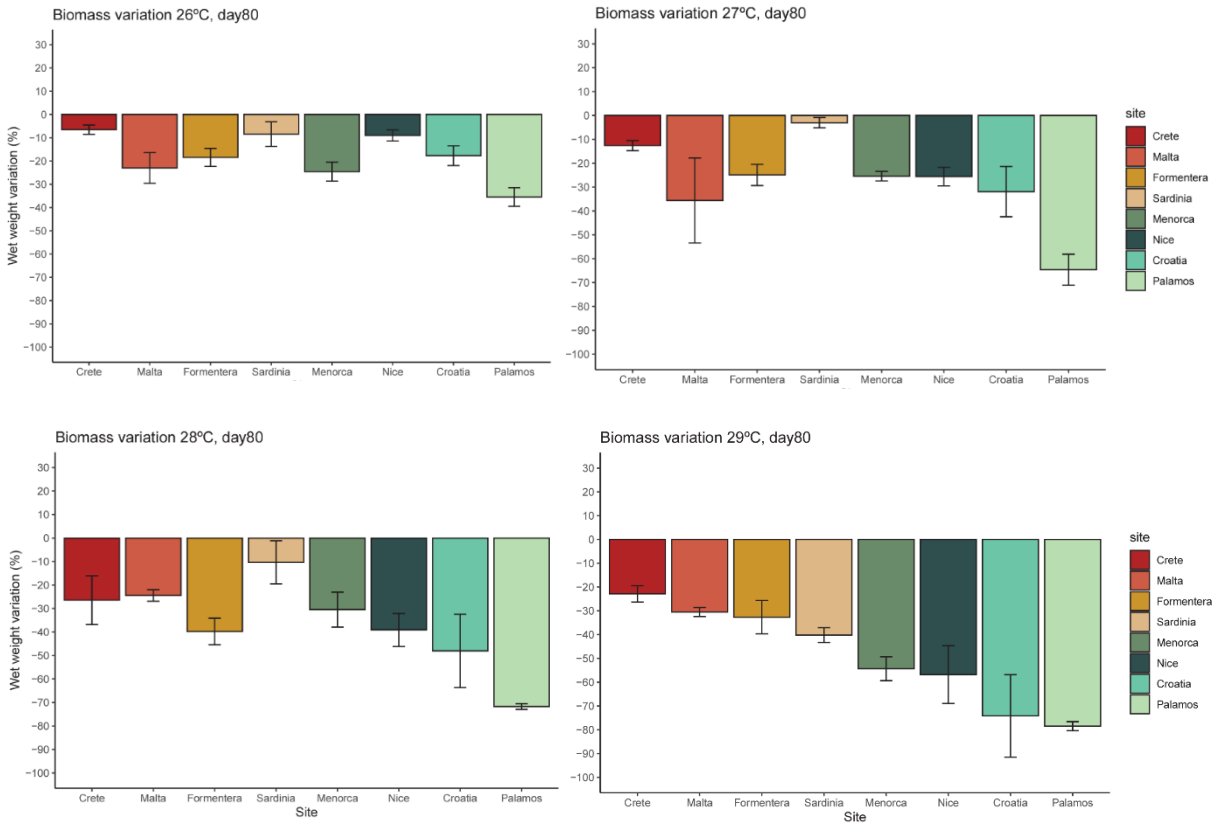


*Figure 21. Wet weight loss (mean ± SE) at the end of the experiment on Ericaria crinita. The colour gradient on the x-axis is a graphic support to arrange the populations in relation to their thermal regime of origin (from warm to cold thermal regimes).*

### *4.4 Conclusions*

The exposure to long-term chronic warm temperature conditions affected the fitness and survival of *E. crinita*, with sustained temperatures above 28°C causing considerable biomass losses (>40%). Populations dwelling in the warm range of the species distribution were more tolerant to the high temperatures than the populations from the cold thermal regimes. Actually, populations such as Catalonia were already highly affected by temperatures of 27°C, whereas populations from warmer areas only showed similar levels of damage when exposed to 29°C. This experiment, therefore, demonstrated local thermal adjustments, in accordance with the marked differences in thermal conditions that are found within *E. crinita* distribution range. It can be expected that future temperature conditions in the Mediterranean Sea, where mean summer temperatures can reach up to 31 °C, might have a great impact on shallow marine forests and strongly compromise the viability of many canopy-forming species.

The mechanisms involved in the intraspecific variability of these species remain unknown but might be related to local adaptation processes and/or physiological plasticity through acclimatization. The underlying nature of such variability requires further methodological approaches such as genetic studies assessing the connectivity between populations, transcriptomic assessments or reciprocal transplant experiments.

Understanding how different populations respond to stressful conditions can give us essential information for conservation prioritization. On the one hand, those populations dwelling in the cold range of the species distribution might be the main candidates for future restoration interventions. On the other hand, populations from the warm range could serve as donors to restore the vulnerable populations and to help preserve their integrity and resilience to future thermal regimes.

# Chapter 5 – Ocean acidification impairs seagrass performance under thermal stress in shallow and deep water

SL28 Contributors: Fabio Bulleri, Chiara Ravaglioli

## *5.1 Introduction*

Ocean acidification (OA), resulting from rising anthropogenic $CO_2$ emissions, is projected to affect all marine areas from deep waters to shallow coastal habitats (Linares et al., 2015; Nagelkerken & Connell, 2015; Luo et al., 2016; Sunday et al., 2017). Although the effects of climate change on marine ecosystems have been extensively investigated over the past few decades, the relative impact of OA on marine life is still debated (Doney et al., 2009; Kroeker et al., 2013; Genin et al., 2020; Cornwall et al., 2021). The response of marine organisms to OA varies broadly, mostly due to differences in the investigated physiological traits and levels of biological organization, hindering predictions of the future performance of marine organisms in combination with other environmental factors (Kroeker et al., 2010, 2017; Gao et al., 2012; Koch et al., 2013; Calosi et al., 2017; Sunday et al., 2017; Cornwall et al., 2020).

Seagrasses are commonly considered carbon-limited under current levels of dissolved $CO_2$ and an increase of dissolved inorganic carbon (DIC) due to OA could enhance their photosynthetic efficiency, growth rate and biomass (Koch et al., 2013; Borum et al., 2016; Zimmerman, 2021). However, these effects have been shown to vary among seagrass species, depending on their carbon concentration mechanisms and growth strategies (Campbell & Fourqurean, 2013; Ow et al., 2015; Cox et al., 2016; Maberly et al., 2022), as well as on local environmental settings, such as temperature, light and nutrients availability (Palacios & R, 2007; Alexandre et al., 2012; Martínez-Crego et al., 2014; Cox et al., 2016; Ravaglioli et al., 2017; Zimmerman et al., 2017; Zayas-Santiago et al., 2020).

To date, previous studies on the effect of OA on seagrasses have been conducted in shallow habitats, neglecting the wide bathymetric distribution of seagrass meadows (Duarte, 1991). This is at odds with the fact that light availability is also an important driver of plant photosynthesis and is depth dependent (Hepburn et al., 2011; Hu et al., 2012; Zimmerman, 2021). Thus, seagrass responses to OA may also vary with light availability (Ow et al., 2016; Schneider et al., 2018; Collier et al., 2018). Previous studies, testing for the effects of OA and light intensity on shallow plants, found positive effects

of elevated $CO_2$ on plant photosynthesis at sub-saturating irradiance, suggesting that low light intensity may increase plant reliance on $CO_2$ uptake due to the high energetic requirements of $HCO^{3-}$ uptake, accumulation and conversion to $CO_2$ (Ow et al., 2016; Schneider et al., 2018). However, plants from contrasting depths exhibit a wide range of variations, from genetic differentiation to changes in physiological and morphological traits, that can be related to local light conditions (Ralph et al., 2006; Sharon et al., 2011; Olivé et al., 2013; Dattolo et al., 2014, 2017; Procaccini et al., 2017). This might have led to an adaptive differentiation between shallow and deep plants of key metabolic processes, including carbon metabolism and photo-acclimation strategies, to maintain a positive carbon balance under different light environments (Dattolo et al., 2014; Procaccini et al., 2017). Nonetheless, how the effects of OA vary between shallow and deep plants remains unexplored.

Plants can react to OA by activating a series of early cellular responses, including expression of antioxidant and macromolecule damage sensors, and genes coding for proteins that help to adjust cellular physiology and metabolism to avoid cell damage or death (Lauritano et al., 2015; Ruocco et al., 2017; Piro et al., 2020). Such changes at the cellular level could affect resource allocation among biological processes due to the increased energy demand for repair and/or defense processes( Ruocco et al., 2017; Scartazza et al., 2017), potentially leading to shifts in plant performance under suboptimal environmental conditions. For example, temperature stress has been recently shown to outweigh the benefits (if any) of elevated $CO_2$ on different seagrass species, leading to a reduction in plant photosynthesis, growth and biomass (Repolho et al., 2017; Collier et al., 2018). Indeed, warming seawater temperatures beyond Topt has been shown to cause plant metabolic impairment, due to increased respiration and loss of fixed carbon, oxidative stress and protein degradation (Koch et al., 2013; Collier et al., 2017; Nguyen et al., 2021), potentially leading to the allocation of additional energy to physiological stress response pathways (Nguyen et al., 2021). However, it is unknown how underlying shifts in plant metabolism may drive responses at higher levels of organization and influence whole-plant tolerance to multiple stressors. Within this context, studies encompassing different levels of biological organization, from molecular to physiological and morphological levels, and considering variability in irradiance and seawater temperature are necessary to predict seagrass responses in a future climate.

As part of the work in SL28, we performed a mesocosm experiment to investigate how the response of the seagrass (*Posidonia oceanica)* to OA varied according to different light regimes that characterized shallow and deep meadows. The experiment was performed during the period of annual plant growth (end of May - early July) and repeated

in two years, 2021 and 2022, which were characterized by average seawater temperature and by a prolonged anomalous warm water event, respectively (see Materials and Methods section for further details of the experimental conditions). These varying thermal conditions provided a unique opportunity to assess how a marine heatwave can influence the effects of OA and light availability on *P. oceanica* . The response of both shallow and deep plants to OA were investigated at different levels of biological organization, by combining biochemical (oxidative stress levels and total antioxidant capacity) and physiological (photosynthetic efficiency and leaf content of photosynthetic pigments and secondary metabolites) analyses and plant growth. In addition, in the 2022 experiment, we also assessed the expression of photosynthesis- and stress-related genes (CAB151, CAT, HSP90, OZ_SP) in order to deepen our understanding of the mechanisms underpinning plant response to combined OA and thermal stress.

The effects of OA on *P. oceanica* were expected to vary with light availability and seawater temperature. Specifically, we hypotheised that low light conditions would increase seagrass reliance on $CO_2$ due to the higher energetic cost of using $HCO^{3-}$ as an alternative carbon substrate for photosynthesis (Hu et al., 2012; Koch et al., 2013; Ow et al., 2016). Thus, at seawater temperatures unlikely to cause thermal stress, we further hypothesized that enhanced $CO_2$ could provide the greatest benefit to deep plants, by enhancing their productivity and growth. Alternatively, OA might have limited effects on deep compared to shallow plants, if enhanced $CO_2$ availability would exceed the energetic capacity for its assimilation under low light availability (Zimmerman, 2021). On the other hand, we expected that thermal stress, by increasing respiratory loss of carbon and impairing plant energetic balances (Koch et al., 2013; Marín-Guirao et al., 2016, 2017; Nguyen et al., 2021), could enhance the allocation of additional energy to defense and/or repair processes (e.g., antioxidant capacity, protein turnover, carbon reserve translocation) expected under OA (Lauritano et al., 2015; Ruocco et al., 2017), thereby resulting in reduced plant productivity and growth. This impact could be predicted as more severe on plants from the deep-water meadow, since they evolved in a relatively colder and darker environment and, thus, might be more negatively affected by extreme heat events (Marín-Guirao et al., 2016, 2017).

### *5.2 Material and Methods*

Seagrass collection and experimental treatments

The experiment was run twice at the annual peak of plant growth, between the end of May and the beginning of July, 2021 and 2022. Satellite-derived SST in the study area,

the coast off Livorno (NW Mediterranean, 43° 28' 45.005'' N, 10° 17' 30.001'' E), indicated the occurrence of a prolonged warm water event during May-July 2022 (Figure 23). The summer of 2022 was the hottest on record for Europe (https://climate.copernicus.eu/copernicus-2022-was-year-climate-extremes-record-high-temperatures-and-rising-concentrations). The mean (±SE) seawater temperature during the study period (end of May – July) was 23.4 ± 0.28 °C and 25.7 ± 0.25 °C for the 2021 and 2022, respectively. Fragments of *Posidonia oceanica* rhizomes bearing several vertical shoots (5 – 20), were collected by divers from well-preserved meadows, located off the coast of Livorno, on May 28th 2021 and June 10th 2022. On both sampling dates, plant fragments were collected at two different depths (~ 5 m and ~ 20 m). Plant material was kept in dark coolers filled with ambient seawater and rapidly transported to the mesocosm facility located at the Aquarium of Livorno.

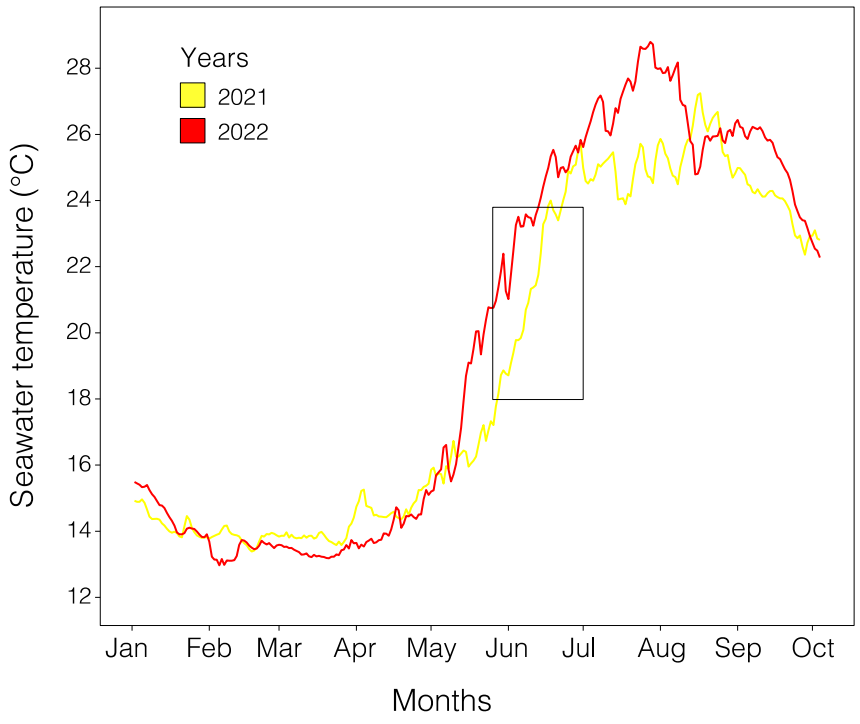


*Figure 22. Daily satellite-derived sea surface temperature at the study site, during January – October 2021 and 2022. Yellow and red lines indicate the satellite-derived sea surface temperature for 2021 and 2022, respectively. The rectangle shows the period of the experiments.*

Plant fragments of similar size and vertical shoot number were carefully selected and individually attached to the bottom of eight plastic cages filled with small cobbles (in 2021, 4 and 3 fragments for each cage, bearing 7 – 18 and 10 – 20 vertical shoots for shallow and deep depth conditions, respectively; in 2022, 5 fragments for each cage, bearing 5 – 14 vertical shoots for both depths). All the response variables were assessed

on intermediate vertical shoots, while shoot-apical meristems were not selected in order to avoid intra-clonal differences in plant responses (Ruocco et al., 2021). Two cages were then randomly placed in each of the four independent glass aquaria (500 L) and filled with fresh seawater, which was filtered and sterilized with UV. Each aquarium was then randomly assigned to each of the four combinations of pH (ambient vs. low pH) and depth (shallow vs. deep). Each aquarium was equipped with three (two Silvermoon Reef Blu 895 and one Silvermoon Marine 895) and two (one Silvermoon Reef Blu 895 and one Silvermoon Marine 895) LED lamps for shallow and deep depths, respectively, which allow the simulation of light diel fluctuation and light intensity. Irradiance levels in experimental tanks were adjusted according to the origin of the plants: ~300 µmol photons $m^{-2}$ $s^{-1}$ above the canopy for shallow plants and ~100 µmol photons $m^{-2}$ $s^{-1}$ for deep plants, both with a light regime of 14:10 h (light:dark cycle). Seawater temperature was independently controlled in each tank by a chiller (Teco TK 500) and monitored using HOBO data loggers along the course of the experiments. Seawater was maintained at a constant temperature of 19.2 ± 0.1 °C and 22.7± 0.1 °C for the first and second years, respectively, according to natural field values at the moment of plant sampling. *P. oceanica* plants in all aquaria were allowed to acclimatize to laboratory conditions for approximately ten days during both experiments (2021 and 2022). Subsequently, pH was independently decreased in the tanks assigned to low pH treatment by bubbling the seawater in sumps with $CO_2$ gas. The pH level in the tanks was monitored with pH sensors as a proxy to control for $CO_2$ input. The sensors provided feedback to a control system that regulated the pH levels in each experimental tank by bubbling $CO_2$ gas into the sumps as required. The two pH treatments were established to compare present-day values with those expected by the end of the century under the scenario RCP 8.5, in which emissions are highest and without specific climate mitigation strategies (Riahi et al., 2011). Plants were maintained under these experimental conditions for three weeks during both years. In 2021, pHNBS was monitored several times a day throughout the experiment by using a portable pH meter (Hach HQ2100). The average values (± SE) at the shallow depth tanks were 8.270 ± 0.003 and 7.798 ± 0.004 for ambient and low pH treatments, respectively. In the deep-water treatment tanks, the pH values were 8.196 ± 0.003 and 7.698 ± 0.004 for ambient and low pH, respectively (Figure 24). In 2022, pHNBS was continuously monitored using HOBO data loggers along the course of the experiment. The mean (± SE) values at the shallow depth were 8.359 ± 0.0003 and 7.781 ± 0.0001 for ambient and low pH treatments, respectively, while those at the deep depth were 8.240 ± 0.0002 and 7.643 ± 0.0002 for ambient and low pH, respectively (Figure 25). For both years, salinity was measured weekly using a conductivity meter and total alkalinity samples were collected weekly from

each aquarium and measured using an automated potentiometric titration with a Methrom 848 Titrino plus system and applying the Gran method. Samples were filtered (Sartorius GFF 0.45 µm) and weighed (22.0000 ± 0.0100 g) prior to titration. The TA values were calculated in the pH range 3.3-3.8 according to the equation developed by Sass and Ben-Yaakov (1977). The HCl titrant (~0.05 mol/L) was calibrated before each session with a seawater Certified Reference Materials from A. Dickson's laboratory (Dickson et al., 2003). Samples were measured in triplicates (internal) and the average precision was better than ±2 µmol·kg-1.

Carbonate system variables were then calculated from measured pH, total alkalinity, temperature and salinity values using the seacarb R package (Gattuso et al., 2015). Unfortunately, for the second year, total alkalinity samples were lost during laboratory procedures and, thus, carbonate system variables were available only for the first year (Table 5).

*Table 5: Carbonate chemistry variables (mean ± SE) measured in each tank exposed to different experimental conditions (Shall = shallow depth, Deep = deep depth, ApH = ambient pH, LpH = low pH), throughout the first year experiment (2021). AT: total alkalinity; pH; Temp: temperature; Sal: salinity; $pCO_2$: the partial pressure of $CO_2$ in seawater; Ωcalc: the saturation state of seawater for calcite; Ωarag: the saturation state of seawater for aragonite; $HCO^{3-}$: the bicarbonate ion concentration; $CO_3^{2-}$: the carbonate ion concentration*

| **Nominal treatment** | **$A_T$ (µmol $kg^{-1}$)** | **pH** | **Temp (°C)** | **Sal (PSU)** | **$pCO_2$ (µatm)** |
|---|---|---|---|---|---|
| Shall, ApH | 2676± 7 | 8.30 ± 0.01 | 19.33 ± 0.09 | 36.7 ± 0.1 | 214 ± 5 |
| Shall, LpH | 2742 ± 5 | 7.87± 0.01 | 19.48 ± 0.10 | 36.9 ± 0.1 | 729 ± 16 |
| Deep, ApH | 2626 ± 6 | 8.22 ± 0.01 | 19.20 ± 0.12 | 36.7 ± 0.1 | 270 ± 10 |
| Deep, LpH | 2807 ± 7 | 7.76 ± 0.03 | 19.32 ± 0.12 | 36.9 ± 0.2 | 1027 ± 68 |
| **Nominal treatment** | **$\Omega_{calc}$** | **$\Omega_{arag}$** | **$HCO_3^-$ (µmol $kg^{-1}$)** | **$CO_3^{2-}$ (µmol $kg^{-1}$)** | |
| Shall, ApH | 8.16 ± 0.10 | 5.31 ± 0.06 | 1840 ± 10 | 346 ± 4 | |
| Shall, LpH | 3.91 ± 0.06 | 2.55 ± 0.04 | 2343 ± 8 | 166 ± 3 | |
| Deep, ApH | 6.96 ± 0.15 | 4.52 ± 0.10 | 1911 ± 18 | 295 ± 6 | |
| Deep, LpH | 3.18 ± 0.16 | 2.07 ± 0.10 | 2484 ± 12 | 135 ± 6 | |

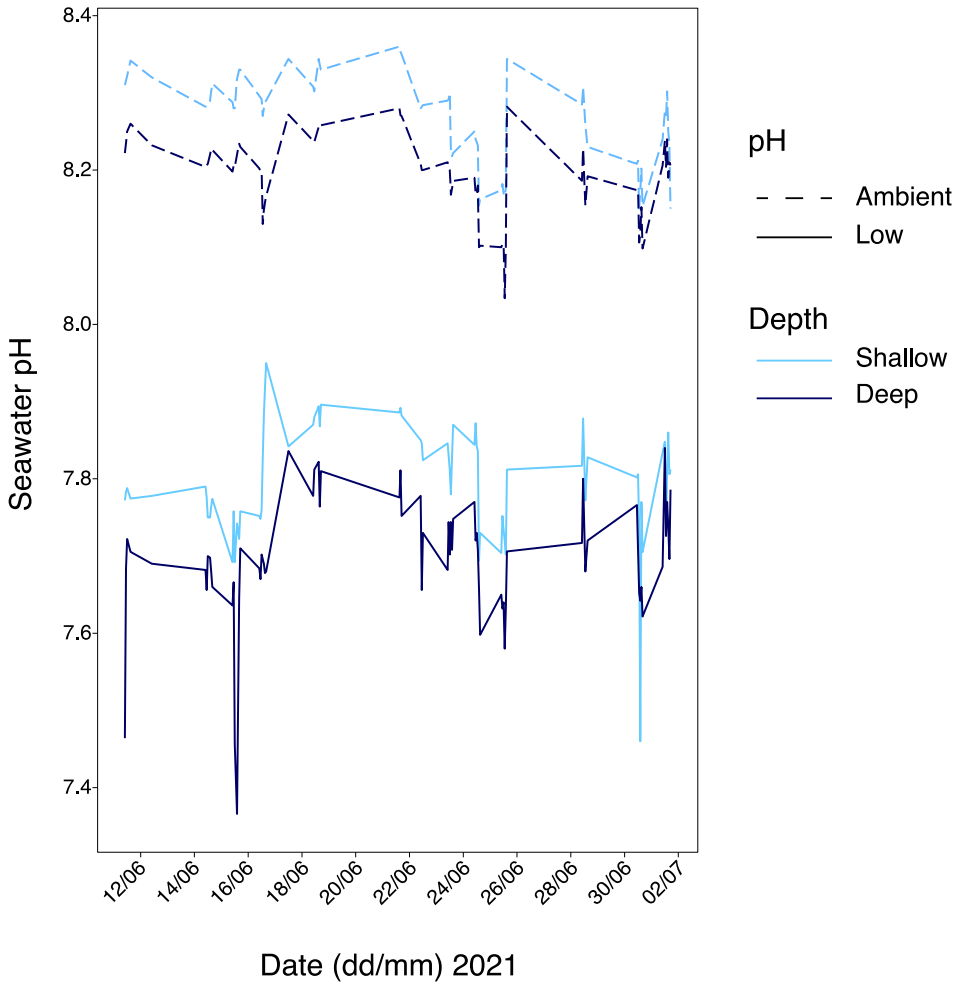


*Figure 23. Time series of daily seawater pH values for different combinations of pH (ambient and low) and depth (shallow and deep), measured along the course of the first year (2021).*

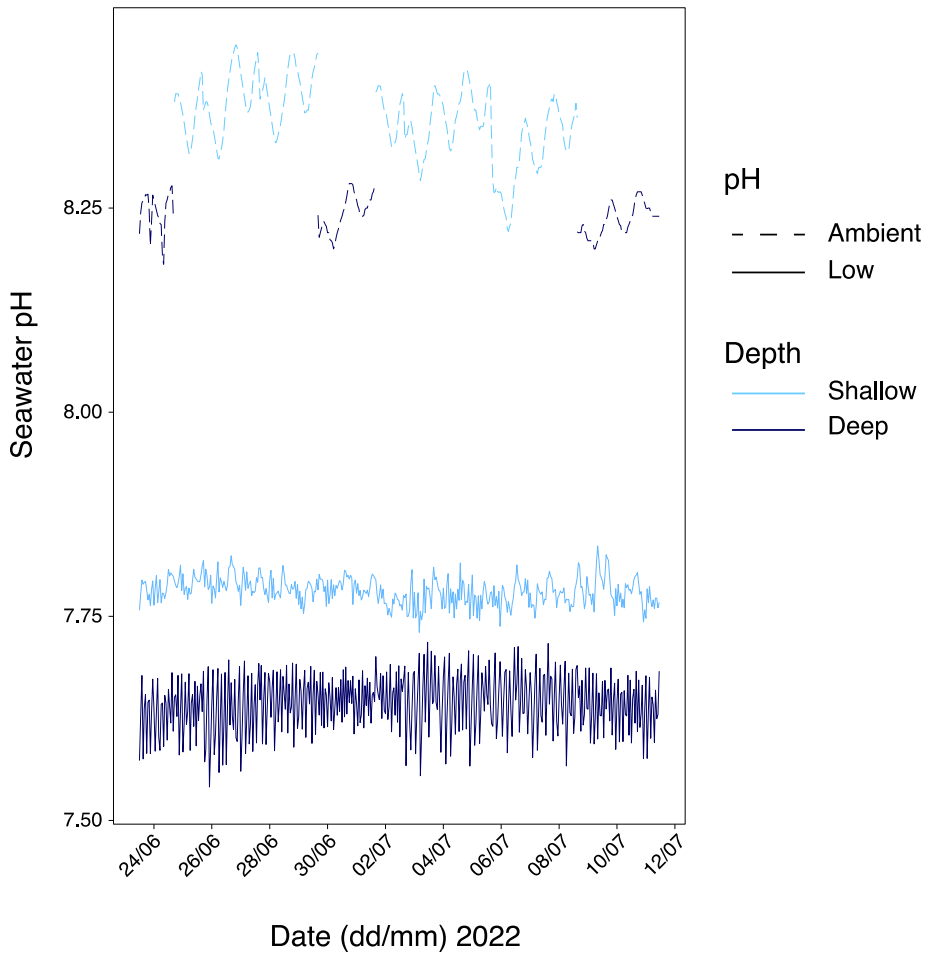


*Figure 24. Time series of hourly seawater pH for different combinations of pH (ambient and low) and depth (shallow and deep), measured along the course of the second year experiment (2022). pH measurements were obtained by using three high-resolution HOBO data loggers, two of which were deployed in the two tanks exposed to low pH treatments (solid lines) throughout the experiment, while the third sensor was alternated between shallow and deep tanks maintained at ambient pH (dotted lines).*

Gene expression analysis

Gene expression was analysed at the end of the second year (early July 2022). For each aquarium, intermediate leaves were sampled on three randomly selected shoots of different rhizomes. Tissue from each leaf was then rapidly cleared of epiphytes with a razor blade, towel-dried and immediately stored in RNAlater solution. Samples were then preserved one night at 4 °C and stored at – 20 °C until RNA extraction. Total RNA from fully developed leaves of *P. oceanica* was extracted with the AurumTM Total RNA Mini Kit (BIO-RAD, Hercules, CA, USA.), following the manufacturer's protocol. A section of about 7 cm-long leaf tissue (corresponding to about 80–100 mg) was ground to a fine powder with a pestle in a mortar containing liquid nitrogen. Samples were then

homogenized through a Mixer Mill MM300 (QIAGEN, Hilden, Germany) and tungsten carbide beads (3 mm) for 3 min at 20.1 Hz. The quality and purity of the total RNA was checked using NanoDrop (ND-1000 UV-Vis spectrophotometer; NanoDrop Technologies, Wilmington, DE, USA) and 1% agarose gel electrophoresis. RNA was used when Abs260 nm/Abs280 nm and Abs260 nm/Abs230 nm ratios were >1.8 and 1.8 < x < 2, respectively. The RNA concentration was accurately determined by the QubitTM RNA BR Assay kit (Thermo Fisher Scientific, Waltham, MA USA) using the Qubit 2.0 Fluorometer (Thermo Fisher Scientific).

Total RNA (500 ng) from each sample was retro-transcribed into cDNA with the iScriptTM cDNA synthesis kit (BIO-RAD), according to the manufacturer's protocol. As genes of interest, a Chlorophyll a-b binding protein (CAB151, Mazzuca et al., 2013) and three transcripts related to stress responses and detoxification processes (HSP90, Oz_SP, CAT), already tested in *P. oceanica* in natural acidification conditions (Lauritano et al., 2015), were selected. To normalise target gene expression, we used as reference genes (RG) the 60s ribosomal protein L23a (L23) and the Ribosomal RNA 18S (18S) as reference genes (RG), which have previously displayed a stable expression in *P. oceanica* under a range of different conditions (Serra et al., 2012; Lauritano et al., 2015).

RT-qPCR reactions were carried out as outlined in Lauritano et al. (2015). Briefly, each reaction consisted in 5 µl Fast SYBR® Green Master Mix (Applied Biosystems), 1 µl cDNA (1:5 diluted) template, and 4 µl of 0.7 pmol µl-1 primers. The thermal profile of the reactions was as follows: 95 °C for 20 s, 40 times 95 °C for 1 s, and 60 °C for 20 s in the Viia7 Real Time PCR System (Applied Biosystem). After normalizing by each primer efficiency, the relative gene expression values were calculated as the negative differences in cycles to cross the threshold value (− ΔCT) between the reference genes and the respective target genes (− ΔCT = CTreference − CTtarget). Fold expression changes were calculated as: Fold expression change = ±2(|(– ΔCT treatment) – (– ΔCTcontrol)|).

All RT-qPCR reactions were conducted in triplicate, and each assay included three no-template negative controls.

2.3. Lipid peroxidation and total antioxidant capacity determination

At the end of both experiments, six shoots of different rhizomes were randomly sampled in each aquarium for analyses of lipid peroxidation (LPO) and total antioxidant capacity (TAC). For the first year, both LPO and TAC were assessed on 5 replicate shoots at deep-water /low pH treatments and, for the second year, LPO was assessed on 3 shoots from the shallow-water/ambient pH treatments, due to the loss of 1 and 3

samples, respectively, during laboratory procedures. Once in the laboratory, sample leaves were immediately frozen at − 80 °C until biochemical analyses. All samples were carefully checked and specimens colonized by epiphytes were discarded. Malondialdehyde (MDA), a by-product of LPO, extraction and quantification were performed following Costa et al. (2015) methodology. Briefly, ~ 300 mg of frozen leaf tissue was powdered and suspended in 5.0 mL of ethanol (80%). The extract was homogenized and then centrifuged at 3000 × g for 10 min at 4 °C. Supernatant (1.0 mL) was added to 1.0 mL of 20% trichloroacetic acid (TCA) with 0.65% thiobarbituric acid (TBA) and 0.01% butylated hydroxytoluene (BHT) solution. Two blanks were used to verify the correct functioning of the test. All samples were first heated (90 °C, 25min), then cooled for 15 min and again centrifuged (3000 × g, 4 °C, 10 min). Absorbance was measured at 440, 532 and 600 nm (BioTek Synergy HT micro-plate reader) and MDA equivalents were expressed in nmol MDA/g FW (Fresh Weight). TAC was measured using ferric reducing antioxidant power (FRAP) assay, following the method described by Benzie and Strain (1996) and adapted by Capó et al. (2020). Powdered samples were homogenized in five volumes (w/v) of 50 mM Tris–HCl buffer, 1 mM EDTA, pH 7.5 using a small sample dispersing system (ULTRA-TURRAX®Disperser, IKA). Homogenates were centrifuged at 9000 × g, 10 min, 4 °C. Then, 20 µL of homogenates were incubated for 30 min with a solution of ferric chloride (2 mM) and 2,4,6-Tris (2-pyridyl)-s-triazine (TPTZ) in acetate buffer pH 3.6. After incubation absorbance was measured at 593 nm and results were expressed as µmol FRAP/L.

Plant photosynthetic efficiency

In vivo chlorophyll fluorescence measurements were performed on *P. oceanica* leaves with a diving-PAM fluorometer (Walz, Germany). Effective quantum yield, an estimate of the photosynthetic efficiency of photosystem II (PSII) in light-adapted plants, was measured between 11:00 and 13:00 at the end of both experiments, by the saturating-light method on leaves. For each aquarium, measurements were performed on the second youngest leaf of 8 and 6 shoots for shallow and deep-water treatments, respectively, during the 2021 experiment and on 10 different shoots for both depths during the 2022 experiment. The effective quantum yield was expressed as Fv/Fm′ = Fm′ – F/Fm′, where F is the fluorescence yield of a leaf measured before the application of a saturating light pulse; Fm′ is the maximum fluorescence yield induced by a saturating light pulse (Genty et al., 1989).

Photosynthetic pigments and secondary metabolites determination

At the end of both experiments, intermediate leaves of 6 shoots were randomly collected from each aquarium to quantify the content of photosynthetic pigments, phenols, and flavonoids. In the laboratory, leaves were washed, cleared of epiphytes using a razor blade and stored at - 80 °C until analysis. The frozen leaves were lyophilized and then ground for 15 s in a steel balls mill (Retsch GmbH & Co. KG, Haan, Germany) cooled with dry ice. Leaf powder was stored at - 30 °C until analyzed.

The photosynthetic pigments were measured after their extraction from the powdered leaves. Briefly, 2 mg of flour for each sample were extracted with 2 ml of acetone: Tris-HCl 0.5 M, pH 7.8 (80:20, v/v) on a magnetic stirrer for 30 min in a cold room (5 °C). The extract was centrifuged at 13,500 g and 5 °C for 10 min. Supernatant absorbances were read against a blank made with the extraction solvent at 430, 537, 647, and 663 nm, with a double beam Lambda 25 (Perkin-Elmer, Milan, Italy) spectrophotometer. The absorbance readings were converted into µmoles/ml following Sims and Gamon (2002) and finally expressed as µmoles/g DW. Each sample extraction was repeated five times.

Total phenols were extracted from the leaf powder following Bolser et al. (1998). An aliquot of 5 mg of leaf powder was extracted with 1 mL of cold 50% methanol in water, on a magnetic stirrer for about 16 hrs at 5 °C. The extracted total phenols were then centrifuged for 15 min at 13,500 g and 5 °C. Each extraction was performed in three replicates.

Polyphenols were assayed based on the Folin-Ciocalteu method (Singleton & Rossi, 1965). Briefly, 100 µl of extract were brought to 625 µl with distilled water and added with 125 µl of Folin-Ciocalteu reagent (Sigma-Aldrich, Milan, Italy). After vortexing, the sample was kept in the dark for 6 min and then, 1250 µl of 7% Na2CO3 and 1000 µl of distilled water were added. The sample was vortexed and kept in the dark for 90 min. The colored reaction product was read at 760 nm, against a blank reaction mixture, where water replaced the phenolic extract. The amount of total phenols was estimated from a calibration curve made with gallic acid and the results were expressed as mmoles of gallic acid equivalents per gram of DW.

The flavonoid assay was based on the colorimetric method described by Dewanto et al. (2002). Briefly, 200 µl of extract were brought to 1500 µl with distilled water and added with 75 µl of a 5% NaNO2 solution. The mixture was vortexed and kept in the dark for 6 min; afterwards, 150 µl of a 10% AlCl3·6H2O solution were added. After vortexing and standing for another 5 min in the dark, 500 µl of 1 M NaOH and 275 µl of distilled water were added. The solution was vortexed again and its absorbance was measured immediately at 510 nm against a blank made by replacing the sample with an equal

volume of distilled water. The amount of flavonoids was estimated from a calibration curve made with catechin and the results were expressed as mmoles of catechin equivalents per gram of DW. Each extract assay had three replicates for a total of nine replicates per sample.

Plant growth

Leaf growth was measured using a modified Zieman's method (Zieman, 1974), for both experiments. After ~ 10 days of acclimation period, shoots of different rhizomes were marked in each aquarium by punching all the leaves together with a needle, just above the ligula of the most external leaf. In the 2021 experiment, plant growth was measured in each aquarium on 8 and 6 replicate shoots for shallow and deep-water treatments, respectively, while, in the 2022 experiment, measurements were performed on 10 replicate shoots for each aquarium. Marked shoots were then collected after 23 and 19 days for the first and second year, respectively. In the laboratory, epiphytes were removed with a razor blade and leaf tissue of each shoot was divided into new material (i.e., leaf tissue below the hole) and old material (i.e., leaf tissue above the hole), dried at 60 °C for 24 h and weighed. Leaf growth rate (mg DW shoot-1 day-1) was estimated as the weight of new tissue produced divided by the time elapsed between the two sampling events.

Statistical analyses

The effects of pH, depth and year on biochemical (lipid peroxidation and total antioxidant capacity) and physiological (photosynthetic efficiency and leaf content of photosynthetic pigments and secondary metabolites) plant responses, and leaf growth rate were analyzed using generalized linear mixed models (GLMMs), assuming a gaussian distribution. The factors pH (ambient vs. low), depth (shallow vs. deep) and year (2021 vs. 2022) were included in the fixed part of the model as predictor variables, while tank was included as a random effect to take into account that replicate shoots were grouped within each tank. Expression levels of selected genes of interest (CAB-151, CAT, HPS90 and PZ-SP) were analyzed using GLMMs, including pH and depth as fixed factors, and tank as a random effect. The GLMMs were run using glmmTMB R package. Post-hoc comparisons were performed with R function emmeans for the significant interaction terms. Residuals were checked with Q-Q plots and plots of standardized residuals versus expected values, using DHARMA R package. The same package was used to assess heteroscedasticity and checked for over-dispersion. All statistical analyses were performed in R version 3.6.1.

### *5.3 Results*

Expression levels of the genes of interest

There was a significant interaction between pH and depth on the expression of the stress-related genes, HSP90 and CAT (Table 5). In particular, the heat shock protein gene HSP90 was significantly up-regulated in deep plants exposed to low pH, while there was no change in HSP90 expression between pH treatments in shallow plants (Figure 26). At low pH, the antioxidant CAT was upregulated and downregulated in deep and shallow-water treatments, respectively, compared to those maintained at ambient pH, although post hoc comparisons between pH treatments did not detect significant differences at any depth (Table 5, Figure 26). Finally, although not statistically significant, both deep and shallow plants tended to increase the expression of the stress-related gene OZ_SP at low pH (Table 5, Figure 26).

The expression of the photosynthesis-related gene (CAB-151) did not show significant changes between pH treatments at both depths, although there was a tendency for CAB expression to be down-regulated under low pH (Table 6, Figure 26. Relative expression (ΔCT) of stress- and photosynthetic-related genes in deep depth – low pH, shallow depth – low pH vs. control conditions (deep depth – ambient pH, shallow depth – ambient pH; x-axis) for the second year (mean ± SE). Table 5, Figure 26).

*Table 6: Results of Generalized Linear Mixed Models (GLMMs) used to assess the effects of pH (ambient = ApH, low = LpH) and depth (shallow = Shall, deep = Deep) on CT of target genes at the end of the second experimental run. Coefficients and standard errors for pH and depth are reported for the fixed effects, while estimate of variance (2) and standard deviations (SD) for tank are reported for the random effects. *P < 0.05, **P < 0.01, ***P < 0.001*

| Effect | HSP90 | OZ_SP | CAT | CAB |
|---|---|---|---|---|
| ***Fixed effects*** | ***Estimate (SE)*** | ***Estimate (SE)*** | ***Estimate (SE)*** | ***Estimate (SE)*** |
| Intercept | -3.74 (0.46)*** | -5.13 (0.77)*** | -2.76 (0.75)*** | -5.34 (0.80)*** |
| LpH | 3.07 (0.64)*** | 2.03 (1.09) | 2.18 (1.06)* | -0.53 (1.13) |
| Shall | -0.04 (0.64) | 0.86 (1.09) | -0.83 (1.06) | 0.30 (1.13) |
| LpH x Shall | -3.27 (0.91)*** | -0.83 (1.54) | -3.49 (1.5)* | -0.37 (1.60) |
| ***Random effects*** | $\sigma^2$ ***(SD)*** | $\sigma^2$ ***(SD)*** | $\sigma^2$ ***(SD)*** | $\sigma^2$ ***(SD)*** |
| Tank | 1.1e-10 (1.1e-05) | 5.4e-10 (2.3e-05) | 4.8e-10 (2.18e-05) | 6.5e-10 (2.5e-05) |
| Residual | 6.2e-01 (7.9e-01) | 1.8 (1.3) | 1.7 (1.3) | 1.9 (1.4) |
| | ***Post-hoc contrasts*** | | ***Post-hoc contrasts*** | |
| | HSP90 (pH x depth) | | CAT (pH x depth) | |
| | Shall: ApH = LpH | | Shall: ApH = LpH | |
| | Deep: ApH < LpH** | | Deep: ApH = LpH | |

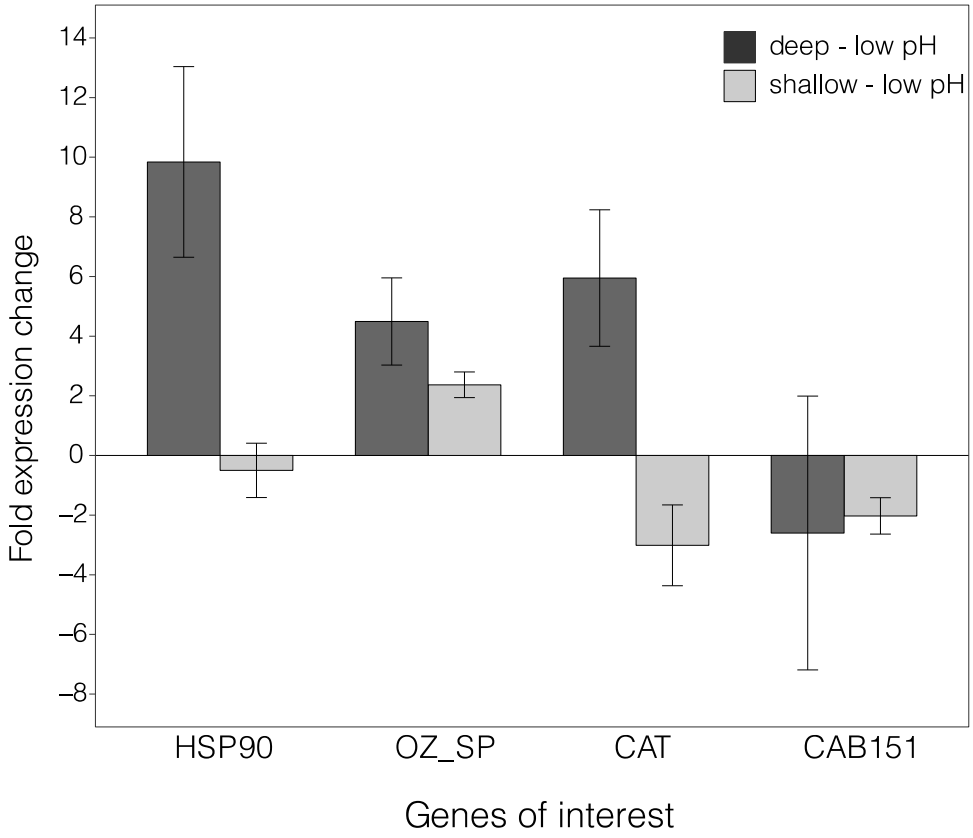


*Figure 25. Relative expression (ΔCT) of stress- and photosynthetic-related genes in deep depth – low pH, shallow depth – low pH vs. control conditions (deep depth – ambient pH, shallow depth – ambient pH; x-axis) for the second year (mean ± SE).*

Biochemical responses of *P. oceanica* to experimental treatments

There was a significant interaction among pH, depth and year on the lipid peroxidation (LPO) of *P. oceanica* (Table 6). In 2021, there were no differences in LPO between pH treatments while, in 2022, LPO was significantly higher under low than ambient pH at both depths and this trend was more pronounced in shallow than in deep-water treatments (Figure 27a).

There was a significant interaction between depth and year on the total antioxidant capacity (TAC) of *P. oceanica*, regardless of pH. In 2021, TAC was higher in shallow than in deep plants while, in 2022, TAC was greater in deep than in shallow plants (Table 6, Figure 27b).

*Table 7: Results of Generalized Linear Mixed Models (GLMMs) used to assess the effects of pH (ambient = ApH, low = LpH), depth (shallow = Shall, deep = Deep) and year (Year1 - 2021, Year2 - 2022) on lipid peroxidation (LPO) and total antioxidant capacity (TAC). Coefficients and standard errors (SE) for pH, depth and year are reported for the fixed effects, while estimate of variance (□2) and standard deviations (SD) for tank are reported for the random effects. *P < 0.05, **P < 0.01, ***P < 0.001. IData sqrt (x+1) and IIData log (x+1) transformed.*

| Effect | Lipid peroxidation[II] | Total antioxidant capacity[I] |
|---|---|---|
| ***Fixed effects*** | ***Estimate (SE)*** | ***Estimate (SE)*** |
| Intercept | 0.39 (0.09)*** | 4.84 (1.67)** |
| LpH | 0.03 (0.13) | 0.22 (2.48) |
| Shall | 0.24 (0.12)* | 9.49 (2.10)** |
| Year2 | 1.06 (0.12)*** | 18.07 (2.36)*** |
| LpH x Shall | -0.10 (0.18) | -2.22 (3.81) |
| Shall x Year2 | -0.71 (0.19)*** | -11.15 (3.74)** |
| LpH x Year2 | 0.26 (0.18) | -0.09 (3.43) |
| LpH x Shall x Year2 | 0.59 (0.26)* | -1.66 (5.07) |
| ***Random effects*** | ***$\sigma^2$ (SD)*** | ***$\sigma^2$ (SD)*** |
| Tank | 1.1e-12 (1.02e-06) | 1.2e-08 (0.0001) |
| Residual | 4.6e-02 (2.14e-01) | 1.7e+01 (4.0955) |
| | ***Post-hoc contrasts*** | ***Post-hoc contrasts*** |
| | (pH x depth x year) | (depth x year) |
| | Year1 (Shall: ApH =LpH) | Year1: Shall > Deep*** |
| | Year1 (Deep: ApH =LpH) | Year2: Shall < Deep* |
| | Year2 (Shall: ApH < LpH)*** | |
| | Year2 (Deep: ApH <LpH)* | |

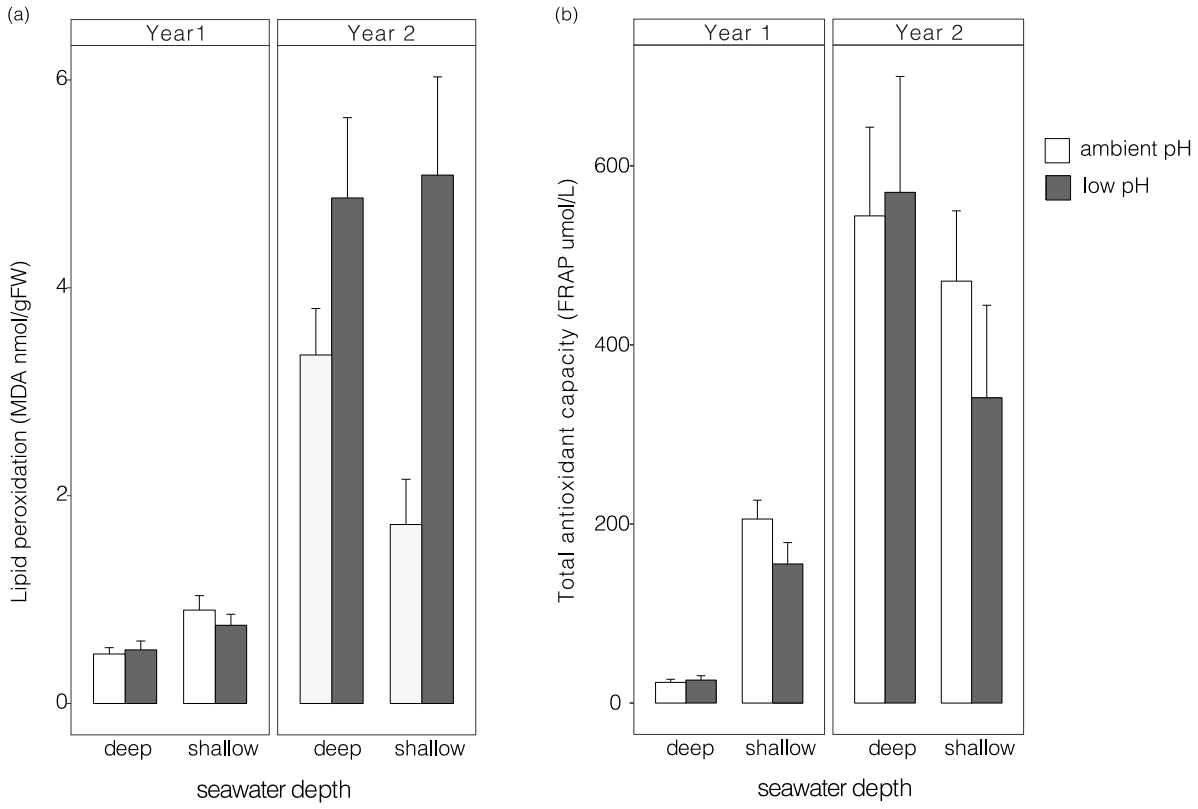


*Figure 26. Mean ± SE levels of (a) lipid peroxidation (MDA, nmol/gFW) and (b) total antioxidant capacity (FRAP, μmol/L) in shallow and deep P. oceanica plants under ambient and low pH conditions, for both years.*

Physiological responses and leaf growth of *P. oceanica* under experimental treatments

There was a significant interaction between pH and year on the photosynthetic efficiency of *P. oceanica,* regardless of depth conditions (Table 7). In 2021, there were no differences in the effective quantum yield between pH levels while, in 2022, low pH significantly decreased the effective quantum yield (Fig. 28a). In addition, in both years, plant photosynthetic efficiency was significantly higher in deep than shallow-water treatments (Table 7, Fig. 28a).

There was a significant interaction between pH and year on leaf content of chlorophyll a, regardless of depth treatment (Table 7). In 2021, there were no differences in the chlorophyll a content between pH treatments, while low pH significantly decreased chlorophyll a concentration in 2022 (Fig. 28b). Although not statistically significant, the content of chlorophyll b and carotenoids tended to be lower at low than at ambient pH in 2022 (Table 7, Fig. 28c, d) and were significantly higher in deep than shallow-water treatments in both years (Table 7, Fig. 28c, d). Although not statistically significant, there was also a tendency for chlorophyll a concentration to be higher in deep-water treatments, in both years (Table 7, Fig. 28b).

*Table 7: : Results of Generalized Linear Mixed Models (GLMMs) used to assess the effects of pH (ambient = ApH, low = LpH), depth (shallow = Shall, deep = Deep) and year (Year1 - 2021, Year2 - 2022) on the effective quantum yield and leaf content of photosynthetic pigments (chlorophyll a, b and carotenoids) and secondary metabolites (flavonoids and phenols). Coefficients and standard errors (SE) for pH, depth and year are reported for the fixed effects, while estimates of variance (σ2) and standard deviation (SD) per tank are reported for the random effects. *P < 0.05, **P < 0.01, ***P < 0.001*

| Effect | Effective quantum yield | Chlorophyll *a* | Chlorophyll *b* |
|---|---|---|---|
| ***Fixed effects*** | ***Estimate (SE)*** | ***Estimate (SE)*** | ***Estimate (SE)*** |
| Intercept | 0.64 (0.04)*** | 4.45 (0.24)*** | 1.97 (0.12)*** |
| LpH | 0.03 (0.06) | 0.24 (0.34) | 0.05 (0.15) |
| Shall | -0.19 (0.06)*** | -0.58 (0.34) | -0.39 (0.15)** |
| Year2 | 0.06 (0.05) | -0.23 (0.34) | -0.10 (0.15) |
| LpH x Shall | -0.01 (0.08) | -0.65 (0.47) | -0.18 (0.21) |
| Shall x Year2 | 0.06 (0.07) | -0.02 (0.49) | 0.16 (0.21) |
| LpH x Year2 | -0.22 (0.07)** | -1.21 (0.49)* | 0.27 (0.21) |
| LpH x Shall x Year2 | 0.07 (0.10) | 0.49 (0.68) | 0.11 (0.29) |
| ***Random effects*** | ***σ² (SD)*** | ***σ² (SD)*** | ***σ² (SD)*** |
| Tank | 1.9e-12 (1.4e-06) | 5.6e-11 (7.5e-06) | 6.7e-13 (8.2e-07) |
| Residual | 1e-02 (1.02e-01) | 3.6e-01 (6e-01) | 6.6e-02 2(.6e-01) |
| | ***Post-hoc contrasts*** (pH x year) | ***Post-hoc contrasts*** (pH x year) | |
| | Year1: ApH = LpH | Year1: ApH = LpH | |
| | Year2: ApH > LpH*** | Year2: ApH > LpH*** | |

| Effect | Carotenoids | Phenols | Flavonoids |
|---|---|---|---|
| ***Fixed effects*** | ***Estimate (SE)*** | ***Estimate (SE)*** | ***Estimate (SE)*** |
| Intercept | 2.81 (0.14)*** | 43.73 (12.94)*** | 21.18 (8.64)* |
| LpH | 0.03 (0.2) | -16.49 (18.31) | -8.55 (12.22) |
| Shall | -0.43 (0.2)* | 156.55 (18.31)*** | 110.3 (12.22)*** |
| Year2 | -0.03 (0.2) | 96.13 (18.31)*** | 74.85 (12.22)*** |
| LpH x Shall | -0.31 (0.28) | 0.5 (25.05) | -10.47 (16.73) |
| Shall x Year2 | 0.04 (0.29) | -228.52 (25.88)*** | -146.34 (17.28)*** |
| LpH x Year2 | -0.28 (0.29) | 4.14 (25.88) | 2.44 (17.28) |
| LpH x Shall x Year2 | 0.42 (0.4) | 7.97 (36.02) | 5.85 (24.05) |
| ***Random effects*** | ***σ² (SD)*** | ***σ² (SD)*** | ***σ² (SD)*** |
| Tank | 9e-12 (3e-06) | 6.9e-16 (8.3e-78) | 3.2e-84 (1.8e-42) |
| Residual | 1.2e-01 (3.5e-01) | 1e+03 (3.17e+01) | 4.5e+02 (2.1e+01) |
| | | ***Post-hoc contrasts*** (pH x year) | ***Post-hoc contrasts*** (pH x year) |
| | | Year1: ApH > LpH*** | Year1: ApH > LpH*** |
| | | Year2: ApH < LpH*** | Year2: ApH < LpH*** |

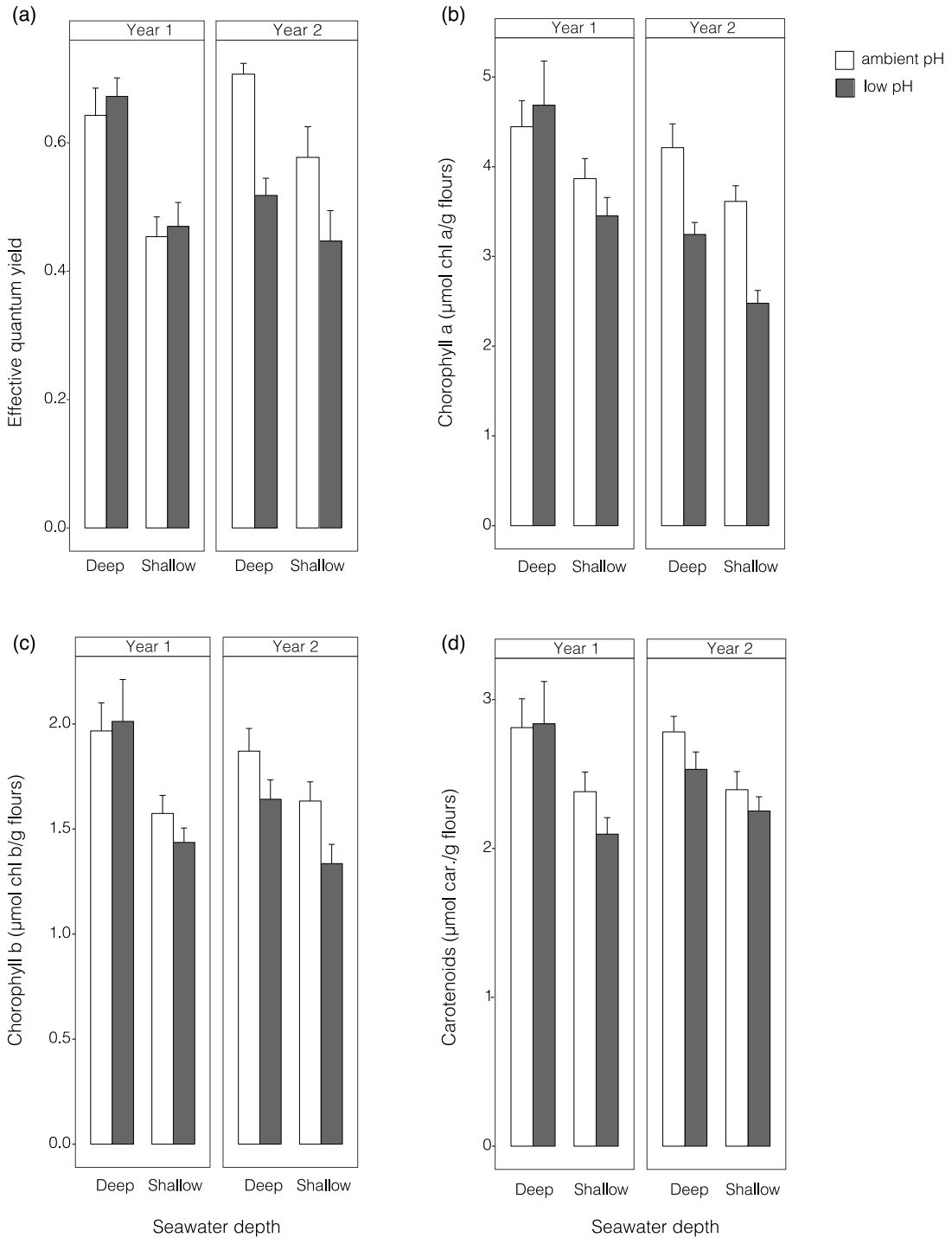


*Figure 27. (a) Photosynthetic efficiency and content (µg g-1) of (b) chlorophyll a, (c) chlorophyll b and (d) carotenoids in leaves of shallow and deep plants under ambient and low pH conditions, for both years. Values are mean ± SE.*

There was a significant interaction between depth and year on flavonoid and phenol contents in *P. oceanica* leaves, regardless of pH levels (Table 7). In 2021, leaf secondary metabolites were significantly lower in deep than in shallow-water treatments while, in year 2022, their concentrations were significantly higher in deep than in shallow-water treatments (Figure 29).

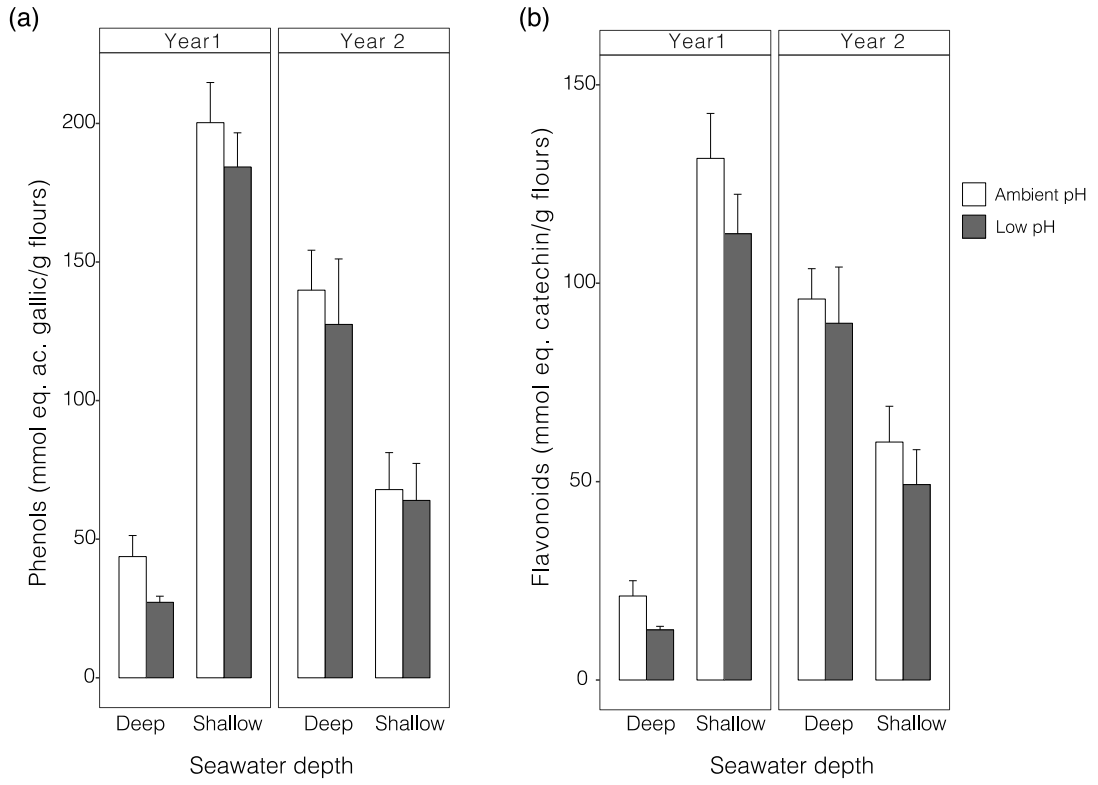


*Figure 28. Mean content of (a) phenols (mmol eq. ac. gallic g-1) and (b) flavonoids (mmol eq. catechin g-1) in leaves of shallow and deep plants under ambient and low pH conditions, for both years.*

Finally, leaf growth rate in 2022 was significantly lower than 2021, regardless of pH and depth treatments (Table 8, Figure 30).

*Table 8: Results of Generalized Linear Mixed Models (GLMMs) used to assess the effects of pH (ambient = ApH, low = LpH), depth (shallow = Shall, deep = Deep) and year (Year1 - 2021, Year2 - 2022) on plant growth rate. Coefficients and standard errors (SE) for pH, depth and year are reported for the fixed effects, while estimates of variance (□2) and standard deviation (SD) per tank are reported for the random effects. *P < 0.05, **P < 0.01, ***P < 0.001.*

| Effect | Growth rate |
|---|---|
| ***Fixed effects*** | ***Estimate (SE)*** |
| Intercept | 4.59 (0.58)*** |
| LpH | 0.45 (0.82) |
| Shall | -0.97 (0.77) |
| Year2 | -1.57 (0.77)* |
| LpH x Shall | 0.71 (1.08) |
| Shall x Year2 | 1.44 (1.04) |
| LpH x Year2 | -0.32 (1.11) |
| LpH x Shall x Year2 | -1.14 (1.48) |
| ***Random effects*** | $\sigma^2$ ***(SD)*** |
| Tank | 7.7e-10 (2.8e-05) |
| Residual | 2 (1.4) |

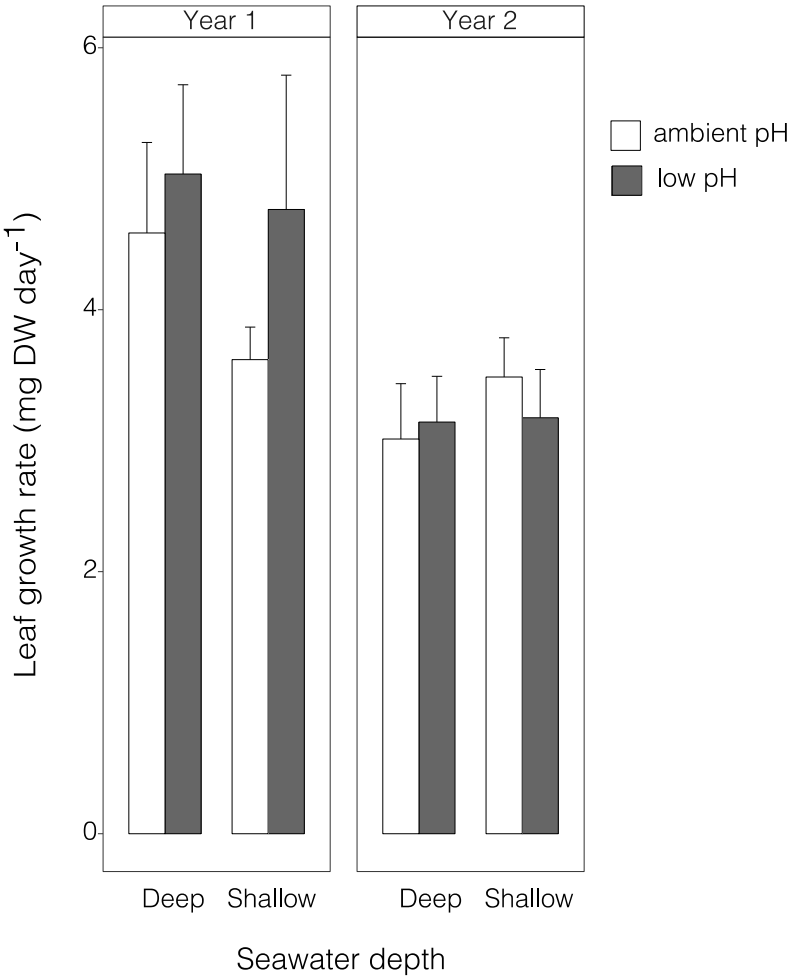


*Figure 29. Leaf growth (mg DW/shoot day, mean ± SE) of shallow and deep plants under ambient and low pH conditions, for both years.*

### *5.4 Discussion*

Thermal stress due to the 2022 heatwave overwhelmed the effects of OA on plant productivity, suggesting that the predicted intensification of extreme heat events will be a main driver of seagrass responses under future climate conditions. Under average seawater temperature conditions unlikely to cause thermal stress, there were no effect of short-term elevation of $CO_2$ on plant performance at both depths, indicating that *Posidonia oceanica* is not limited by current seawater inorganic carbon concentration, regardless of light availability. In contrast, OA exacerbated thermal stress, causing an increase and a decrease of plant lipid peroxidation and photosynthetic performance, respectively, with deep plants also showing signs of heat stress-induced damage (i.e., over-expression of heat shock proteins and activation of antioxidant system).

Seagrasses are generally thought to benefit from OA because they are able to use both $CO_2$ and $HCO_{3-}$ for photosynthesis, but, due to the higher affinity for $CO_2$, often result in C-limitation under current DIC (Hall-Spencer et al., 2008; Koch et al., 2013; Sunday et al., 2017). Nonetheless, results from field and mesocosm studies are contrasting, with effects of elevated $CO_2$ on seagrass productivity and biomass ranging from positive to neutral, largely as a consequence of variations in species physiology and life-history traits (Jiang et al., 2010; Campbell & Fourqurean, 2013; Ow et al., 2015; Cox et al., 2015, 2016; Zimmerman, 2021).

Here, we found that the effects of elevated $CO_2$ levels varied between both years, which were characterized by markedly different seawater thermal conditions. Under average seawater temperature during 2021, there were no effect of elevated $CO_2$ on all the response variables analysed in shallow and deep *P. oceanica*. This is in line with previous experiments showing limited (if any) production stimulation for shallow *P. oceanica* stands under future OA (Cox et al., 2015, 2016; Berlinghof et al., 2022), reflecting the ability of *P. oceanica* to use bicarbonate as carbon substrate for photosynthesis more efficiently than other seagrass species (Koch et al., 2013; Zimmerman, 2021).

The lack of an effect of OA in the deep-water treatments is in contrast with the general view that low light availability may increase plant reliance on $CO_2$ diffusion due to the high energetic requirement of $HCO^{3-}$ use for photosynthesis (Koch et al., 2013; Ow et al., 2016; Collier et al., 2018). Therefore, even species that are able to use $HCO^{3-}$ might be expected to positively respond to elevated $CO_2$ at limiting light levels (Koch et al., 2013; Ow et al., 2016). However, previous studies are based on shallow-water plants exposed to different light conditions (Ow et al., 2016), neglecting the fact that deep-water plants that developed under reduced light conditions might have evolved different molecular and photo-physiological mechanisms to maintain a balance between light harvesting and cellular metabolism (Dattolo et al., 2014, 2017). Under these circumstances, any further increase in $CO_2$ concentration may exceed the energetic capacity for its assimilation (Zimmerman, 2021).

Regardless of $CO_2$ level, photosynthetic pigment content and efficiency were higher in deep than in shallow *P. oceanica* plants. This may be an acclimation strategy to maintain a positive carbon balance and growth under low irradiance level, as previously reported for other seagrass species at their deeper distribution limits (Sharon et al., 2011; Beca-Carretero et al., 2019). In addition, under average seawater temperatures, deep stands of *P. oceanica* did not show any sign of cellular stress, as

indicated by lower levels of total antioxidant activity and secondary metabolites (i.e., flavonoids and total phenols), suggesting a successful adaptation to deep-water light conditions tested in this study. Our results are in agreement with those of Dattolo et al. (2014), who found that shallow *P. oceanica* plants (~5 m depth) activated specific defence mechanisms (e.g., antioxidant enzymes and xanthophyll-cycle related genes) to avoid photo-damage and maintain high photosynthetic performance, in contrast to deep plants (~ 25 m depth) that appeared to be photo-relaxed. However, it is worth noting that a further decrease in light availability (40 µmol photons $m^{-2}$ $s^{-1}$) has been shown to negatively affect vertical shoots of *P. oceanica* at different levels of biological organization, suggesting that there might be a light shortage limit below which plants show severe stress responses (Ruocco et al., 2021). Additional experiments are, thus, needed to improve our ability to make projections of the effects of OA on seagrass beds under lower chronic light shortage.

Importantly, plants from both depths, exposed to a prolonged anomalous warm water event (+3 °C during the period of plant growth) and maintained at increased $CO_2$ levels, showed a significant increase in lipid peroxidation (as a signal of oxidative damage to cell membranes) and an up-regulation of the stress-related gene (OZ-species), suggesting a limited capacity of *P. oceanica* to cope with both stressors in combination. Thermal stress can cause plant metabolic impairment due to oxidative stress (e.g., accumulation of reactive oxygen species), alteration of membrane fluidity and protein structure (e.g., protein unfolding and/or degradation) (Nguyen et al., 2021). In addition, seagrasses exposed to OA have been recently shown to increase the expression of antioxidant- and stress-related genes, indicating a cellular stress response of plants to elevated CO2 (Lauritano et al., 2015; Ravaglioli et al., 2017; Ruocco et al., 2017; Piro et al., 2020), even if they may well adapt to future acidified oceans (Hall-Spencer et al., 2008; Takahashi et al., 2016). This means that also plants, which are generally highly tolerant to OA, can be affected by elevated $CO_2$ during heatwaves. To the best of our knowledge, no previous studies have investigated the combined effects of OA and thermal stress on molecular and biochemical pathways of both shallow- and deep-water plants, despite the fact that they may act as an early-warning of seagrass collapse (Ceccherelli et al., 2018).

The combined effect of OA and seawater warming negatively affected the performance of photosynthetic machinery of *P. oceanica*, by reducing plant photosynthetic efficiency, leaf pigment content and, to some extent, the expression of the photosynthesis-related gene (CAB), regardless of depth. Thermal stress has been shown to adversely affect the functioning of the photosynthetic apparatus of different

seagrass species, through the damaging of PSII activity, inactivation of Rubisco and degradation of photosynthetic pigments (Marín-Guirao et al., 2016; Nguyen et al., 2021). On the other hand, OA could mitigate the negative effects of warming on plant productivity, by enhancing photosynthesis and reducing respiratory loss of fixed carbon (Zimmerman et al., 2017; Egea et al., 2018; Zayas-Santiago et al., 2020; Rodríguez et al., 2022). Indeed, the few studies that have experimentally tested the cumulative effects of these stressors on seagrass physiology have produced contrasting results, likely due to variations in seagrass responses to increasing $CO_2$ (Repolho et al., 2017; Egea et al., 2018; Collier et al., 2018). In particular, OA could offset thermal stress in species that respond positively to elevated $CO_2$, enhancing light harvesting mechanisms and photosynthetic efficiency (Egea et al., 2018), but not in carbon-saturated species (Repolho et al., 2017; Collier et al., 2018). Our results support previous findings of a limited stimulation of *P. oceanica* production under $CO_2$ levels predicted by the end of the century (Cox et al., 2015, 2016; Berlinghof et al., 2022) and bring new evidence that future OA could exacerbate the negative impacts of thermal stress on this species, as recently found for other tropical seagrasses (Collier et al., 2018). The negative impacts of both stressors on *P. oceanica* may be the result of an increased energy allocation to repair and defence processes rather than productivity, due to metabolic impairment, as reported for other photosynthetic organisms under stressful conditions (Gao et al., 2012; Briggs & Carpenter, 2019).

We also found a general reduction in the growth rate of *P. oceanica* in the warmer year (2022), as previously documented by other studies (Collier et al., 2011, 2018; Traboni et al., 2018; Nguyen et al., 2021). Although thermal stress decreased plant growth at both depths, the expression of heat shock proteins, such as HSP90, was greater in deep than shallow-water plants. Heat shock proteins, including HSP90, play a fundamental role as molecular chaperones to fix non-functional proteins or prevent their accumulation and they are commonly considered an early-warning response of plants exposed to warming and extreme heat events (Marín-Guirao et al., 2016; Nguyen et al., 2021). In agreement with our result, Marín-Guirao et al. (2016) reported a differential molecular response to heat stress among *P. oceanica* plants from contrasting depths (5 m vs. 25 m depths), with deep-water plants increasing the expression of heat shock proteins to much higher levels than shallow-water plants.

Thermal stress also increased the expression of the antioxidant CAT, the total antioxidant capacity and the leaf content of secondary metabolites (flavonoids and total phenols) in deep plants, regardless of pH levels. The stimulation of antioxidant systems indicated the activation of different defensive mechanisms in deep-water plants to

detoxify reactive oxygen species (ROS), as previously reported for other aquatic and terrestrial plants exposed to thermal stress (De Silva & Asaeda, 2018; Ruiz-Montoya et al., 2021). Likewise, the greater content of phenols and flavonoids in deep-water plants under thermal stress could indicate the stimulation of the antioxidant capacity. Indeed, secondary compounds can be involved in plant protection against a variety of abiotic and biotic stressors (Brandt & Koch, 2003; Arnold et al., 2008; Vergés et al., 2008; De Silva & Asaeda, 2018; Mannino & Micheli, 2020; Ruiz-Montoya et al., 2021) and their accumulation under heat stress has been reported in different terrestrial plants (Wahid, 2007; Mierziak et al., 2014; Commisso et al., 2016), likely indicating their ability to reduce ROS production (Mierziak et al., 2014). These patterns suggest that individuals of *P. oceanica* within the same population, but at different depths, might be thermally adapted to their local conditions (Dattolo et al., 2014; Procaccini et al., 2017), thus resulting in differences in tolerance to heat stress. Our results are in line with previous studies, showing that plants living in more stable and/or colder environments are less tolerant to temperature stress than those from more fluctuating and/or warmer habitats (e.g., populations from different latitudes or water depths (Franssen et al., 2014; Marín-Guirao et al., 2016).

In summary, both shallow and deep *P. oceanica* plants appear to be unaffected by future OA when not exposed to thermal stress, suggesting that their photosynthetic rates are not carbon-limited under current $CO_2$ levels. In contrast, elevated $CO_2$ levels in combination with seawater warming reduced plant performance and productivity, likely by causing metabolic impairment. The results of our study add to mounting evidence that elevated $CO_2$ concentration will not offset the negative impacts of temperature stress on seagrasses, at least for those species showing limited or no photosynthetic enhancement under elevated $CO_2$ (Repolho et al., 2017; Collier et al., 2018).

Seagrasses rank among the most productive ecosystems on Earth, enhance the abundance and diversity of associated organisms (Ralph et al., 2006; Orth et al., 2006; Hughes et al., 2009) and could play a pivotal role in mitigating climate-driven loss of biodiversity (Bulleri et al., 2018; Falkenberg et al., 2021). Indeed, seagrass meadows, like other photosynthetic organisms, can modify seawater chemistry through their metabolic activities (Unsworth et al., 2012; Hendriks et al., 2014; Ricart et al., 2021), potentially providing climatic refugia for OA stress-sensitive species (e.g., calcifying organisms), by either temporarily increasing pH levels or enhancing the adaptive capacity of the threatened organisms (Falkenberg et al., 2021). Therefore, our results suggest that climate-driven changes in seagrass productivity may challenge the adaptability of associated organisms to lower pH and the ability of seagrass meadows to

act as future climate refugia. Our findings highlight the importance of raising the awareness of the effects of OA on seagrass meadows in combination with other environmental stressors when planning suitable climate-ready solutions and mitigation measures that preserving biodiversity and ecosystem functioning in the face of climate change.

## Chapter 6 – Response of *Posidonia oceanica* from different islands of the Tuscan Archipelago to a marine heatwave

SL28 Contributors: Fabio Bulleri, Chiara Ravaglioli, Ludovica Pedicini

### *6.1 Introduction*

Marine ecosystems are threatened by global climate changes, including seawater warming and acidification and increasing intensity and frequency of extreme events, such as storms, floodings and heat waves.

Extreme events, defined as period over which environmental conditions exceed the average values from a previous reference period, have been shown to cause mass mortalities, range shifts and the establishment of novel ecosystems in the marine realm (Wernberg et al., 2013; Harris et al., 2018; Bulleri et al., 2021). On the other hand, extreme events, can actively select more resistant genotypes when threshold of tolerance are not exceeded (Coleman & Wernberg, 2020). When such variation among individuals has a heritable basis, it can sustain population ability to rapidly adapt to changing conditions.

Stress memory describes plant hardening to environmental stress, in the form of changes in individual phenotype, following the exposure to adverse conditions. Within-generation phenotypic plasticity represents the capability of a genotype to generate different phenotypes when exposed to different environmental conditions (Pigliucci, 2005). Such differences can be either reversible or irreversible, according to the life-stage at which they occur. For instance, previous exposure to heatwaves has been shown to regulate the response of seagrasses to subsequent warming events (DuBois et al., 2020)

On short temporal scales such as those encompassed by modern climate variability, phenotypic plasticity, i.e., the ability of an organism to generate different phenotypes when exposed to different biotic or abiotic conditions, within and among individuals of a population could increase their acclimation capacity, i.e., species ability to cope with increasingly adverse environmental conditions. Importantly, somatic DNA mutations or epigenetic modifications underpin phenotypic plasticity, which is, therefore, genetically based (Pazzaglia et al., 2021). Within this context, assessing the potential of species to adapt to novel environmental conditions is key for devising sounded conservation strategies.

Past occurrence of climate extremes may have already selected more resistant genotypes within extant populations (Coleman & Wernberg, 2020; Stipcich et al., 2022). Thus, populations at sites characterized by high and low intensity and frequency of

extreme events could be predicted to be, respectively, more and less resistant to future MHW. Identifying these populations is key for devising climate-ready conservation and restoration practices and requires assessing the relationship between past climate extremes and resistance/resilience to stressors. While warming trends are global, rates of change vary at a hierarchy of spatial scales and there is, indeed, evidence of significant variations of climate extremes at local to regional scales (Burrows et al., 2011).

The seagrass, *P. oceanica*, is a key habitat-former in the Mediterranean Sea, sustaining biodiversity and ecosystem functioning and providing key services to humans (e.g. coastal protection, carbon sequestration, enhanced water quality, nursery provisioning) (Barbier et al., 2011) Nonetheless, anthropogenic perturbations operating at local to regional scales (i.e. eutrophication, anchoring, pollution, trawling), in combination with global climate changes have caused the decline of this species throughout the basin (Telesca et al., 2015). Due to its ecological value, *P. oceanica* is currently, central to nature-based solutions (e.g., conservation and restoration) for mitigating the effects of climate change in marine environments. However, devising sounded climate-ready solutions requires assessing which populations could be more worth of protection under or more suitable as donors of individuals for restoring loss meadows under future climate scenarios.

Common garden experiment, allowing the comparison of different population from different genotypes or population under common environmental conditions, represent a power full to assess phenotypic plasticity (Pazzaglia et al., 2021). Here, taking advantage of work performed in Task 2.3, we used this approach, to test the hypothesis that plants of *Posidonia oceanica* from sites across the Tuscan Archipelago that were exposed to more intense and frequent warming events in the last three decades would a) differ in physiological (i.e., photosyntethic efficiency, pigment and secondary metabolite content) and biochemical features (i.e., C/N ratio, alkaline phosphatases, lipid peroxidation and total antioxidant capacity) and b) would be more tolerant to a simulated future MHW would be higher in plants from sites.

### *6.2 Materials and methods*

Using maps of cumulative MHW severity in the Tuscan Archipelago, generated in Task 2.3 (Figure 31), we identified seven sites characterized by the presence of *P. oceanica*, two on the mainland (Antignano: 43°29'15.59"N; 10°19'34.91"E and Punta Ala: 42°49'27.98"N; 10°45'00.75"E) and five on islands (Elba: 42°44'58.08"N; 10°24'29.38"E, Capraia: 43°01'03"N; 9°49'32"E, Giannutri: 42°15'48.08"N; 11°06'32.09"E, Gorgona: 43°25'55.51"N; 9°54'31.27"E and Giglio: 42°21'10.36"N; 10°55'24.72"E). All of these sites were characterized by the presence of extensive *Posidonia oceanica* meadows that were exposed to particularly intense and frequent heatwaves in the last two decades (Figure 32). Thus, the selection of the study sites allowed encompassing a broad gradient of CHS, with values ranging from 361.01 (Giglio Island) to 443.96 (Gorgona Island).

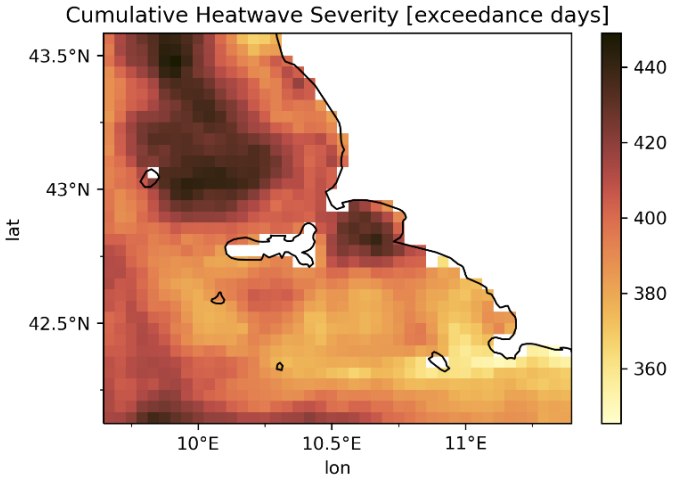


*Figure 30. Maps of Cumulative Heatwaves Severity (CHS) in the Tuscan Archipelago (top).*

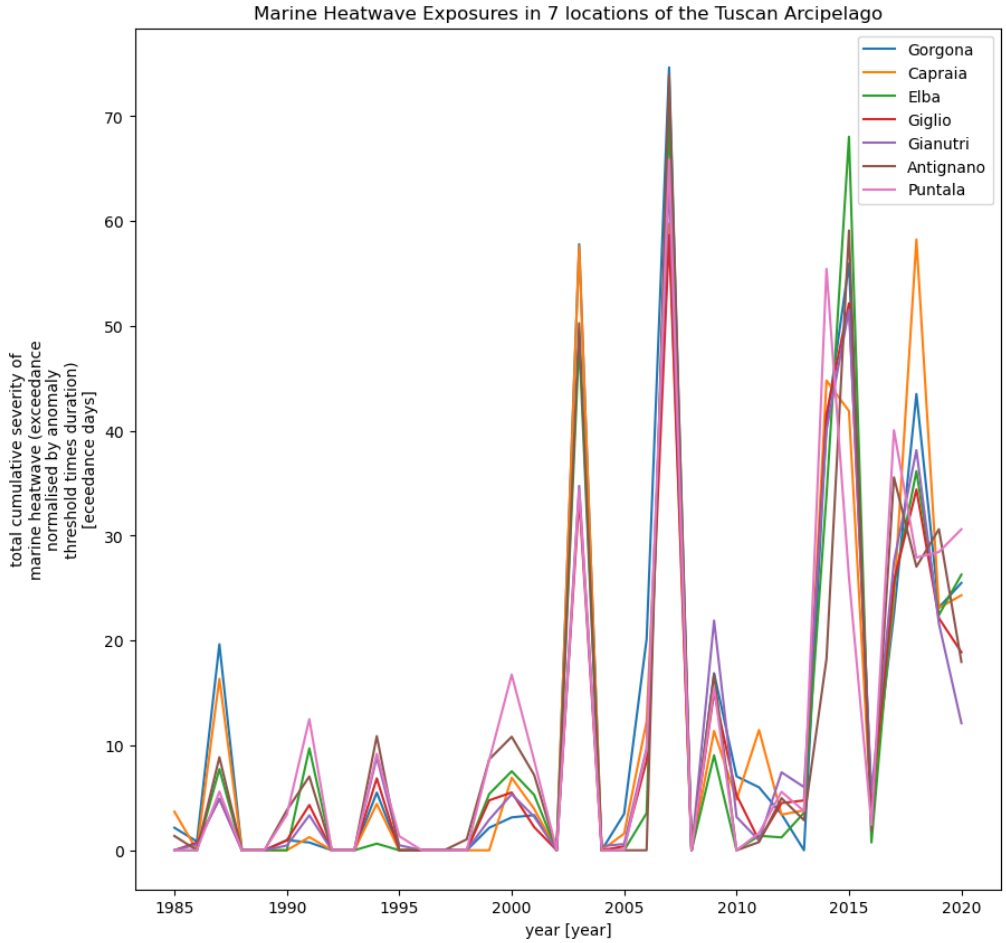


*Figure 31. Total Cumulative Heatwaves Severity (CHS) in the period 1985 – 2020 at the seven study sites selected in the Tuscan Archipelago*

At each site, 12 rhizomes of *P. oceanica*, about 30 cm long, bearing apical growth meristems and 3-5 vertical shoots, were collected at a depth of about 5 m during the last week of July 2022. Rhizomes were collected at a distance > 10 m one from another in order to minimize the probability of repeatedly sampling the same clone. Samples were kept in dark coolers filled with ambient seawater and immediately transported to mesocosms facilities at the Acquario di Livorno. The mesocosms were six glass tanks (80 cm length x 80 cm width x 70 cm height), each filled with 500 l of filtered seawater and sterilized with UV. Two rhizomes from each site were randomly assigned to each of the six tanks, three of which were then exposed to a simulated MHW, while the remaining were left at ambient temperature (i.e., controls). Rhizomes were attached to the bottom of plastic trays filled with small cobbles using plastic cable tiles, at a distance of about 30 cm one from another. Rhizomes in a tank were randomly distributed and, hence, interspersed. Each aquarium was equipped with three (two Silvermoon Reef Blu 895 and

one Silvermoon Marine 895) LED lamps, allowing the simulation of light diel fluctuation and light intensity. Irradiance levels in experimental tanks were ~300 µmol photons m-2 s-1 above the canopy, with a light regime of 14:10 h (light:dark cycle). During one week acclimation period, water temperature in all tanks was maintained at 25 °C according to the mean field values recorded in July. Subsequently, the temperature in half of the tanks was increased at a rate of 1 °C $d^{-1}$ to 30.5 °C, which represents extreme summer seawater temperature projected for the end of the century. The characteristics of the MHW were calculated following Hobday et al. (2016). The reference mean seawater temperature within the region of interest was obtained from daily satellite observations over the period 1981-2022 and used to identify MHWs for simulated SSTs over the period 2023-2100, following the high emission scenario (RCP 8.5). Daily satellite SST observations were obtained from Mediterranean Sea SST analysis L4 available at Copernicus Marine Service and simulated SST data were obtained from simulation models implemented in the fifth phase of the Coupled Model Intercomparison Project (CMIP5) at https://esgf-node.llnl.gov/search/cmip5/. Plants exposure to heat stress lasted 5-days after that temperature returned again to control conditions. Plant responses were evaluated after 5 days of exposure to the treatments and after a recovery period of one week.

Plant photosynthetic efficiency

In vivo Chlorophyll fluorescence measurements were performed on *P. oceanica* leaves with a diving-PAM fluorometer (Walz, Germany). Effective quantum yield, an estimate of the photosynthetic efficiency of photosystem II (PSII) in light-adapted plants, was measured between 11:00 and 13:00 a.m. after five days of experimental treatments and at the end of the experiment (after a recovery period of 5 days), using the saturating-light method. For each aquarium, measurements were performed on the second youngest leaf of 2 shoots of 2 rhizomes (1-2 technical replicate per leaf). The effective quantum yield was expressed as ΔF/Fm' = Fm' – F/Fm', where F is the fluorescence yield of a leaf measured before the application of a saturating light pulse; Fm' is the maximum fluorescence yield induced by a saturating light pulse (Genty et al., 1989).

Photosynthetic pigments and secondary metabolites

At the end of the experiment, intermediate leaves of the shoots were randomly collected from each aquarium to quantify the content of photosynthetic pigments, phenols and flavonoids. In the laboratory, leaves were washed, cleaned from epiphytes using a razor blade and stored at -80 °C until analysis. One leaf from 2 shoots was randomly collected from each aquarium to quantify the content of photosynthetic pigments (Chlorophyll-a

and b, carotenoids), phenols, and flavonoids. Leaves were cleared from of epiphytes using a razor blade and stored at - 80 °C until analysis. Frozen leaves were lyophilized and grounded for 15 s in a steel balls mill (Retsch GmbH & Co. KG, Haan, Germany) that was cooled using dry ice. This powder was sieved through a 160 mesh (104 µm) and stored at – 30 °C before further analysis.

From 2 mg of flour for each sample, photosynthetic pigments were extracted with 2 ml of acetone:Tris-HCl 0.5 M, pH 7.8 (80:20, v/v) on a magnetic stirrer for 30 min in a cold room (5 °C). The extract was centrifuged at 13,500 g and 5 °C for 10 min. Supernatant absorbances were read against a blank made with the extraction solvent at 430, 537, 647, and 663 nm, with a double beam Lambda 25 (Perkin-Elmer, Milan, Italy) spectrophotometer. The absorbance readings were converted into µmoles/ml following (Sims & Gamon, 2002) and expressed as µmoles/g DW. Three technical replicates were done for each sample.

According to Bolser et al. (1998), total phenolics were extracted from an aliquot of 5 mg of leaves powder, with 1 mL of cold 50% methanol in water, on a magnetic stirrer for about 16 hrs at 5 °C. The extracted total phenolics extract was then centrifuged for 15 min at 13,500 g and 5 °C.

Polyphenols were quantified using the Folin-Ciocalteu method (Singleton et al., 1999). One hundred µl of extract were brought to 625 µl with distilled water and added with 125 µl of Folin-Ciocalteu reagent (Sigma-Aldrich, Milan, Italy). Samples were vortexed and was kept under dark conditions for 6 min before adding 1250 µl of 7% $Na_2CO_3$ and 1000 µl of distilled water. Samples were then vortexed and kept in the dark for 90 min. The coloured reaction product was read at 760 nm, against a blank reaction mixture, where water replaced the phenolics extract. The amount of total phenols was estimated from a calibration curve made with gallic acid and the results were expressed as nmoles of gallic acid equivalents per gram of DW.

Flavonoid assays were based on the colorimetric method of (Dewanto et al. 2002). Two-hundred µl of extract were diluted to 1500 µl with distilled water and added of 75 µl of a 5% NaNO2 solution. The mixture was vortexed and kept in the dark for 6 min; afterwards, 150 µl of a 10% AlCl3·6H2O solution were added. After vortexing and standing for another 5 min in the dark, 500 µl of 1 M NaOH and 275 µl of distilled water were added. The solution was vortexed again and its absorbance was measured immediately at 510 nm against a blank made by replacing the sample with an equal volume of distilled water. The amount of flavonoids was estimated from a calibration curve made with catechin

and the results were expressed as nmoles of catechin equivalents per gram of DW. Each extract assay had three replicates for a total of nine replicates per sample.

Leaf C/N ratio

Analyses were performed on dried *P. oceanica* leaves. Dried tissues were homogenized by accurately cutting and fine grinding dried tissues to obtain enough sample to test. Analyses were performed in triplicate to evaluate mean (SD values) of total organic carbon (TOC), and total nitrogen (TN) levels and results were expressed as % dry weight (d.w.). Levels of TOC, and TN were determined by acid digestion and chemical titration respectively according to DM n. 196/89 part II (TOC), and DM 185/99 met. XIV.3 (TN). Limit of quantifications were 0.001 % (TN) and 0.01 % (TOC).

Lipid peroxidation and total antioxidant capacity determination

At the end of both experiments, two shoots of different rhizomes were randomly sampled in each aquarium for analyses of lipid peroxidation (LPO), alkaline phosphatases (ALP) and total antioxidant capacity (TAC). Leaves with a very small epiphyte load were selected and immediately frozen at −80 °C until biochemical analyses. Malondialdehyde (MDA), a by-product of LPO, extraction and quantification were performed according to Costa et al. (2015). About 300 mg of frozen leaf tissue was powdered and suspended in 5.0 mL of ethanol (80%). The extract was homogenized and then centrifuged at 3000 × g for 10 min at 4°◦C. The supernatant (1.0 mL) was added to 1.0 mL of 20% trichloroacetic acid (TCA) with 0.65% thiobarbituric acid (TBA) and 0.01% butylatedhydroxytoluene (BHT) solution. Two blanks were used to verify the correct functioning of the test. All samples were first heated (90°◦C, 25min), then cooled for 15 min and again centrifuged (3000 × g, 4◦C, 10 min). Absorbance was measured at 440, 532 and 600 nm (BioTek Synergy HT micro-plate reader) and MDA equivalents were expressed in nmol MDA/g FW (Fresh Weight). TAC was measured using a ferric reducing antioxidant power (FRAP) assay, according to (Benzie & Strain 1996) and modified by (Capo et al. 2020). Powdered samples were homogenized in five volumes (w/v) of 50 mM Tris–HCl buffer, 1 mM EDTA, pH 7.5 using a small sample dispersing system (ULTRA-TURRAX® Disperser, IKA). Homogenates were centrifuged at 9000 ×g, 10 min, 4 °C. Then, 20 µL of homogenates were incubated for 30 min with a solution of ferric chloride (2 mM) and 2,4,6-Tris (2-pyridyl)-s-triazine (TPTZ) in acetate buffer pH 3.6. After incubation absorbance was measured at 593 nm and results were expressed as µmol FRAP/L.

Statistical analyses

Data were analysed using linear mixed models with the lmer package, v. 1.1-26 (Bates et al. 2015). The CHS and the treatment (exposed to MHW versus control) were treated as a fixed effects, while the tank was included in the random part of the model. Type III Analysis of Variance with the Satterthwaite's method was used to test for fixed effects included in the model by means of the 'anova' function. Model assumptions were visually checked by means of Q-Q and fitted versus residual plots. All analyses were performed in R studio v. 2022.07.2.

### *6.3 Results*

Although marginally significant (p = 0.069), there was a trend for plant photosynthetic efficiency to increase with CHS at Time 1 (Table 8 , Figure 34a). There was no effect of the exposure of plants to the experimental MHW at Time 1 or at Time 2 (Table 8 , Figure 33a,b).

Likewise, the concentration of phenols and flavonoids was not affected by the experimental MHW, but varied across the CHW gradient (Table 8, Figure 35). In both cases, concentrations decreased with increasing CHS values.

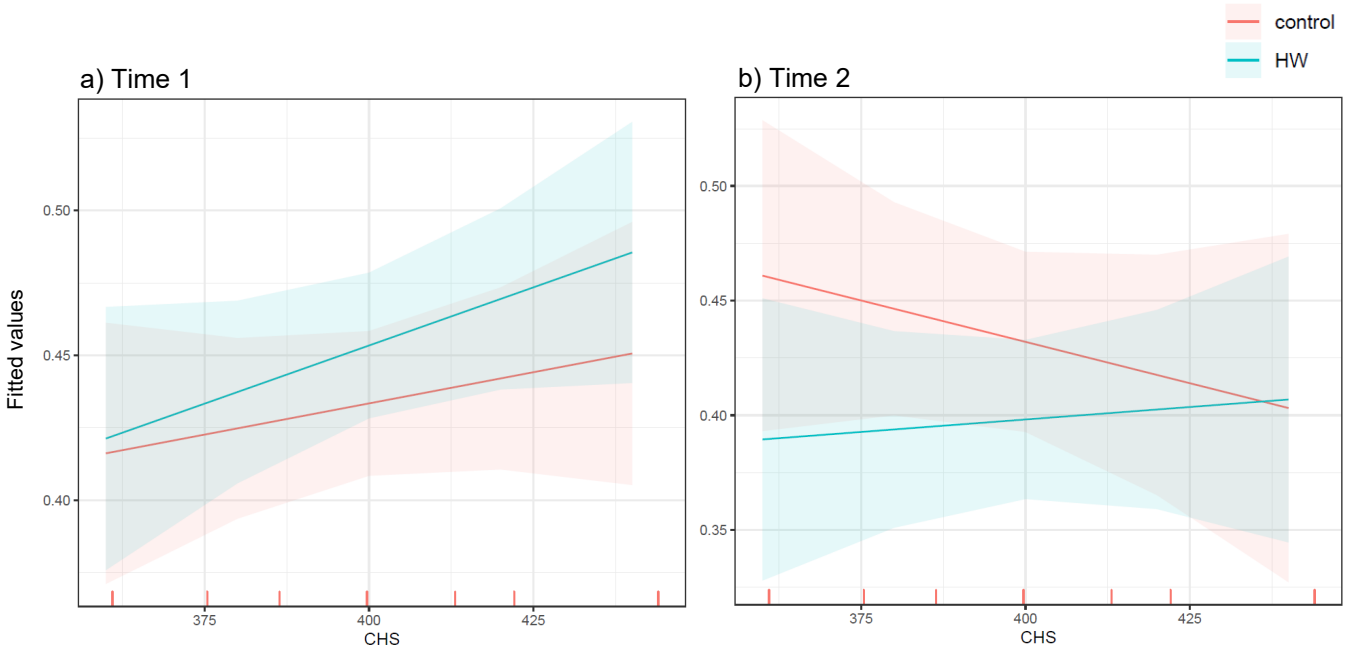


*Figure 32: The relationship between photosynthetic efficiency, expressed as effective quantum yield (fitted values with 95% CI) and CHS in leaves from plants experimentally exposed to a MHW or maintained at ambient temperature at different study sites, at Time 1 (a) and Time 2 (b).*

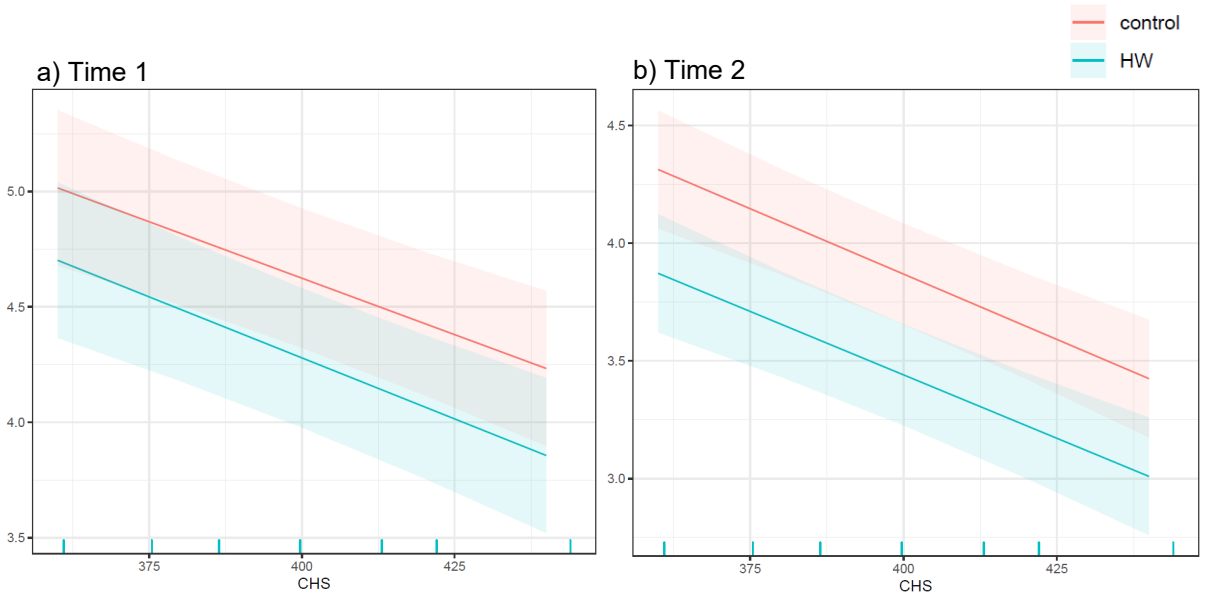


*Figure 33. Variation in the concentration of a) Chla, b) Chlb and c) Carotenoids (fitted values with 95% CI) in leaves from plants experimentally exposed to a MHW or maintained at ambient temperature across the CHS gradient.*

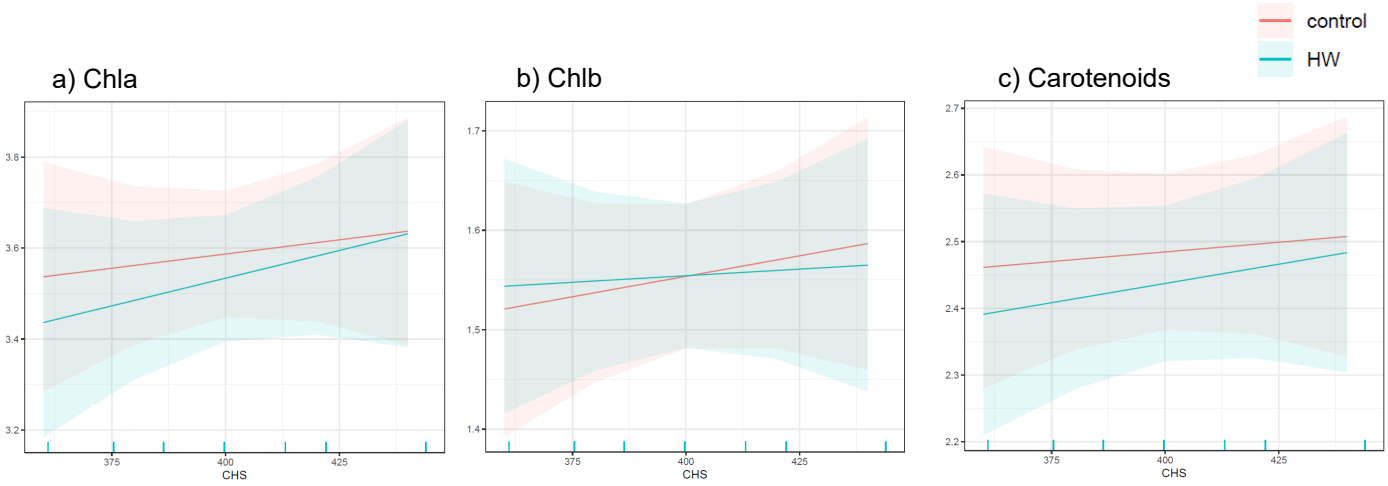


*Figure 34. . Variation in Phenols and Flavonoids concentrations (fitted values with 95% CI) in leaves from plants experimentally exposed to a MHW or maintained at ambient temperature across the CHS gradient.*

*Table 8: Type III ANOVA results for fixed effect parameters included in the linear mixed model testing the effects of site and treatment on P. oceanica plants.*

| | | **EQY - Time 1** | | | **EQY - Time 2** | | |
|---|---|---|---|---|---|---|---|
| *Source of variation* | df | MS | *F* | *P* | MS | *F* | *P* |
| CHS | 1 | 0.086 | 3.325 | 0.069 | 0.008 | 0.252 | 0.616 |
| Treatment | 1 | 0.006 | 0.226 | 0.635 | 0.034 | 1.047 | 0.187 |
| CHS x Treatment | 1 | 0.008 | 0.302 | 0.583 | 0.029 | 0.876 | 0.350 |
| | | **Chla** | | | **Chlb** | | |
| *Source of variation* | df | MS | *F* | *P* | MS | *F* | *P* |
| CHS | 1 | 0.600 | 0.969 | 0.326 | 0.052 | 0.333 | 0.564 |
| Treatment | 1 | 0.076 | 0.123 | 0.726 | 0.014 | 0.088 | 0.767 |
| CHS x Treatment | 1 | 0.062 | 0.100 | 0.752 | 0.014 | 0.088 | 0.767 |
| | | **Carotenoids** | | | **Phenols** | | |
| *Source of variation* | df | MS | *F* | *P* | MS | *F* | *P* |
| CHS | 1 | 0.132 | 0.491 | 0.484 | 36.464 | 58.203 | <0.001 |
| Treatment | 1 | 0.021 | 0.078 | 0.780 | 0.000 | 0.001 | 0.979 |
| CHS x Treatment | 1 | 0.015 | 0.054 | 0.816 | 0.055 | 0.088 | 0.766 |
| | | **Flavonoids** | | | | | |
| *Source of variation* | df | MS | *F* | *P* | | | |
| CHS | 1 | 103317 | 73.64 | < 0.001 | | | |
| Treatment | 1 | 3511 | 2.503 | 0.114 | | | |
| CHS x Treatment | 1 | 2073 | 1.477 | 0.225 | | | |

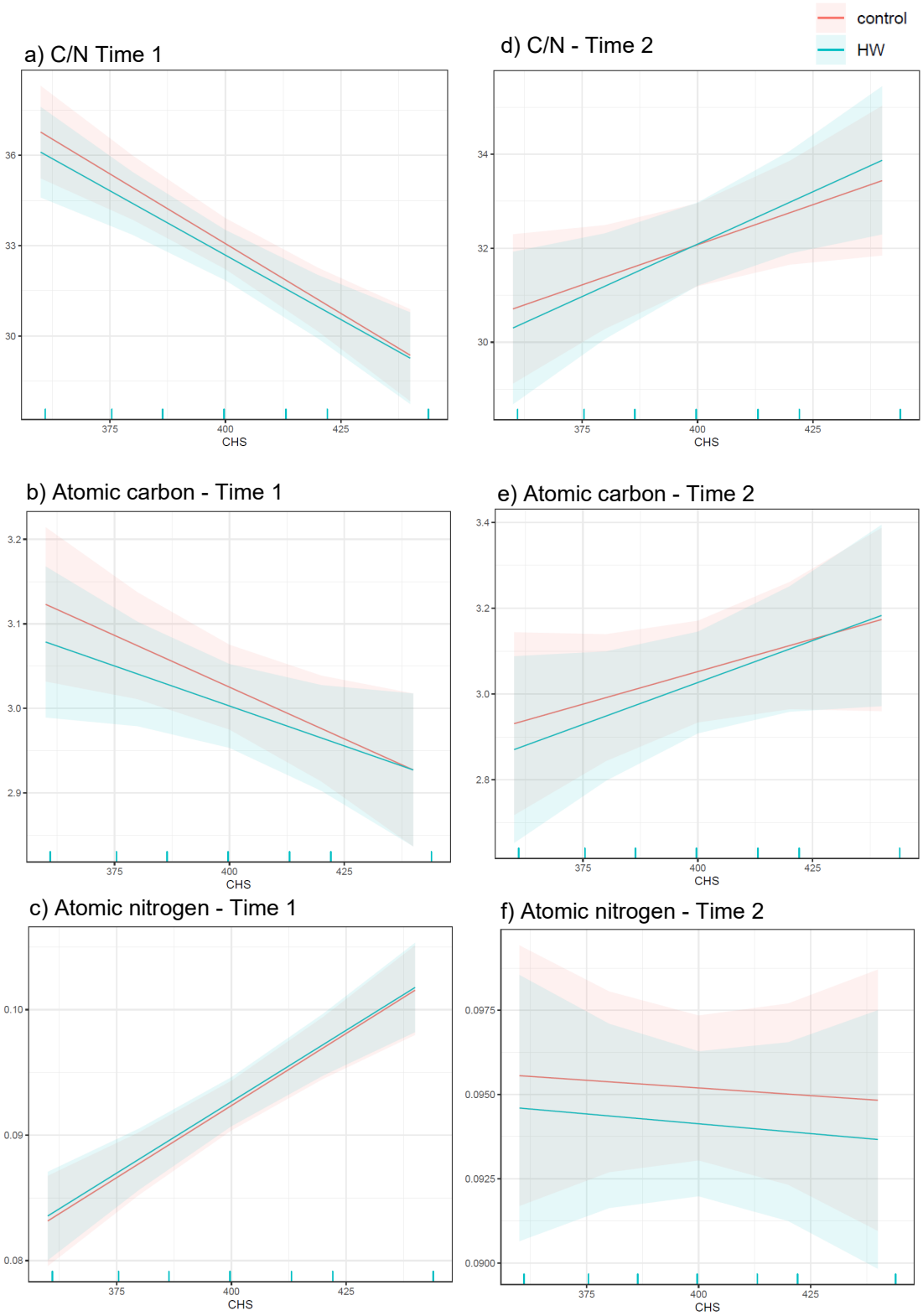


*Figure 35. Variation in leaf C/N ratio, atomic carbon and atomic nitrogen (fitted values with 95% CI) in leaves from plants experimentally exposed to a MHW or maintained at ambient temperature across the CHS gradient, at a-c) Time 1 and d-f) Time 2.*

The C/N ratio in leaf tissues varied across the CHS gradient at both Time 1 and Time 2, but it was not affected by the MHW (Table 9, Fig. 36). However, the C/N ratio

decreased with increasing CHS values at Time 1 (Fig. 36a), as a result of declining and increasing trends in atomic carbon and nitrogen, respectively, with CHS (Fig 36b-c).

The opposite pattern emerged at Time 2, since there was a positive relationship between C/N ratio and CHS (Table 9, Fig. 36d). This was generated by increasing C content when leaf tissues from sites towards the upper end of the CHS gradient.

*Table 9. Type III ANOVA results for fixed effect parameters included in the linear mixed model testing the effects of site and treatment on C/N ratio, atomic carbon and atomic nitrogen in P. oceanica leaves at times 1 and 2.*

| | | **C/N ratio - Time 1** | | | **Carbon - Time 1** | | | **Nitrogen - Time 1** | | |
|---|---|---|---|---|---|---|---|---|---|---|
| *Source of variation* | df | MS | *F* | *P* | MS | *F* | *P* | MS | *F* | *P* |
| CHS | 1 | 471.01 | 62.55 | <0.001 | 0.280 | 10.508 | <0.01 | $3.11e^{-03}$ | 75.388 | <0.001 |
| Treatment | 1 | 0.96 | 0.13 | 0.721 | 0.005 | 0.208 | 0.649 | $1.30e^{-07}$ | 0.003 | 0.955 |
| CHS x Treatment | 1 | 0.75 | 0.10 | 0.753 | 0.005 | 0.173 | 0.678 | $7.00e^{-08}$ | 0.002 | 0.967 |
| | | **C/N ratio - Time 2** | | | **Carbon - Time 2** | | | **Nitrogen - Time 2** | | |
| *Source of variation* | df | MS | *F* | *P* | MS | *F* | *P* | MS | *F* | *P* |
| CHS | 1 | 89.86 | 11.15 | <0.01 | 0.699 | 4.820 | <0.05 | $6.25e^{-06}$ | 0.131 | 0.718 |
| Treatment | 1 | 1.57 | 0.19 | 0.659 | 0.013 | 0.087 | 0.768 | $2.00e^{-10}$ | 0.000 | 0.998 |
| CHS x Treatment | 1 | 1.59 | 0.20 | 0.657 | 0.011 | 0.076 | 0.783 | $9.44e^{-08}$ | 0.002 | 0.965 |

At Time 1, differences in the alkaline phosphatases (ALP) concentration between control and MHW plants varied across the CHS gradient (Table 10, Fig. 37a). In particular, ALP concentrations did not vary in control plants, while concentrations in plants exposed to the experimental MHW decreased with increasing CHS values.

At Time 2, there was no significant effect of the MHW on the ALP concentration (Table 10), which did not vary across the CHS gradient (Fig. 37b).

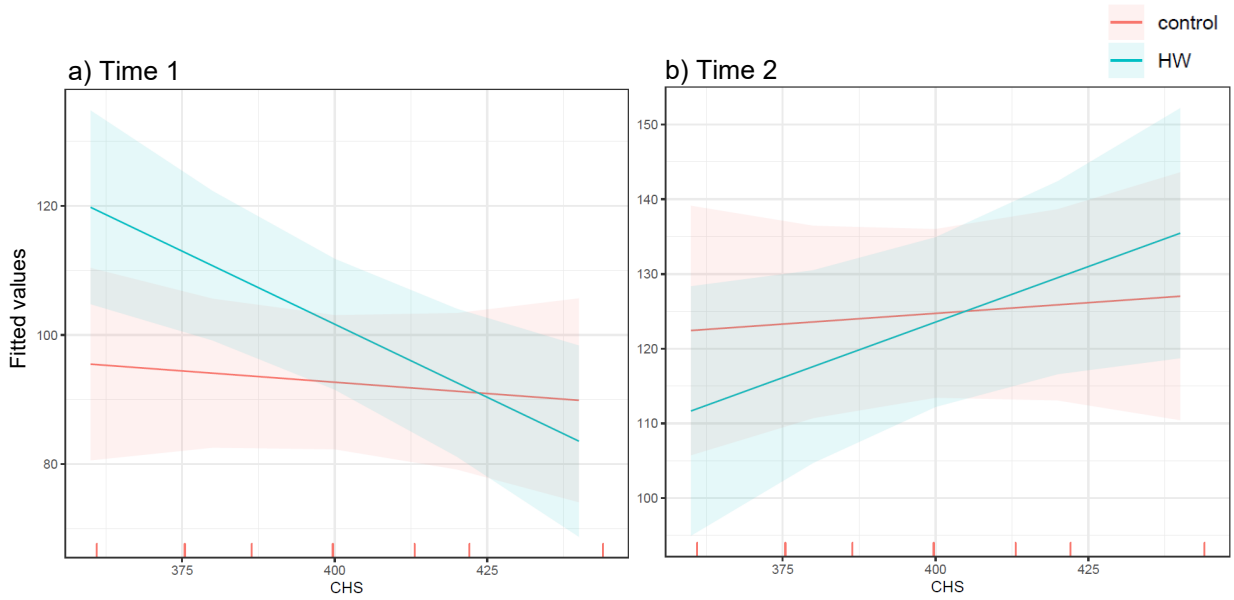


*Figure 36. Variation in Alkaline phosphatase (ALP) concentration (fitted values with 95% CI) in leaves from plants experimentally exposed to a MHW or maintained at ambient temperature across the CHS gradient, at a) Time 1 and b) Time 2.*

*Table 10: Type III ANOVA results for fixed effect parameters included in the linear mixed model testing the effects of site and treatment on ALP, LPO and TAC in P. oceanica leaves*

| | | **ALP-Time 1** | | | **ALP-Time 2** | | |
|---|---|---|---|---|---|---|---|
| *Source of variation* | df | MS | *F* | *P* | MS | *F* | *P* |
| CHS | 1 | 3671.3 | 7.056 | <0.01 | 1846.75 | 2.662 | 0.107 |
| Treatment | 1 | 21.96.8 | 4.222 | <0.05 | 859.39 | 1.239 | 0.269 |
| CHS x Treatment | 1 | 1968.2 | 3.783 | 0.056 | 846.39 | 1.220 | 0.273 |
| | | **LPO-Time 1** | | | **LPO-Time 2** | | |
| *Source of variation* | df | MS | *F* | *P* | MS | *F* | *P* |
| CHS | 1 | 0.109 | 0.392 | 0.533 | 0.154 | 0.425 | 0.516 |
| Treatment | 1 | 0.025 | 0.090 | 0.765 | 0.251 | 0.694 | 0.407 |
| CHS x Treatment | 1 | 0.025 | 0.091 | 0.764 | 0.215 | 0.596 | 0.443 |
| | | **TAC-Time 1** | | | **TAC-Time 2** | | |
| *Source of variation* | df | MS | *F* | *P* | MS | *F* | *P* |
| CHS | 1 | 1984.50 | 1.343 | 0.251 | 817.54 | 12.01 | <0.001 |
| Treatment | 1 | 73.62 | 0.050 | 0.824 | 155.20 | 2.297 | 0.134 |
| CHS x Treatment | 1 | 49.65 | 0.034 | 0.855 | 132.27 | 1.958 | 0.166 |

There was no effect of the experimental MHW on lipid peroxidation (LPO) (Table 2) which did not vary across the CHS gradient, at both times of measurement (Fig. 38)

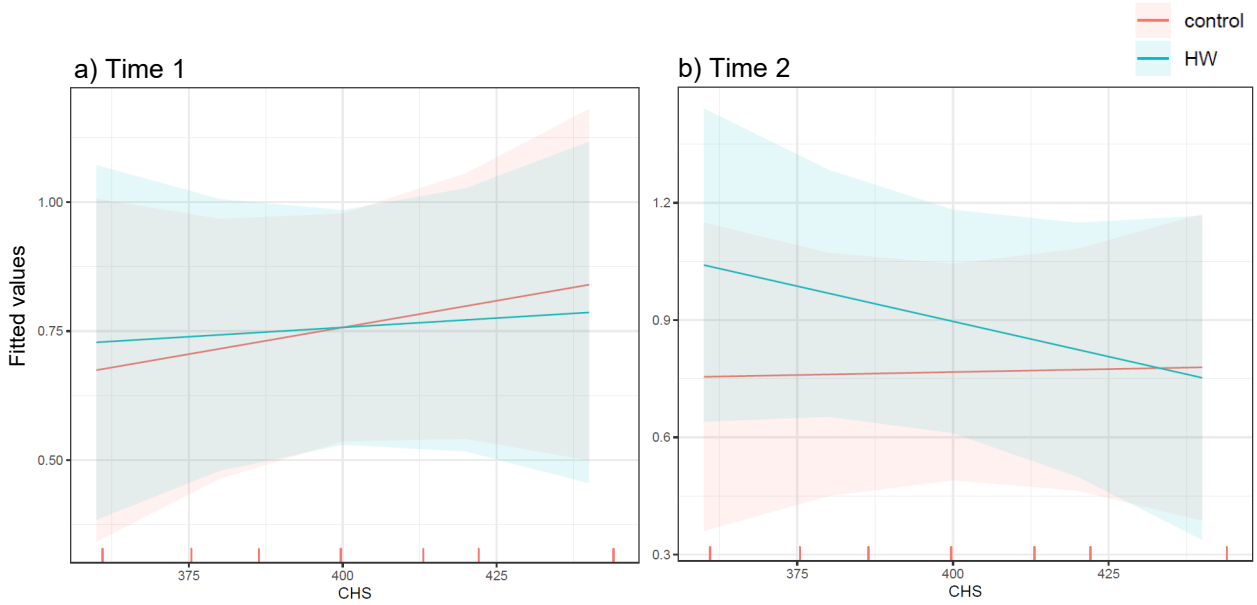


*Figure 37. Variation in Lipid Peroxidation (LPO) concentration (fitted values with 95% CI) in leaves from plants experimentally exposed to a MHW or maintained at ambient temperature across the CHS gradient, at a) Time 1 and b) Time 2.*

There was no variation in total antioxidant capacity (TAC) between MHW treatments or across the CHS gradient Time 1 (Table 12, Fig. 39a). In contrast, at Time 2, TAC levels decreased when moving towards the upper end of the CHS gradient, irrespective of MHW treatments (Table 12, Fig. 39a)

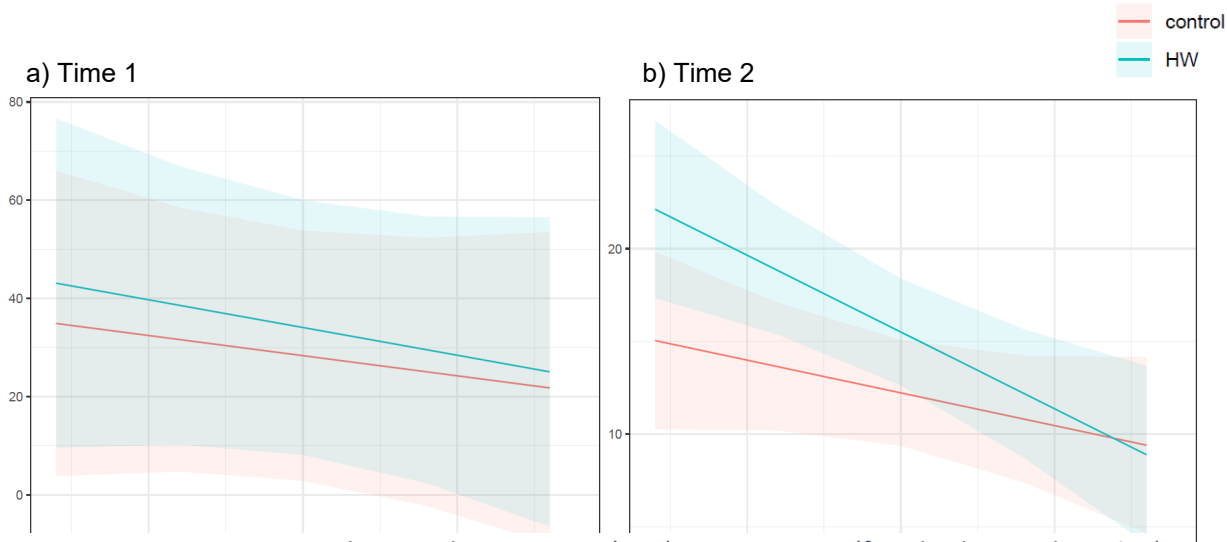


*Figure 38. Variation in total antioxidant capacity (TAC) concentration (fitted values with 95% CI) in leaves from plants experimentally exposed to a MHW or maintained at ambient temperature across the CHS gradient, at a) Time 1 and b) Time 2.*

### *6.4 Discussion*

*Posidonia oceanica* plants from sites exposed to different regimes of cumulative marine heatwave severity in the last three decades differed in some physiological and biochemical features. For instance, at Time 1, irrespective of the experimental MHW treatment, C/N ratio and the concentrations of phenols and flavonoids in plants decreased with increasing CHS, while the photosynthetic efficiency showed the opposite pattern. This suggests that variations in recent exposure to MHW plants may have shaped regional-scale patterns in differences in plant physiology and biochemistry, in accordance with previous findings of disturbance events being able to regulate the response of clonally reproducing organisms, such as seagrasses, to future extreme events (DuBois et al., 2020).

The lowering of the C/N ratio in plants from sites at the upper end of the CHS gradient was the result of decreasing C content and increasing N content and indicates a lower nutritional status of plants (Lee et al., 2004). Reduced C content could be explained by increasing respiration rates under thermal stress which would foster the release of carbon as $CO_2$ (Stipcich et al., 2022). At the same time, MHW would cause the accumulation of leaf N to sustain the production of amino acids (Stipcich et al., 2022). Given that these plants from high CHS sites had a higher photosynthetic efficiency, lower carbon content could be the result of prolonged periods in which plants were physiologically impaired and, hence, a signature of past warming events.

Previous studies have found a down-regulation in the expression of genes underpinning phenols production in *Zostera marina* response to seawater warming (Jakobsson-Thor et al., 2020). Likewise, reduced phenol concentrations have been identified as a promising indicator of stress levels in *P. oceanica* (Ceccherelli et al., 2018). Phenols are often correlated with herbivore defence in seagrasses (Ravaglioli et al., 2018). Reduced resistance to herbivores, due to weaker chemical defences, coupled with enhanced leaf palatability, due to the lower C/N, could imply the exposure plants at the upper end of the CHS gradient to elevated grazing pressure.

Although the ecological role of flavonoids is yet to be fully elucidated, they seem to be implicated in the reduction of oxidative stress (Dybsland et al., 2021). Here, there was a decrease in the concentration of flavonoids with increasing CHS which may indicate that plants that have been frequently exposed to intense warming events have a lower ability to cope with adverse environmental conditions.

In general, the exposure to a MHW, characterized by an intensity and duration predicted for the end of the century under the RCP 8.5 scenario had no dramatic negative effects on plants of *Posidonia oceanica*, independently from the collection site across the Tuscan Archipelago. For instance, there was no response to the heatwave in terms of photosynthetic efficiency, C/N ratio or concentration of photosynthetic pigments in leaves. This suggests a generalized resistance to thermal stress of *P. oceanica* from this region which is at odds with model projections of functional extinctions of this species in the Mediterranean basin (Jorda et al., 2012; Chefaoui et al., 2018). Although mortality of this seagrass during warm summers has been documented (Diaz-Almela et al., 2009; Marba & Duarte, 2010), recent experimental studies indicate evidence of resistance of shallow-water plants of *P. oceanica* to warming events (Marin-Guirao et al., 2017; Nguyen et al., 2021). On the other hand, the collapse of *P. oceanica,* as a consequence of environmental stress can be sudden and not anticipated by evident phenological changes (Ceccherelli et al., 2018). In addition, the exposure to multiple extreme events could, over a long period, cause declines. For instance, Stipcich et al. (2022) found that rhizome biomass decreased with increasing frequency of marine heatwaves (Stipcich et al., 2022).

Nonetheless, the exposure to the experimental MHW caused an increase in the alkaline phosphatases (ALP) in plants from sites towards the lower end of the CHS gradient. An increase in ALP was documented in *P. oceanica* plants experimentally exposed to elevated temperatures and was associated with increasing demand of energy to sustain elevated rated of $N_2$ fixation (Garcia-Marquez et al., 2022). $N_2$ fixation has

been reported in leaves and roots of *P. oceanica* and have been demonstrated to increase with warming (Garcias-Bonet et al., 2019). Such an increase in ALP was not evident in plants from sites at the upper end of the CHS gradient, suggesting that the exposure to the experimental MHW might not have been sufficient to trigger an increase in $N_2$ fixation rates in these plants, suggesting lower susceptibility to extreme warming events.

In summary, plants belonging to populations from different sites across the Tuscan Archipelago and the mainland of Tuscany appear to be characterized by differences in the physiological and biochemical properties of their leaf tissues. These differences suggesting that local environmental and biological conditions may have selected locally adapted phenotypes. While bringing some evidence for a generalized resistance of *P. oceanica* to MHW, our study also suggests, to some extent, that plants that have been historically exposed to a greater CHS could have a higher tolerance to thermal stress. Whether further investigation is necessary to buttress our findings of variations in the susceptibility of *P. oceanica* to extreme warming events and to identify the underpinning molecular mechanism(s), populations at sites characterized by higher CHS levels (i.e., Gorgona and Capraia islands and Punta Ala on the mainland of Tuscany) appear to be those that should be given priority for conservation within this region.

# Chapter 7 – FutureMARES protocol on temperature ramping experiments for thermal tolerance assessment in seaweeds

Contributors: Francisco Arenas, Sofía Hernández-Chan

## *7.1 Introduction*

Thermal stress (TS) occurs when an organism is exposed to temperatures beyond its thermal comfort zone, which is the particular range of temperatures that a species can endure without adverse impacts on its health or performance, thereby ensuring the proper functioning of physical processes. If the temperature surpasses these thermal comfort thresholds for a prolonged period, an organism may experience the impairment of vital functions, accumulation of injuries, and ultimately, death (Angilletta, 2009). Quantifying heat resistance has been accomplished through various methods, making it difficult to compare results across different studies. The most common measures include (i) the temperature that leads to the loss of motor function or functional collapse (known as critical thermal maximum or knockdown temperature) and (ii) the temperature at which 50% of a population succumbs to heat stress (Cooper et al,. 2008).

Here, we followed recommendations by Rezende et al. (2010) to apply relatively rapid ramping conditions when conducting studies about the phenotypic variation and/or the effects of thermal acclimation to critical thermal limits. Although fast ramping rates may not always reflect ecological realism, they help to minimize the impact of uncontrolled variables in experimental settings (like acclimation or individual hardening).

Our approach aims to define the "**thermal tolerance landscape**" for different populations/species by determining their **survival probability to a given thermal stress event**, as a function of both the **duration** and **intensity** of the thermal stress experienced. This method hereby applied is based on the approach suggested by (Rezende et al. 2014) and used by other authors, i.e. (Jorgensen et al. 2021).

In ectoderms, the “time-to-coma” or “time-to-dead” decreases exponentially with temperature. Thus, the coma or dead times can be represented as a Thermal Death Time (TDT) curve that shows the threshold relationship between temperature and time, which is exponential.

TDT curves are frequently represented with the Temperature in the X-axis, but can also be plotted the other way around in a more intuitive way, where curves show heat tolerance varies with the intensity and duration of the thermal stress, and are characterized by two parameters CTmax and z, from (Peralta-Maraver & Rezende, 2020).

Hence, the **Thermal tolerance**, which defines the temperature at which species experience knockdown or death (Tcrit), depends on two key parameters: the constant thermal sensitivity (z) which is suggested to be unique for each species, and the upper critical thermal limit (**CTmax**). **CTmax** is defined as the temperature that results in knockdown or death of the species at $\mathbf{\log_{10}.t = 0}$, i.e. one single time unit (Rezende et al. 2014). The relationship between these parameters can be modelled linearly by the following equation:

$$\mathbf{T_{crit} = CTmax - z \,.\, \log_{10} t}$$

In this protocol, ramping experiments will be conducted for the different populations of the targeted species to determine the parameters **z** and **CTmax** for each species.

### *7.2 Experimental procedure*

In a ramp experiment, temperature is continuously increased at a fixed rate over the course of different temporal intervals. Once temperature surpasses the critical level, i.e. baseline level for thermal stress, the rate of injury in test subjects will increase exponentially over time until individuals undergo severe functional impairment and/or death (Jørgensen et al., 2021).

Combinations of ramps with different speeds (i.e. durations) provide insights into the different rates of thermal tolerance between test groups. To better estimate each specific thermal tolerance, we propose to run 4 ramping temperature essays with different durations, namely: 3H; 6H; 12H; and 24H

We used chlorophyll fluorescence with a PAM device to assess the health status of our fronds during the ramping experiments. Fluorescence measures like quantum yield (Fv/fm: basal fluorescence/maximum fluorescence) can be used to provide information on the state of photosystem II, as a good manifestation of stress in plants or algae (Maxwell & Johnson, 2000). We use Fv/fm ratios from saturation pulses, and values are usually placed between 0 and 1; lower values (usually < 0.5 for brown seaweeds) indicate the deteriorating health of the algae as a result of the stress exposure.

To obtain proper identification of the fronds' health status, at least 3 PAM measurements per frond (with the optic fibre placed in different positions onto the frond) must be taken every time. Once yield values start to decline frequencies should increase to identify properly the critical temperature and time for each frond.

Sample collection: We will use 10 to 15 sections of algal fronds per species will be needed, that is, for a total of 4 ramps, at least around 100 different individual samples to account for possible mortality. Only vegetative structures should be collected, preferably apical young sections of the fronds without marks of herbivory

Laboratory adjustment period: A 10-day post-sampling laboratory adjustment period Seawater should be at a constant optimal growth temperature (in Portugal, 16ºC should fit most intertidal species, around 14º C for Norwegian samples). A realistic photoperiod should be configured in order to provide the algae with good lighting during this period

Equipment: 1 Intertidal Chamber © or a similar device able to control rising temperatures in a very controlled way. 1 Pulse-Amplitude-Modulation (PAM) chlorophyll fluorometer (here we used a Waltz JUNIOR-PAM). Titanium water heaters. Seawater pump to mixture Aquarium air pumps. Individual label for algal fronds

Summary of procedure: Prepare the intertidal chamber with filtered seawater and a temperature similar to those in the acclimation/adjustment tanks. Program the chamber temperature programme to be the same temperature as in the adjustment tanks. Algal fronds must be individually identified before being placed in the upper section of the experimental tank. Make sure the seawater is mixing properly in the experimental tanks. Before any ramping temperature experiment begins, a set of “T0” saturation pulse measurements are to be taken for each sample (3 light pulses should be made by frond). Configure the temperature controller of the intertidal chamber accordingly to your desired temperature ramps and durations. Annotate initial and final time & temperatures from your temperature-controlling device at the beginning and the end of each set of Fv/fm measures. Next Fv/Fm measures should be taken hourly during the experiment as the temperature rises progressively, and at least with half-hour intervals once the temperature reaches 25 ºC or an Fv/Fm value inferior to 0.6 (in our experiences seaweeds did not show any damage signal below this temperature, but you should check this in your species). For the shortest experiment (3h), we strongly recommend taking SAT pulse measurements as continuously as possible once the Fv/Fm values start to plunge. Saturation pulses can be taken directly underwater on the submerged fronds to optimize measurement frequency. Optionally, the experiment can be prematurely ended once the lectures of Fv/Fm values of every sample are **null** or below the 0.1 mark for each of the measure replicates. Once the experiment is over, the fronds are not expected to be able to recover from the inflicted thermal stress and thus should be discarded.

### *7.3 Analyses of data and preliminary results*

Analyses of data. A complete script in R to analyse data from ramping experiments with seaweeds is now available for the FutureMARES partners (Figure 40).

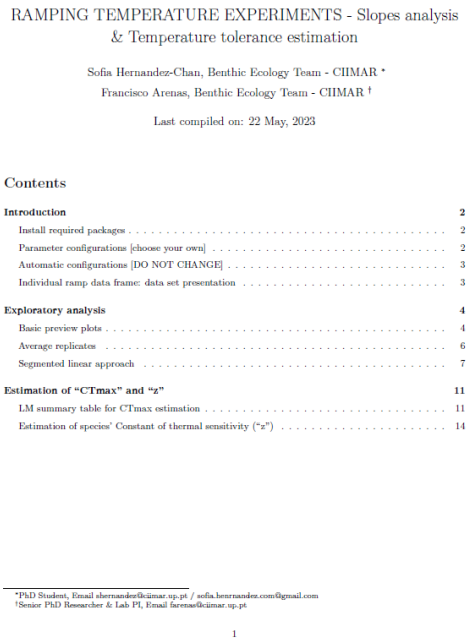

RAMPING TEMPERATURE EXPERIMENTS - Slopes analysis
& Temperature tolerance estimation

Sofia Hernandez-Chan, Benthic Ecology Team - CIIMAR *
Francisco Arenas, Benthic Ecology Team - CIIMAR †

Last compiled on: 22 May, 2023

Contents



*PhD Student, Email shernandez@ciimar.up.pt / sofia.henrandez.com@gmail.com
†Senior PhD Researcher & Lab PI, Email farenas@ciimar.up.pt

1

*Figure 39: Protocol to perform slope analyses and Temperature tolerance parameters*

The script allows to estimate directly from experimental data the CTmax and the (i.e. the temperature that would result in knockdown or death at log10 t = 0 that corresponds, by definition, to 1 min) and the constant of thermal susceptibility z, which describes how thermal tolerance decays with the duration of the heat challenge (i.e. the net reduction in $T_{crit}$ resulting from a tenfold increase in exposure time).

Our first trials comparing populations across the Atlantic distribution range of some intertidal species are now undergoing and some preliminary results are available (Figure 41). We plan to run trials at different laboratories using the Intertidal chamber which will be operative across the FutureMARES partners this summer.
Our first tests using populations from France, Norway and Portugal suggest interesting findings. ANCOVA (analyses of covariance) demonstrated species-specific differences across population but with a common pattern across species. The populations from Norway always showed lower CTmax than those from Portugal.

Furthermore some differences among species were also obvious (Figure 41). In the case of *Ascophyllum nodosum* no differences in Ctmax-Time relationships were

found for populations from Portugal and France while Norway had a smaller intercept value (i.e. lower theoretical thermal maximum). In *Fucus vesiculosus*, population from France and Norway did not exhibited any difference but Portuguese population exhibited a larger CTmax. Finally, in the case of *Fucus serratus*, we found a gradient of increasing CTmax from Portugal to Norway. In this case slopes where also significantly different.

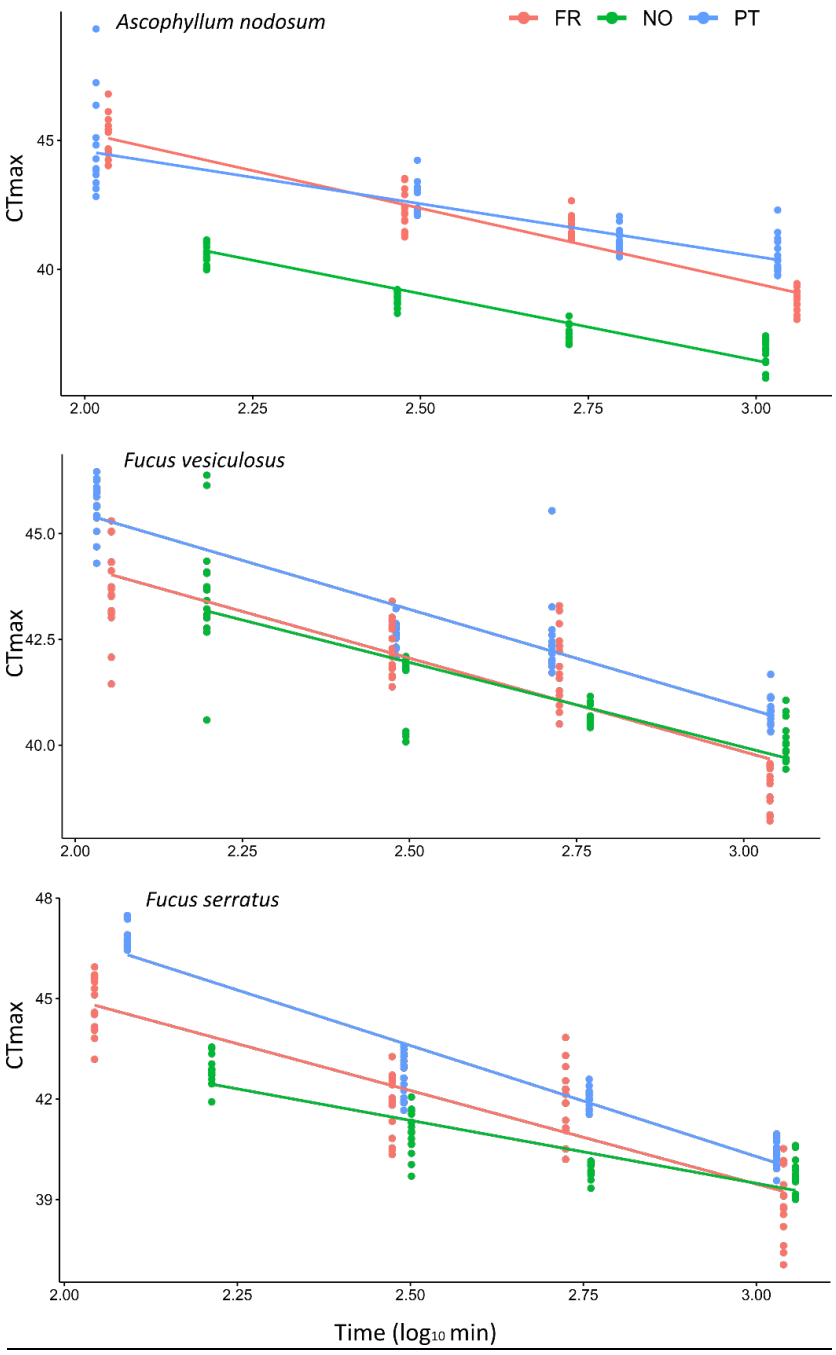


*Figure 40: CTmax-Time(log10 min-1)relationships for three different , see Rezende et al (2014) for Ascophyllum nodosum, Fucus vesiculosus and Fucus serratus in three different populations from Norway, France and Portugal.*

## Chapter 8 - General conclusions

Assessing species vulnerability to global climate change is a complex task that requires the integration of multiple lines of data and information (Figure 42). According to the IPCC fourth assessment report (2007) and common usage in the field of conservation and CCVA (Climate Change Vulnerability Assessment) of species, vulnerability to climate change results from the interaction of exposure to environmental stressors, the sensitivity to those stressors, and the adaptive capacity to cope with stressors (Foden et al., 2019). These same elements are combined in a different way in Climate Risk Assessments conducted in the IPCC fifth assessment report (AR5) and employed in FutureMARES WP5.

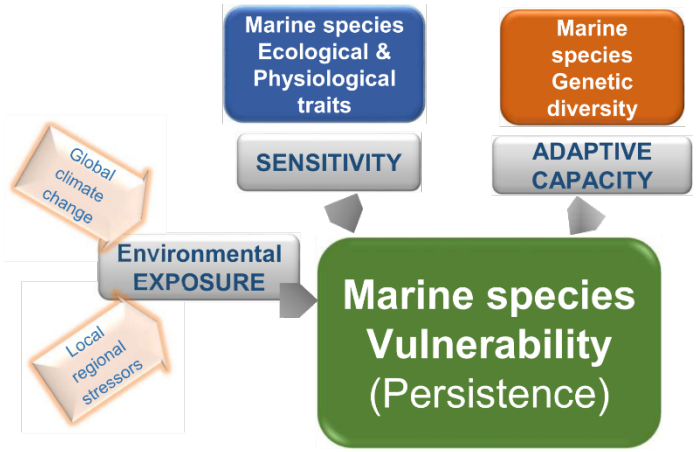


*Figure 41. Marine species vulnerability as a function of Exposure, Sensitivity and Adaptive Capacity (modified from Foden et al. 2019).*

In the last decade, ecological projection techniques such as species distribution models (SDM) have gained prominence as invaluable tools to assess the vulnerability of species to climate change (Sinclair et al., 2010). These modelling approaches involve correlating data on the current distribution of species with observations of recent climate. These correlations are then applied to climate projections to estimate the potential locations where suitable climatic conditions for a species may occur in the future (Willis et al., 2015).

Correlative approaches are often criticized for their inability to offer some understanding of the underlying processes (Sinclair et al., 2010; Peck et al., 2018). One way to increase the robustness of correlative SDMs projections is to use physiological tolerance knowledge that provides a mechanistic basis for inferring range constraints (Evans et al., 2015; Kearney & Porter 2009). However, one limitation of these models is that they often rely on physiological measures obtained from a single population to estimate the ability of an entire species to respond to environmental changes (Lecocq et al., 2019). In other words, models implicitly assume that physiological niches are uniform

across different populations within a species (Peterson, 2011; Bennett et al., 2019), which may not accurately reflect the true variability in responses among populations. Ignoring the potential for such locally-adapted variation greatly risks under- or over-estimating species sensitivity to climate change (Cacciapaglia & van Woesik, 2015).

Although some analyses are still ongoing, experiments performed on habitat-forming species (from gorgonian and oyster reefs to primary producers such as seagrasses and seaweeds) shed new light on the adaptive capacity of species by documenting population-specific (regional) differences in thermal tolerance. For example, the results of experiments on European flat oysters revealed that Norwegian populations exhibited superior performance compared to those from the Netherlands. However, additional comparison with a Croatian population was largely inconclusive due to the low health quality of the individuals upon their arrival. The next step are analyses offering insights on whether these observed differences in thermal physiology and growth performance have a genetic basic. So far, three distinct genetic clusters have been identified for the flat oyster in Europe: one comprising the Netherlands and Denmark, another from France, Ireland, and England, and a third exclusive to Spain (Vera et al., 2016).

Task 3.2 included three examples of experiments conducted canopy-forming plants from the Atlantic and Mediterranean Sea that suggest regional, population-specific, differences in thermal tolerance. In the first example, the growth physiology of the Atlantic brown intertidal seaweed *Ascophyllum nodosum* under heatwave conditions was compared across nine populations from Portugal to Norway. These experiments represent some of the first attempts to incorporate realistic atmospheric heatwave gradients in experiments with intertidal species. Due to their inherent complexity, the results are still being analysed. Preliminary findings indicate significant variations among metabolic rates in the populations, with individuals from the Norway having lower Topt and populations from the Portugal showing the highest responses to warming and higher Topt. Atmospheric heatwaves were more deleterious in northern populations, especially when combined with conditions of cold seawater at high tide. Similar, regional (population-specific) differences were also observed in the thermal tolerance experiments done with canopy-forming caespitose algae (*Ericaria crinita*) in the Mediterranean. In this second example, populations of this alga inhabiting the warmer range of the distribution exhibited greater tolerance to high temperatures compared to populations from colder thermal regimes. In a third example, regional-scale differences in thermal tolerance were documented and related to the frequency and magnitude of previous exposure to heatwaves in the seagrass *Posidonia oceanica*. In this case, plants

that have been historically exposed to a greater cumulative heat stress tended to have a higher tolerance to thermal stress.

Beyond large regional comparisons among populations, two of the studies compared the effects of CC stressors on local populations at different water depths in a *Posidonia oceanica* meadow and among local populations with high genetic distinctiveness in the red gorgonian *Paramuricea clavat*a from the Mediterranean Sea. In the first case, it was observed that heat stress-induced damage was more pronounced in populations inhabiting deeper (colder with more stable temperature) waters. However, these responses were likely connected to acclimation response within the species. In the study with the red gorgonian, necrosis rates due to thermal stress were highly variable within populations, with time and even among individuals.

In summary, our results add compelling evidence that local conditions can cause adjustments in physiological responses of marine plants and animals to climate-driven stressors. In general, populations from cooler locations were more sensitive to increased temperature than populations found in warmer locations as has been previously reported (e.g. King et al., 2018). While there is a clear understanding of the presence of evolutionary physiological limits to thermal tolerance in species, particularly concerning upper thermal boundaries, the work reported here in Task 3.2 adds to the increasing body of evidence suggesting intraspecific adjustments of tolerance thresholds of species in response to prevailing local climate conditions (Bennett et al., 2021). By incorporating this information into models projecting climate change impacts, we can enhance our ability to make robust projections of climate impacts on the distribution of species and plan more effective, climate-ready restoration actions for habitat-forming species to preserve and/or enhance marine biodiversity.

## Indexes

### *Index of figures*

### *Index of tables*

### *References*


Alexandre A, Silva J, Buapet P, Björk M, Santos R. 2012. Effects of CO2 enrichment on photosynthesis, growth, and nitrogen metabolism of the seagrass *Zostera noltii*. Ecology and Evolution **2**: 2625–2635.

Angilletta, M. J. 2009. Thermal adaptation : a theoretical and empirical synthesis. Oxford University Press, Oxford ; New York.

Antão, L. H., B. Weigel, G. Strona, M. Hällfors, E. Kaarlejärvi, T. Dallas, Ø. H. Opedal, J. Heliölä, H. Henttonen, O. Huitu, E. Korpimäki, M. Kuussaari, A. Lehikoinen, R. Leinonen, A. Lindén, P. Merilä, H. Pietiäinen, J. Pöyry, M. Salemaa, T. Tonteri, K. Vuorio, O. Ovaskainen, M. Saastamoinen, J. Vanhatalo, T. Roslin, and A.-L. Laine. 2022. Climate change reshuffles northern species within their niches. Nature Climate Change **12**:587-592.

Anton, A., J. L. Randle, F. C. Garcia, S. Rossbach, J. I. Ellis, M. Weinzierl, and C. M. Duarte. 2020. Differential thermal tolerance between algae and corals may trigger the proliferation of algae in coral reefs. Glob Chang Biol **26**:4316-4327.

Arizmendi-Mejía, R., J.-B. Ledoux, S. Civit, A. Antunes, Z. Thanopoulou, J. Garrabou, and C. Linares. 2015. Demographic responses to warming: reproductive maturity and sex influence vulnerability in an octocoral. Coral Reefs **34**:1207-1216.

Arnold TM, Tanner CE, Rothen M, Bullington J. 2008. Wound-induced accumulations of condensed tannins in turtlegrass, *Thalassia testudinum*. Aquatic Botany **89**: 27-33.

Assis, J., E. Á. Serrão, N. C. Coelho, F. Tempera, M. Valero, and F. Alberto. 2018. Past climate changes and strong oceanographic barriers structured low-latitude genetic relics for the golden kelp *Laminaria ochroleuca*. Journal of Biogeography **45**: 2326-2336.

Barbier, E.B., Hacker, S.D., Kennedy, C., Koch, E.W., Stier, A.C. & Silliman, B.R. (2011). The value of estuarine and coastal ecosystem services. Ecological Monographs, **81**: 169-193.

Bates D, Mächler M, Bolker B, Walker S (2015). “Fitting Linear Mixed-Effects Models Using lme4.” Journal of Statistical Software, **67**(1): 1–48.

Bates, A. E., and S. A. Morley. 2020. Interpreting empirical estimates of experimentally derived physiological and biological thermal limits in ectotherms. Canadian Journal of Zoology **98**: 237-244.

Beca-Carretero P, Guihéneuf F, Winters G. 2019. Depth-induced adjustment of fatty acid and pigment composition suggests high biochemical plasticity in the tropical seagrass Halophila stipulacea . Marine Ecology Progress Series, **608**: 105–117.

Bennett, S., C. M. Duarte, N. Marba, and T. Wernberg. 2019. Integrating within-species variation in thermal physiology into climate change ecology. Philos Trans R Soc Lond B Biol Sci **374**: 20180550.

Bennett, S., T. Wernberg, B. Arackal Joy, T. de Bettignies, and A. H. Campbell. 2015. Central and rear-edge populations can be equally vulnerable to warming. Nat Commun **6**: 10280.

Benzie, I.F.F. & Strain, J.J. (1996). The ferric reducing ability of plasma (FRAP) as a measure of "antioxidant power": The FRAP assay. Analytical Biochemistry, **239**: 70-76.

Berlinghof J, Peiffer F, Marzocchi U, Munari M, Quero GM, Dennis L, Wild C, Cardini U. 2022. The role of epiphytes in seagrass productivity under ocean acidification. Scientific Reports **12**: 1–9.

Bertolini, C., S. Rubinetti, G. Umgiesser, R. Witbaard, T. J. Bouma, A. Rubino, and R. Pastres. 2021. How to cope in heterogeneous coastal environments: Spatio-temporally endogenous circadian rhythm of valve gaping by mussels. Sci Total Environ **768**:145085.

Bolser RC, Hay ME, Lindquist N, Fenical W, Wilson D. 1998. Chemical defenses of freshwater macrophytes against crayfish herbivory. Journal of chemical Ecology **24**: 1639–1658.

Borum J, Pedersen O, Kotula L, Fraser MW, Statton J, Colmer TD, Kendrick GA. 2016. Photosynthetic response to globally increasing CO2 of co-occurring temperate seagrass species. Plant, Cell & Environment **39**: 1240–1250.

Brandt LA, Koch EW. 2003. Periphyton as a UV-B filter on seagrass leaves: A result of different transmittance in the UV-B and PAR ranges. Aquatic Botany **76**: 317–327.

Briggs AA, Carpenter RC. 2019. Contrasting responses of photosynthesis and photochemical efficiency to ocean acidification under different light environments in a calcifying alga. Scientific reports **9**: 1–10.

Bulleri F, Eriksson BK, Queirós A, Airoldi L, Arenas F, Arvanitidis C, Bouma TJ, Crowe TP, Davoult D, Guizien K. 2018. Harnessing positive species interactions as a tool against climate-driven loss of coastal biodiversity. PLoS biology **16**: e2006852.

Bulleri, F., Batten, S., Connell, S.D., Benedetti-Cecchi, L., Gibbons, M., Nugues, M.M. et al. (2021). Human pressures and the emergence of novel marine ecosystems. Oceanography and Marine Biology: An Annual Review, Vol **58**: 441.

Burrows, M.T., Schoeman, D.S., Buckley, L.B., Moore, P., Poloczanska, E.S., Brander, K.M. et al. (2011). The Pace of Shifting Climate in Marine and Terrestrial Ecosystems. Science, **334**: 652-655.

Cacciapaglia, C., and R. van Woesik. 2015. Reef-coral refugia in a rapidly changing ocean. Glob Chang Biol **21**:2272-2282.

Calosi P, Melatunan S, Turner LM, Artioli Y, Davidson RL, Byrne JJ, Viant MR, Widdicombe S, Rundle SD. 2017. Regional adaptation defines sensitivity to future ocean acidification. Nature Communications **8**: 13994.

Campbell JE, Fourqurean JW. 2013. Effects of in situ CO2 enrichment on the structural and chemical characteristics of the seagrass Thalassia testudinum. Marine Biology **160**: 1465–1475.

Canty, A., and B. D. Ripley. 2022. boot: Bootstrap R (S-Plus) Functions. R package version 1.3-28.1.

Capdevila, P., B. Hereu, R. Salguero-Gómez, G. Rovira, A. Medrano, E. Cebrian, J. Garrabou, D. K. Kersting, and C. Linares. 2019. Warming impacts on early life stages increase the vulnerability and delay the population recovery of a long-lived habitat-forming macroalga. Journal of Ecology **107**:1129-1140.

Capo, X., Tejada, S., Ferriol, P., Pinya, S., Mateu-Vicens, G., Montero-Gonzalez, I. et al. (2020). Hypersaline water from desalinization plants causes oxidative damage in *Posidonia oceanica* meadows. Science of the Total Environment, **736**.

Carpenter, K. E., M. Abrar, G. Aeby, R. B. Aronson, S. Banks, A. Bruckner, A. Chiriboga, J. Cortés, J. C. Delbeek, L. DeVantier, G. J. Edgar, A. J. Edwards, D. Fenner, H. M. Guzmán, B. W. Hoeksema, G. Hodgson, O. Johan, W. Y. Licuanan, S. R. Livingstone, E. R. Lovell, J. A. Moore, D. O. Obura, D. Ochavillo, B. A. Polidoro, W. F. Precht, M. C. Quibilan, C. Reboton, Z. T. Richards, A. D. Rogers, J. Sanciangco, A. Sheppard, C. Sheppard, J. Smith, S. Stuart, E. Turak, J. E. N. Veron, C. Wallace, E. Weil, and E. Wood. 2008. One-Third of Reef-Building Corals Face Elevated Extinction Risk from Climate Change and Local Impacts. Science **321**:560-563.

Ceccherelli, G., S. Oliva, S. Pinna, L. Piazzi, G. Procaccini, L. Marin-Guirao, E. Dattolo, R. Gallia, G. La Manna, P. Gennaro, M. M. Costa, I. Barrote, J. Silva, and F. Bulleri. 2018. Seagrass collapse due to synergistic stressors is not anticipated by phenological changes. Oecologia **186**:1137-1152.

Cerrano, C., G. Bavestrello, C. N. Bianchi, R. Cattaneo-vietti, S. Bava, C. Morganti, C. Morri, P. Picco, G. Sara, S. Schiaparelli, A. Siccardi, and F. Sponga. 2000. A catastrophic mass-mortality episode of gorgonians and other organisms in the Ligurian Sea (North-western Mediterranean), summer 1999. Ecol Lett **3**:284-293.

Chefaoui, R. M., C. M. Duarte, and E. A. Serrao. 2018. Dramatic loss of seagrass habitat under projected climate change in the Mediterranean Sea. Global Change Biology **24**:4919-4928.

Chust G, Villarino E, McLean M, Mieszkowska N, Benedetti-Cecchi L, Bulleri F, Ravaglioli C, Borja A, Muxika I, Fernandes-Salvador JA, Ibaibarriaga L, Villate F, Iriarte A, Uriarte I, Zervoudaki S, Carstensen J, Somerfield PJ, Queirós AM, Auber A, Hidalgo M, Coll M, Garrabou J, Gómez-Gras D, Ramírez F, Margarit N, Lepage M, Dambrine C, Lobry J, Peck MA, de la Barra P, van Leeuwen A, Rilov G,0 Yeruham E, Lindegren M (Submitted) Cross-basin and cross-taxa patterns in biodiversity turnover in warming seas. Nature Communications

Coleman, M. A., and T. Wernberg. 2017. Forgotten underwater forests: The key role of fucoids on Australian temperate reefs. Ecology and Evolution **7**:8406-8418.

Coleman, M. A., G. Wood, K. Filbee-Dexter, A. J. P. Minne, H. D. Goold, A. Vergés, E. M. Marzinelli, P. D. Steinberg, and T. Wernberg. 2020. Restore or Redefine: Future Trajectories for Restoration. Frontiers in Marine Science **7**.

Coleman, M.A. & Wernberg, T. (2020). The Silver Lining of Extreme Events. Trends in Ecology & Evolution, 35: 1065-1067.
Collier CJ, Langlois L, Ow Y, Johansson C, Giammusso M, Adams MP, O'Brien KR, Uthicke S. 2018. Losing a winner: thermal stress and local pressures outweigh the positive effects of ocean acidification for tropical seagrasses. New Phytologist **219**: 1005–1017.
Collier CJ, Ow YX, Langlois L, Uthicke S, Johansson CL, O'Brien KR, Hrebien V, Adams MP. 2017. Optimum Temperatures for Net Primary Productivity of Three Tropical Seagrass Species. Frontiers in Plant Science **8**. https://doi.org/10.3389/fpls.2017.01446
Collier CJ, Uthicke S, Waycott M. 2011. Thermal tolerance of two seagrass species at contrasting light levels: Implications for future distribution in the Great Barrier Reef. Limnology and Oceanography **56**: 2200–2210.
Connell, S.D., Doubleday, Z.A., Foster, N.R., Hamlyn, S.B., Harley, C.D.G., Helmuth, B., Kelaher, B.P., Nagelkerken, I., Rodgers, K.L., Sarà, G., Russell, B.D., 2018. The duality of ocean acidification as a resource and a stressor. Ecology **99(5),** 1005–1010. https://doi. org/10.1002/ecy.2209
Commisso M, Toffali K, Strazzer P, Stocchero M, Ceoldo S, Baldan B, Levi M, Guzzo F. 2016. Impact of phenylpropanoid compounds on heat stress tolerance in carrot cell cultures. Frontiers in Plant Science **7**: 1439.
Cooper, B. S., B. H. Williams, and M. J. Angilletta. 2008. Unifying indices of heat tolerance in ectotherms. Journal of Thermal Biology **33**:320-323.
Cornwall CE, Comeau S, DeCarlo TM, Larcombe E, Moore B, Giltrow K, Puerzer F, D'alexis Q, McCulloch MT. 2020. A coralline alga gains tolerance to ocean acidification over multiple generations of exposure. Nature Climate Change **10**: 143–146.
Cornwall CE, Comeau S, Kornder NA, Perry CT, van Hooidonk R, DeCarlo TM, Pratchett MS, Anderson KD, Browne N, Carpenter R. 2021. Global declines in coral reef calcium carbonate production under ocean acidification and warming. Proceedings of the National Academy of Sciences **118**: e2015265118.
Costa MM, Barrote I, Silva J, Olivé I, Alexandre A, Albano S, Santos R. 2015. Epiphytes modulate *Posidonia oceanica* photosynthetic production, energetic balance, antioxidant mechanisms, and oxidative damage. Frontiers in Marine Science **2**: 111.
Coumou, D., and S. Rahmstorf. 2012. A decade of weather extremes. Nature Climate Change **2**:491-496.
Cox TE, Gazeau F, Alliouane S, Hendriks IE, Mahacek P, Le Fur A, Gattuso J-P. 2016. Effects of in situ CO2 enrichment on structural characteristics, photosynthesis, and growth of the Mediterranean seagrass *Posidonia oceanica* . Biogeosciences **13**: 2179–2194.
Cox TE, Schenone S, Delille J, Díaz-Castañeda V, Alliouane S, Gattuso J-P, Gazeau F. 2015. Effects of ocean acidification on *Posidonia oceanica* epiphytic community and shoot productivity. Journal of Ecology **103**: 1594–1609.
Cramer, W., J. Guiot, M. Fader, J. Garrabou, J.-P. Gattuso, A. Iglesias, M. A. Lange, P. Lionello, M. C. Llasat, S. Paz, J. Peñuelas, M. Snoussi, A. Toreti, M. N. Tsimplis, and E. Xoplaki. 2018. Climate change and interconnected risks to sustainable development in the Mediterranean. Nature Climate Change **8**:972-980.
Crisci, C., J. B. Ledoux, K. Mokhtar-Jamai, M. Bally, N. Bensoussan, D. Aurelle, E. Cebrian, R. Coma, J. P. Feral, M. La Riviere, C. Linares, P. Lopez-Sendino, C. Marschal, M. Ribes, N. Teixido, F. Zuberer, and J. Garrabou. 2017. Regional and local environmental conditions do not shape the response to warming of a marine habitat-forming species. Sci Rep **7**:5069.
Crisci, C., N. Bensoussan, J. C. Romano, and J. Garrabou. 2011. Temperature anomalies and mortality events in marine communities: insights on factors behind differential mortality impacts in the NW Mediterranean. PLoS One **6**:e23814.
Darmaraki, S., S. Somot, F. Sevault, P. Nabat, W. D. Cabos Narvaez, L. Cavicchia, V. Djurdjevic, L. Li, G. Sannino, and V. D. Sein. 2019. Future evolution of Marine Heatwaves in the Mediterranean Sea. Climate Dynamics **53**:1371-1392.
Dattolo E, Marín-Guirao L, Ruiz JM, Procaccini G. 2017. Long-term acclimation to reciprocal light conditions suggests depth-related selection in the marine foundation species *Posidonia oceanica*. Ecology and Evolution **7**: 1148–1164.
Dattolo E, Ruocco M, Brunet C, Lorenti M, Lauritano C, D'Esposito D, de Luca P, Sanges R, Mazzuca S, Procaccini G. 2014. Response of the seagrass *Posidonia oceanica* to different light environments: Insights from a combined molecular and photo-physiological study. Marine Environmental Research **101**: 225–236.

De Silva HC, Asaeda T. 2018. Stress response and tolerance of the submerged macrophyte Elodea nuttallii (Planch) St. John to heat stress: a comparative study of shock heat stress and gradual heat stress. Plant Biosystems - An International Journal Dealing with all Aspects of Plant Biology **152**: 787–794.

Dewanto V, Wu X, Adom KK, Liu RH. 2002. Thermal processing enhances the nutritional value of tomatoes by increasing total antioxidant activity. Journal of agricultural and food chemistry 50: 3010–3014.

Diaz-Almela, E., N. Marba, R. Martinez, R. Santiago, and C. M. Duarte. 2009. Seasonal dynamics of *Posidonia oceanica* in Magalluf Bay (Mallorca, Spain): Temperature effects on seagrass mortality. Limnology and Oceanography **54**:2170-2182.

Dickson AG, Afghan JD, Anderson GC. 2003. Reference materials for oceanic CO2 analysis: a method for the certification of total alkalinity. Marine Chemistry **80**: 185–197.

Díez, I., N. Muguerza, A. Santolaria, U. Ganzedo, and J. M. Gorostiaga. 2012. Seaweed assemblage changes in the eastern Cantabrian Sea and their potential relationship to climate change. Estuarine, Coastal and Shelf Science **99**:108-120.

Doney SC, Fabry VJ, Feely RA, Kleypas JA. 2009. Ocean Acidification: The Other CO2 Problem. Annual Review of Marine Science **1**: 169–192.

Doney SC, Ruckelshaus M, Emmett Duffy J, Barry JP, Chan F, English CA, Galindo HM, Grebmeier JM, Hollowed AB, Knowlton N, et al. 2011. Climate Change Impacts on Marine Ecosystems. Annual Review of Marine Science **4**: 11–37.

Duarte CM. 1991. Seagrass depth limits. Aquatic botany 40: 363–377.

DuBois, K., S. L. Williams, and J. J. Stachowicz. 2020. Previous exposure mediates the response of eelgrass to future warming via clonal transgenerational plasticity. Ecology **101**: e03169

Dybsland, C. S., T. Bekkby, K. H. Enerstvedt, O. M. Kvalheim, E. Rinde, and M. Jordheim. 2021. Variation in Phenolic Chemistry in Zostera marina Seagrass along Environmental Gradients. Plants-Basel **10**.

Egea LG, Jiménez-Ramos R, Vergara JJ, Hernández I, Brun FG. 2018. Interactive effect of temperature, acidification and ammonium enrichment on the seagrass Cymodocea nodosa. Marine Pollution Bulletin **134**: 14–26.

Eggert, A. 2012. Seaweed Responses to Temperature.

Evans, T. G., S. E. Diamond, and M. W. Kelly. 2015. Mechanistic species distribution modelling as a link between physiology and conservation. Conserv Physiol **3**:cov056.

Falkenberg LJ, Scanes E, Ducker J, Ross PM. 2021. Biotic habitats as refugia under ocean acidification. Conservation Physiology **9**: coab077.

Feldmann, J. 1934. Les Laminariacées de la Méditerranée et leur répartition géographique. Bull. Stat. Aquic. et Pêche Castiglione **2**.

Feldmann, J. 1937. Recherches sur la végétation marine de la Médoterranée: la côte des Albères. Revue Algologique **10**:1-340.

Foden, W. B., B. E. Young, H. R. Akcakaya, R. A. Garcia, A. A. Hoffmann, B. A. Stein, C. D. Thomas, C. J. Wheatley, D. Bickford, J. A. Carr, D. G. Hole, T. G. Martin, M. Pacifici, J. W. Pearce-Higgins, P. J. Platts, P. Visconti, J. E. M. Watson, and B. Huntley. 2019. Climate change vulnerability assessment of species. Wiley Interdisciplinary Reviews-Climate Change **10**.

Franssen SU, Gu J, Winters G, Huylmans A-K, Wienpahl I, Sparwel M, Coyer JA, Olsen JL, Reusch TBH, Bornberg-Bauer E. 2014. Genome-wide transcriptomic responses of the seagrasses Zostera marina and Nanozostera noltii under a simulated heatwave confirm functional types. Marine Genomics **15**: 65–73.

Gao K, Xu J, Gao G, Li Y, Hutchins DA, Huang B, Wang L, Zheng Y, Jin P, Cai X, et al. 2012. Rising CO2 and increased light exposure synergistically reduce marine primary productivity. Nature Climate Change **2**: 519–523.

Garcia-Marquez, M. G., V. Fernandez-Juarez, J. C. Rodriguez-Castaneda, and N. S. R. Agawin. 2022. Response of *Posidonia oceanica* (L.) Delile and Its Associated N-2 Fixers to Different Combinations of Temperature and Light Levels. Frontiers in Marine Science **8**.

Garcias-Bonet, N., R. Vaquer-Sunyer, C. M. Duarte, and N. Marba. 2019. Warming effect on nitrogen fixation in Mediterranean macrophyte sediments. Biogeosciences **16**:167-175.

Garrabou, J., and J. G. Harmelin. 2002. A 20-year study on life-history traits of a harvested long-lived temperate coral in the NW Mediterranean: insights into conservation and management needs. Journal of Animal Ecology **71**:966-978.

Garrabou, J., D. Gómez-Gras, A. Medrano, C. Cerrano, M. Ponti, R. Schlegel, N. Bensoussan, E. Turicchia, M. Sini, V. Gerovasileiou, N. Teixido, A. Mirasole, L. Tamburello, E. Cebrian, G. Rilov, J.-B. Ledoux, J. B. Souissi, F. Khamassi, R. Ghanem, M. Benabdi, S. Grimes, O. Ocaña, H. Bazairi, B. Hereu, C. Linares, D. K. Kersting, G. la Rovira, J. Ortega, D. Casals, M. Pagès-Escolà, N. Margarit, P. Capdevila, J. Verdura, A. Ramos, A. Izquierdo, C. Barbera, E. Rubio-Portillo, I. Anton, P. López-Sendino, D. Díaz, M. Vázquez-Luis, C. Duarte, N. Marbà, E. Aspillaga, F. Espinosa, D. Grech, I. Guala, E. Azzurro, S. Farina, M. Cristina Gambi, G. Chimienti, M. Montefalcone, A. Azzola, T. P. Mantas, S. Fraschetti, G. Ceccherelli, S. Kipson, T. Bakran-Petricioli, D. Petricioli, C. Jimenez, S. Katsanevakis, I. T. Kizilkaya, Z. Kizilkaya, S. Sartoretto, R. Elodie, S. Ruitton, S. Comeau, J.-P. Gattuso, and J.-G. Harmelin. 2022. Marine heatwaves drive recurrent mass mortalities in the Mediterranean Sea. Global Change Biology **28**:5708-5725.

Garrabou, J., D. Gómez-Gras, J.-B. Ledoux, C. Linares, N. Bensoussan, P. López-Sendino, H. Bazairi, F. Espinosa, M. Ramdani, S. Grimes, M. Benabdi, J. B. Souissi, E. Soufi, F. Khamassi, R. Ghanem, O. Ocaña, A. Ramos-Esplà, A. Izquierdo, I. Anton, E. Rubio-Portillo, C. Barbera, E. Cebrian, N. Marbà, I. E. Hendriks, C. M. Duarte, S. Deudero, D. Díaz, M. Vázquez-Luis, E. Alvarez, B. Hereu, D. K. Kersting, A. Gori, N. Viladrich, S. Sartoretto, I. Pairaud, S. Ruitton, G. Pergent, C. Pergent-Martini, E. Rouanet, N. Teixidó, J.-P. Gattuso, S. Fraschetti, I. Rivetti, E. Azzurro, C. Cerrano, M. Ponti, E. Turicchia, G. Bavestrello, R. Cattaneo-Vietti, M. Bo, M. Bertolino, M. Montefalcone, G. Chimienti, D. Grech, G. Rilov, I. Tuney Kizilkaya, Z. Kizilkaya, N. Eda Topçu, V. Gerovasileiou, M. Sini, T. Bakran-Petricioli, S. Kipson, and J. G. Harmelin. 2019. Collaborative Database to Track Mass Mortality Events in the Mediterranean Sea. Frontiers in Marine Science **6**.

Garrabou, J., R. Coma, N. Bensoussan, M. Bally, P. ChevaldonnÉ, M. Cigliano, D. Diaz, J. G. Harmelin, M. C. Gambi, D. K. Kersting, J. B. Ledoux, C. Lejeusne, C. Linares, C. Marschal, T. PÉRez, M. Ribes, J. C. Romano, E. Serrano, N. Teixido, O. Torrents, M. Zabala, F. Zuberer, and C. Cerrano. 2009. Mass mortality in Northwestern Mediterranean rocky benthic communities: effects of the 2003 heat wave. Global Change Biology **15**:1090-1103.

Gattuso J-P, Epitalon J-M, Lavigne H, Orr J, Gentili B, Hagens M, Hofmann A, Mueller J-D, Proye A, Rae J. 2015. Package 'seacarb'. Preprint at http://cran. r-project. org/package= seacarb.

Genin A, Levy L, Sharon G, Raitsos DE, Diamant A. 2020. Rapid onsets of warming events trigger mass mortality of coral reef fish. Proceedings of the National Academy of Sciences **117**: 25378–25385.

Genty B, Briantais J-M, Baker NR. 1989. The relationship between the quantum yield of photosynthetic electron transport and quenching of chlorophyll fluorescence. Biochimica et Biophysica Acta (BBA) - General Subjects **990**: 87–92.

Giaccone, G. 1969. Note Sistematiche ed Osservazioni Fitosociologiche Sulle Laminariales del Mediterraneo Occidentale. Giornale botanico italiano **103**:457-474.

Giaccone, G., and A. Bruni. 1973. Le *Cystoseire* e la vegetazione sommersa del Mediterraneo. Veneto Scienze, Lettere ed Arti **131**:59-103.

Gómez Garreta, A. 2000. Flora phycologica iberica. Vol. 1. Fucales, Murcia.

Gomez-Gras, D., C. Linares, A. Lopez-Sanz, R. Amate, J. B. Ledoux, N. Bensoussan, P. Drap, O. Bianchimani, C. Marschal, O. Torrents, F. Zuberer, E. Cebrian, N. Teixido, M. Zabala, S. Kipson, D. K. Kersting, I. Montero-Serra, M. Pages-Escola, A. Medrano, M. Frleta-Valic, D. Dimarchopoulou, P. Lopez-Sendino, and J. Garrabou. 2021. Population collapse of habitat-forming species in the Mediterranean: a long-term study of gorgonian populations affected by recurrent marine heatwaves. Proc Biol Sci **288**:20212384.

Gomez-Gras, D., N. Bensoussan, J. B. Ledoux, P. Lopez-Sendino, C. Cerrano, E. Ferretti, S. Kipson, T. Bakran-Petricioli, E. A. Serrao, D. Paulo, M. A. G. Coelho, G. A. Pearson, J. Boavida, I. Montero-Serra, M. Pages-Escola, A. Medrano, A. Lopez-Sanz, M. Milanese, C. Linares, and J. Garrabou. 2022. Exploring the response of a key Mediterranean gorgonian to heat stress across biological and spatial scales. Sci Rep **12**:21064.

Goudet, J. 2005. hierfstat, a package for r to compute and test hierarchical F-statistics. Molecular Ecology Notes **5**:184-186.

Hall-Spencer, J. M., R. Rodolfo-Metalpa, S. Martin, E. Ransome, M. Fine, S. M. Turner, S. J. Rowley, D. Tedesco, and M. C. Buia. 2008. Volcanic carbon dioxide vents show ecosystem effects of ocean acidification. Nature **454**:96-99.

Harris, R.M.B., Beaumont, L.J., Vance, T.R., Tozer, C.R., Remenyi, T.A., Perkins-Kirkpatrick, S.E. et al. (2018). Biological responses to the press and pulse of climate trends and extreme events. Nature Climate Change **8**: 579-587.

Haure, J., C. Penisson, S. Bougrier, and J. P. Baud. 1998. Influence of temperature on clearance and oxygen consumption rates of the flat oyster Ostrea edulis: determination of allometric coefficients. Aquaculture **169**:211-224.

Hendriks IE, Olsen YS, Ramajo L, Basso L, Steckbauer A, Moore TS, Howard J, Duarte CM. 2014. Photosynthetic activity buffers ocean acidification in seagrass meadows. Biogeosciences **11**: 333–346.

Hepburn CD, PRITCHARD DW, CORNWALL CE, McLEOD RJ, BEARDALL J, RAVEN JA, HURD CL. 2011. Diversity of carbon use strategies in a kelp forest community: implications for a high CO2 ocean. Global Change Biology **17**: 2488–2497.

Hoegh-Guldberg, O., E. S. Poloczanska, W. Skirving, and S. Dove. 2017. Coral reef ecosystems under climate change and ocean acidification. Frontiers in Marine Science **4**.

Hoffmann, A. A., and C. M. Sgro. 2011. Climate change and evolutionary adaptation. Nature **470**:479-485.

Hu X, Burdige DJ, Zimmerman RC. 2012. δ13C is a signature of light availability and photosynthesis in seagrass. Limnology and Oceanography **57**: 441–448.

Hughes AR, Williams SL, Duarte CM, Heck Jr KL, Waycott M. 2009. Associations of concern: declining seagrasses and threatened dependent species. Frontiers in Ecology and the Environment **7**: 242–246.

Hughes, T. P., J. T. Kerry, M. Álvarez-Noriega, J. G. Álvarez-Romero, K. D. Anderson, A. H. Baird, R. C. Babcock, M. Beger, D. R. Bellwood, R. Berkelmans, T. C. Bridge, I. R. Butler, M. Byrne, N. E. Cantin, S. Comeau, S. R. Connolly, G. S. Cumming, S. J. Dalton, G. Diaz-Pulido, C. M. Eakin, W. F. Figueira, J. P. Gilmour, H. B. Harrison, S. F. Heron, A. S. Hoey, J. P. A. Hobbs, M. O. Hoogenboom, V. E. Kennedy, C. Y. Kuo, J. M. Lough, R. J. Lowe, G. Liu, M. T. McCulloch, H. A. Malcolm, M. J. McWilliam, J. M. Pandolfi, R. J. Pears, M. S. Pratchett, V. Schoepf, T. Simpson, W. J. Skirving, B. Sommer, G. Torda, D. R. Wachenfeld, B. L. Willis, and S. K. Wilson. 2017. Global warming and recurrent mass bleaching of corals. Nature **543**:373-377.

Jakobsson-Thor, S., J. Brakel, G. B. Toth, and H. Pavia. 2020. Complex Interactions of Temperature, Light and Tissue Damage on Seagrass Wasting Disease in Zostera marina. Frontiers in Marine Science **7**.

Jiang ZJ, Huang X-P, Zhang J-P. 2010. Effects of CO2 Enrichment on Photosynthesis, Growth, and Biochemical Composition of Seagrass Thalassia hemprichii (Ehrenb.) Aschers. Journal of Integrative Plant Biology **52**: 904–913.

Jombart, T. 2008. adegenet: a R package for the multivariate analysis of genetic markers. Bioinformatics **24**:1403-1405.

Jorda, G., N. Marba, and C. M. Duarte. 2012. Mediterranean seagrass vulnerable to regional climate warming. Nature Climate Change **2**:821-824.

Jorgensen, L. B., H. Malte, M. Orsted, N. A. Klahn, and J. Overgaard. 2021. A unifying model to estimate thermal tolerance limits in ectotherms across static, dynamic and fluctuating exposures to thermal stress. Sci Rep **11**:12840.

Kamvar, Z. N., J. C. Brooks, and N. J. Grunwald. 2015. Novel R tools for analysis of genome-wide population genetic data with emphasis on clonality. Front Genet **6**:208.

Kearney, M., and W. Porter. 2009. Mechanistic niche modelling: combining physiological and spatial data to predict species' ranges. Ecol Lett **12**:334-350.

King, N. G., N. J. McKeown, D. A. Smale, and P. J. Moore. 2018. The importance of phenotypic plasticity and local adaptation in driving intraspecific variability in thermal niches of marine macrophytes. Ecography **41**:1469-1484.

Koch, M., G. Bowes, C. Ross, and X.-H. Zhang. 2013. Climate change and ocean acidification effects on seagrasses and marine macroalgae. Global Change Biology **19**:103-132.

Kroeker KJ, Kordas RL, Crim R, Hendriks IE, Ramajo L, Singh GS, Duarte CM, Gattuso J. 2013. Impacts of ocean acidification on marine organisms: quantifying sensitivities and interaction with warming. Global change biology **19**: 1884–1896.

Kroeker KJ, Kordas RL, Crim RN, Singh GG. 2010. Meta-analysis reveals negative yet variable effects of ocean acidification on marine organisms. Ecology Letters **13**: 1419–1434.
Kroeker KJ, Kordas RL, Harley CDG. 2017. Embracing interactions in ocean acidification research: confronting multiple stressor scenarios and context dependence. Biology Letters **13**: 20160802.
Kroeker, K. J., M. C. Gambi, and F. Micheli. 2013. Community dynamics and ecosystem simplification in a high-$CO_2$ ocean. Proc Natl Acad Sci U S A **110**:12721-12726.
Krumhansl, K. A., D. K. Okamoto, A. Rassweiler, M. Novak, J. J. Bolton, K. C. Cavanaugh, S. D. Connell, C. R. Johnson, B. Konar, S. D. Ling, F. Micheli, K. M. Norderhaug, A. Pérez-Matus, I. Sousa-Pinto, D. C. Reed, A. K. Salomon, N. T. Shears, T. Wernberg, R. J. Anderson, N. S. Barrett, A. H. Buschmann, M. H. Carr, J. E. Caselle, S. Derrien-Courtel, G. J. Edgar, M. Edwards, J. A. Estes, C. Goodwin, M. C. Kenner, D. J. Kushner, F. E. Moy, J. Nunn, R. S. Steneck, J. Vásquez, J. Watson, J. D. Witman, and J. E. K. Byrnes. 2016. Global patterns of kelp forest change over the past half-century. Proc Natl Acad Sci U S A **113**:13785-13790.
Larkum, A., R. J. Orth, and C. Duarte. 2007. Seagrasses: Biology. Ecology and Conservation. doi:10.1007/978-1-4020-2983-7.
Lauritano C, Ruocco M, Dattolo E, Buia MC, Silva J, Santos R, Olivé I, Costa MM, Procaccini G. 2015. Response of key stress-related genes of the seagrass *Posidonia oceanica* in the vicinity of submarine volcanic vents. Biogeosciences **12**: 4185–4194.
Lecocq, T., A. Harpke, P. Rasmont, O. Schweiger, and J. Bolliger. 2019. Integrating intraspecific differentiation in species distribution models: Consequences on projections of current and future climatically suitable areas of species. Diversity and Distributions **25**:1088-1100.
Lee, K.S., Short, F.T. & Burdick, D.M. (2004). Development of a nutrient pollution indicator using the seagrass, Zostera marina, along nutrient gradients in three New England estuaries. Aquatic Botany **78**: 197-216.
Liesner, D., L. Fouqueau, M. Valero, M. Y. Roleda, G. A. Pearson, K. Bischof, K. Valentin, and I. Bartsch. 2020. Heat stress responses and population genetics of the kelp Laminaria digitata (Phaeophyceae) across latitudes reveal differentiation among North Atlantic populations. Ecol Evol **10**:9144-9177.
Lima, F. P., and D. S. Wethey. 2009. Robolimpets: measuring intertidal body temperatures using biomimetic loggers. Limnology and Oceanography: Methods **7**:347-353.
Lima, F. P., and D. S. Wethey. 2012. Three decades of high-resolution coastal sea surface temperatures reveal more than warming. Nat Commun **3**:704.
Linares C, Vidal M, Canals M, Kersting DK, Amblas D, Aspillaga E, Cebrián E, Delgado-Huertas A, Díaz D, Garrabou J. 2015. Persistent natural acidification drives major distribution shifts in marine benthic ecosystems. Proceedings of the Royal Society B: Biological Sciences **282**: 20150587.
Linares, C., M. Vidal, M. Canals, D. K. Kersting, D. Amblas, E. Aspillaga, E. Cebrian, A. Delgado-Huertas, D. Diaz, J. Garrabou, B. Hereu, L. Navarro, N. Teixido, and E. Ballesteros. 2015. Persistent natural acidification drives major distribution shifts in marine benthic ecosystems. Proc Biol Sci **282**:20150587.
Linares, C., R. Coma, J. Garrabou, D. Díaz, and M. Zabala. 2008. Size distribution, density and disturbance in two Mediterranean gorgonians:Paramuricea clavataandEunicella singularis. Journal of Applied Ecology **45**:688-699.
Luo, Y., B. P. Boudreau, and A. Mucci. 2016. Disparate acidification and calcium carbonate desaturation of deep and shallow waters of the Arctic Ocean. Nat Commun **7**:12821.
Maberly SC, Stott AW, Gontero B. 2022. The differential ability of two species of seagrass to use carbon dioxide and bicarbonate and their modelled response to rising concentrations of inorganic carbon. Frontiers in Plant Science **13**.
Mannino AM, Micheli C. 2020. Ecological Function of Phenolic Compounds from Mediterranean Fucoid Algae and Seagrasses: An Overview on the Genus Cystoseira sensu lato and *Posidonia oceanica* (L.) Delile. Journal of Marine Science and Engineering **8**.
Marba, N., and C. M. Duarte. 2010. Mediterranean warming triggers seagrass (*Posidonia oceanica* ) shoot mortality. Global Change Biology **16**:2366-2375.
Mariani, S., M. E. Cefalì, E. Chappuis, M. Terradas, S. Pinedo, X. Torras, E. Jordana, A. Medrano, J. Verdura, and E. Ballesteros. 2019. Past and present of Fucales from shallow and sheltered shores in Catalonia. Regional Studies in Marine Science **32**:100824-100824.

Marín-Guirao L, Entrambasaguas L, Dattolo E, Ruiz JM, Procaccini G. 2017. Molecular Mechanisms behind the Physiological Resistance to Intense Transient Warming in an Iconic Marine Plant. Frontiers in Plant Science **8**.

Marín-Guirao L, Ruiz JM, Dattolo E, Garcia-Munoz R, Procaccini G. 2016. Physiological and molecular evidence of differential short-term heat tolerance in Mediterranean seagrasses. Scientific Reports **6**: 28615.

Martínez-Crego B, Olivé I, Santos R. 2014. CO2 and nutrient-driven changes across multiple levels of organization in *Zostera noltii* ecosystems. Biogeosciences **11**: 7237–7249.

Mazzuca S, Björk M, Beer S, Felisberto P, Gobert S, Procaccini G, Runcie J, Silva J, Borges AV, Brunet C. 2013. Establishing research strategies, methodologies and technologies to link genomics and proteomics to seagrass productivity, community metabolism, and ecosystem carbon fluxes. Frontiers in Plant Science **4**: 38.

Mierziak J, Kostyn K, Kulma A. 2014. Flavonoids as Important Molecules of Plant Interactions with the Environment. Molecules **19**: 16240–16265.

Monteiro, C., J. Pereira, R. Seabra, and F. P. Lima. 2022. Fine-scale survey of intertidal macroalgae reveals recent changes in a cold-water biogeographic stronghold. Frontiers in Marine Science **9**.

Morley, S. A., L. S. Peck, J. M. Sunday, S. Heiser, A. E. Bates, and A. Algar. 2019. Physiological acclimation and persistence of ectothermic species under extreme heat events. Global Ecology and Biogeography **28**:1018-1037.

Moyano M, Candebat C, Ruhbaum Y, Álvarez-Fernández S, Claireaux G, Zambonino-Infante J-L, Peck MA (2017) Effects of warming rate, acclimation temperature and ontogeny on the critical thermal maximum of temperate marine fish larvae. PLoS ONE doi.org/10.1371/journal.pone.0179928

Müller, R., T. Laepple, I. Bartsch, and C. Wiencke. 2009. Impact of oceanic warming on the distribution of seaweeds in polar and cold-temperate waters. Botanica Marina **52**:617-638.

Nagelkerken I, Connell SD. 2015. Global alteration of ocean ecosystem functioning due to increasing human CO2 emissions. Proceedings of the National Academy of Sciences **112**: 13272–13277.

Nguyen HM, Ralph PJ, Marín-Guirao L, Pernice M, Procaccini G. 2021. Seagrasses in an era of ocean warming: a review. Biological Reviews **96**: 2009–2030.

Nguyen, H. M., F. Bulleri, L. Marin-Guirao, M. Pernice, and G. Procaccini. 2021. Photo-physiology and morphology reveal divergent warming responses in northern and southern hemisphere seagrasses. Marine Biology **168**: 129

Niell, F. X. 1977. Distribución y zonación de las algas bentónicas en las facies rocosa del sistema intermareal de las Rías Bajas Gallegas. Investigaciones Pesqueras **41**:219-237.

Olabarria, C., I. Gestoso, F. P. Lima, E. Vazquez, L. A. Comeau, F. Gomes, R. Seabra, and J. M. Babarro. 2016. Response of Two Mytilids to a Heatwave: The Complex Interplay of Physiology, Behaviour and Ecological Interactions. PLoS One **11**:e0164330.

Olivé I, Vergara JJ, Pérez-Lloréns JL. 2013. Photosynthetic and morphological photoacclimation of the seagrass *Cymodocea nodosa* to season, depth and leaf position. Marine Biology **160**: 285–297.

Oliver, E. C. J., M. G. Donat, M. T. Burrows, P. J. Moore, D. A. Smale, V. L. Alexander, J. A. Benthuysen, M. Feng, A. Sen Gupta, A. J. Hobday, N. J. Holbrook, S. E. Perkins-Kirkpatrick, H. A. Scannell, S. C. Straub, and T. Wernberg. 2018. Longer and more frequent marine heatwaves over the past century. Nat Commun **9**:1-12.

Oliver, E. C. J., M. T. Burrows, M. G. Donat, A. Sen Gupta, V. L. Alexander, S. E. Perkins-Kirkpatrick, J. A. Benthuysen, A. J. Hobday, N. J. Holbrook, P. J. Moore, M. S. Thomsen, T. Wernberg, and D. A. Smale. 2019. Projected marine heatwaves in the 21st century and the potential for ecological impact. Frontiers in Marine Science **6**:1-12.

Olsen, J. L., F. W. Zechman, G. Hoarau, J. A. Coyer, W. T. Stam, M. Valero, and P. Åberg. 2010. The phylogeographic architecture of the fucoid seaweed *Ascophyllum nodosum*: an intertidal 'marine tree' and survivor of more than one glacial-interglacial cycle. Journal of Biogeography **37**:842-856.

Orth RJ, Carruthers TJB, Dennison WC, Duarte CM, Fourqurean JW, Heck KL, Hughes AR, Kendrick GA, Kenworthy WJ, Olyarnik S, et al. 2006. A Global Crisis for Seagrass Ecosystems. BioScience **56**: 987–996.

Ow YX, Collier CJ, Uthicke S. 2015. Responses of three tropical seagrass species to CO2 enrichment. Marine Biology **162**: 1005–1017.
Ow YX, Uthicke S, Collier CJ. 2016. Light levels affect carbon utilisation in tropical seagrass under ocean acidification. PloS one **11**: e0150352.
Padfield, D., H. O'Sullivan, and S. Pawar. 2021. rTPC and nls.multstart : A new pipeline to fit thermal performance curves in R. Methods in Ecology and Evolution **12**:1138-1143.
Palacios, R Z. 2007. Response of eelgrass Zostera marina to CO2 enrichment: possible impacts of climate change and potential for remediation of coastal habitats. Marine Ecology Progress Series **344**: 1-13.
Parmesan, C. 2006. Ecological and Evolutionary Responses to Recent Climate Change. Annual Review of Ecology, Evolution, and Systematics **37**:637-669.
Pazzaglia, J., Reusch, T.B.H., Terlizzi, A., Marin-Guirao, L. & Procaccini, G. (2021). Phenotypic plasticity under rapid global changes: The intrinsic force for future seagrasses survival. Evolutionary Applications **14**: 1181-1201.
Peck, M.A., Arvanitidis, C., Butenschön, M., Melaku Canu, D., Chatzinikolaou, E., Cucco, A., Domenici, P., Fernandes, J.A., Gasche, L., Huebert, K.B., Hufnagl, M., Jones, M.C., Kempf, A., Keyl, F., Maar, M., Mahévas, S., Marchal, P., Nicolas, D., Pinnegar, J.K., Rivot, E., Rochette, S., Sell, A.F., Sinerchia, M., Solidoro, C., Somerfield, P.J., Teal, R.L., Travers-Trolet, M., van de Wolfshaar, K.E. (2018) Projecting changes in the distribution and productivity of living marine resources: A critical review of the suite of modeling approaches used in the large European project VECTORS. Estuarine, Coastal and Shelf Science 201:40-55
Peralta-Maraver, I., and E. L. Rezende. 2020. Heat tolerance in ectotherms scales predictably with body size. Nature Climate Change **11**:58-63.
Perkins, S. E., V. L. Alexander, and J. R. Nairn. 2012. Increasing frequency, intensity and duration of observed global heatwaves and warm spells. Geophysical Research Letters **39**:1-5.
Peterson, A. T. 2011. Ecological niche conservatism: a time-structured review of evidence. Journal of Biogeography **38**:817-827.
Pigliucci, M. (2005). Evolution of phenotypic plasticity: where are we going now? Trends in Ecology & Evolution, 20, 481-486.
Pineiro-Corbeira, C., R. Barreiro, and J. Cremades. 2016. Decadal changes in the distribution of common intertidal seaweeds in Galicia (NW Iberia). Mar Environ Res **113**:106-115.
Piñeiro-Corbeira, C., R. Barreiro, J. Cremades, and F. Arenas. 2018. Seaweed assemblages under a climate change scenario: Functional responses to temperature of eight intertidal seaweeds match recent abundance shifts. Sci Rep **8**:12978.
Pinna, S., L. Piazzi, G. Ceccherelli, A. Castelli, G. Costa, M. Curini-Galletti, P. Gianguzza, J. Langeneck, R. Manconi, M. Montefalcone, C. Pipitone, A. Rosso, and C. Bonaviri. 2020. Macroalgal forest vs sea urchin barren: Patterns of macro-zoobenthic diversity in a large-scale Mediterranean study. Mar Environ Res **159**:104955-104955.
Pinsky, M. L., A. M. Eikeset, D. J. McCauley, J. L. Payne, and J. M. Sunday. 2019. Greater vulnerability to warming of marine versus terrestrial ectotherms. Nature **569**:108-111.
Piro A, Bernardo L, Serra IA, Barrote I, Olivé I, Costa MM, Lucini L, Santos R, Mazzuca S, Silva J. 2020. Leaf proteome modulation and cytological features of seagrass Cymodocea nodosa in response to long-term high CO2 exposure in volcanic vents. Scientific Reports **10**: 1–13.
Poloczanska, E. S., C. J. Brown, W. J. Sydeman, W. Kiessling, D. S. Schoeman, P. J. Moore, K. Brander, J. F. Bruno, L. B. Buckley, M. T. Burrows, C. M. Duarte, B. S. Halpern, J. Holding, V. C. Kappel, M. I. O'Connor, J. M. Pandolfi, C. Parmesan, F. Schwing, S. A. Thompson, and A. J. Richardson. 2013. Global imprint of climate change on marine life. Nature Climate Change **3**:919-925.
Pörtner, H.O., Peck, M.A. 2010. Climate change impacts on fish and fisheries: towards a cause and effect understanding. Journal of Fish Biology **77**:1745-1779.
Procaccini G, Ruocco M, Marín-Guirao L, Dattolo E, Brunet C, D'Esposito D, Lauritano C, Mazzuca S, Serra IA, Bernardo L. 2017. Depth-specific fluctuations of gene expression and protein abundance modulate the photophysiology in the seagrass *Posidonia oceanica* . Scientific reports **7**: 1–15.
Ralph PJ, Tomasko D, Moore K, Seddon S, Macinnis-Ng CMO. 2006. Human impacts on seagrasses: Eutrophication, sedimentation, and contamination. In: Seagrasses: Biology, Ecology and Conservation.

Ravaglioli C, Lauritano C, Buia MC, Balestri E, Capocchi A, Fontanini D, Pardi G, Tamburello L, Procaccini G, Bulleri F. 2017. Nutrient Loading Fosters Seagrass Productivity under Ocean Acidification. Scientific Reports **7**: 1–14.

Ravaglioli, C., A. Capocchi, D. Fontanini, G. Mori, C. Nuccio, and F. Bulleri. 2018. Macro-grazer herbivory regulates seagrass response to pulse and press nutrient loading. Marine Environmental Research **136**:54-61.

Repolho T, Duarte B, Dionísio G, Paula JR, Lopes AR, Rosa IC, Grilo TF, Caçador I, Calado R, Rosa R. 2017. Seagrass ecophysiological performance under ocean warming and acidification. Scientific Reports **7**: 41443.

Rezende, E. L., L. E. Castañeda, M. Santos, and C. Fox. 2014. Tolerance landscapes in thermal ecology. Functional Ecology **28**:799-809.

Rezende, E. L., M. Tejedo, and M. Santos. 2010. Estimating the adaptive potential of critical thermal limits: methodological problems and evolutionary implications. Functional Ecology **25**:111-121.

Riahi K, Rao S, Krey V, Cho C, Chirkov V, Fischer G, Kindermann G, Nakicenovic N, Rafaj P. 2011. RCP 8.5—A scenario of comparatively high greenhouse gas emissions. Climatic Change **109**: 33.

Ricart AM, Ward M, Hill TM, Sanford E, Kroeker KJ, Takeshita Y, Merolla S, Shukla P, Ninokawa AT, Elsmore K, et al. 2021. Coast-wide evidence of low pH amelioration by seagrass ecosystems. Global Change Biology **27**: 2580–2591.

Richardson, J. L., M. C. Urban, D. I. Bolnick, and D. K. Skelly. 2014. Microgeographic adaptation and the spatial scale of evolution. Trends Ecol Evol **29**:165-176.

Rodríguez A, Moreno-Borges S, Brito A. 2022. Response of Cymodocea nodosa to ocean acidification and warming in the Canary Islands: Direct and indirect effects. Marine Environmental Research **176**: 105603.

Rodríguez-Prieto, C., E. Ballesteros, F. Boisset, and J. Afonso-Carrillo. 2013. Guía de las macroalgas y fanerógamas marinas del Mediterráneo occidental, Barcelona.

Rousset, F. 2008. genepop'007: a complete re-implementation of the genepop software for Windows and Linux. Molecular Ecology Resources **8**:103-106.

Ruiz-Montoya L, Sandoval-Gil JM, Belando-Torrentes MD, Vivanco-Bercovich M, Cabello-Pasini A, Rangel-Mendoza LK, Maldonado-Gutiérrez A, Ferrerira-Arrieta A, Guzmán-Calderón JM. 2021. Ecophysiological responses and self-protective canopy effects of surfgrass (Phyllospadix torreyi) in the intertidal. Marine Environmental Research **172**: 105501.

Ruocco M, Entrambasaguas L, Dattolo E, Milito A, Marín-Guirao L, Procaccini G. 2021. A king and vassals' tale: Molecular signatures of clonal integration in *Posidonia oceanica* under chronic light shortage. Journal of Ecology **109**: 294–312.

Ruocco M, Musacchia F, Olivé I, Costa MM, Barrote I, Santos R, Sanges R, Procaccini G, Silva J. 2017. Genomewide transcriptional reprogramming in the seagrass Cymodocea nodosa under experimental ocean acidification. Molecular Ecology **26**: 4241-4259.

Salois, S. L., T. C. Gouhier, B. Helmuth, F. Choi, R. Seabra, and F. P. Lima. 2022. Coastal upwelling generates cryptic temperature refugia. Sci Rep **12**:19313.

Sanford, E., and M. W. Kelly. 2011. Local Adaptation in Marine Invertebrates. Pages 509-535 *in* C. A. Carlson and S. J. Giovannoni, editors. Annual Review of Marine Science, Vol 3.

Sass E, Ben-Yaakov S. 1977. The carbonate system in hypersaline solutions: Dead Sea brines. Marine Chemistry **5**: 183-199.

Scartazza A, Moscatello S, Gavrichkova O, Buia MC, Lauteri M, Battistelli A, Lorenti M, Garrard SL, Calfapietra C, Brugnoli E. 2017. Carbon and nitrogen allocation strategy in *Posidonia oceanica* is altered by seawater acidification. Science of The Total Environment **607-608**: 954–964.

Schade, H., N. Arneth, M. Powilleit, and S. Forster. 2019. Sand gapers' breath: Respiration of Mya arenaria (L. 1758) and its contribution to total oxygen utilization in sediments. Mar Environ Res **143**:101-110.

Schiel, D. R., and M. S. Foster. 2006. The population biology of large brown seaweeds: Ecological consequences of multiphase life histories in dynamic coastal environments. Annual Review of Ecology, Evolution, and Systematics **37**:343-372.

Schneider G, Horta PA, Calderon EN, Castro C, Bianchini A, da Silva CRA, Brandalise I, Barufi JB, Silva J, Rodrigues AC. 2018. Structural and physiological responses of Halodule wrightii to ocean acidification. Protoplasma **255**: 629–641.

Serra IA, Lauritano C, Dattolo E, Puoti A, Nicastro S, Innocenti AM, Procaccini G. 2012. Reference genes assessment for the seagrass *Posidonia oceanica* in different salinity, pH and light conditions. Marine Biology **159**: 1269–1282.

Shah, A. A., H. A. Woods, J. C. Havird, A. C. Encalada, A. S. Flecker, W. C. Funk, J. M. Guayasamin, B. C. Kondratieff, N. L. Poff, S. A. Thomas, K. R. Zamudio, and C. K. Ghalambor. 2021. Temperature dependence of metabolic rate in tropical and temperate aquatic insects: Support for the Climate Variability Hypothesis in mayflies but not stoneflies. Glob Chang Biol **27**:297-311.

Sharon Y, Levitan O, Spungin D, Berman-Frank I, Beer S. 2011. Photoacclimation of the seagrass Halophila stipulacea to the dim irradiance at its 48-meter depth limit. Limnology and Oceanography **56**: 357–362.

Sims, D.A. & Gamon, J.A. 2002. Relationships between leaf pigment content and spectral reflectance across a wide range of species, leaf structures and developmental stages. Remote Sensing of Environment **81**: 337-354.

Sinclair, B., K. Marshall, M. Sewell, D. Levesque, C. Willett, S. Slotsbo, Y. Dong, C. Harley, D. Marshall, B. Helmuth, and R. Huey. 2016. Can we predict ectotherm responses to climate change using thermal performance curves and body temperatures? Ecol Lett **19**: ele.12686

Sinclair, S. J., M. D. White, and G. R. Newell. 2010. How Useful Are Species Distribution Models for Managing Biodiversity under Future Climates? Ecology and Society **15**.

Singleton, V.L., Orthofer, R. & Lamuela-Raventos, R.M. (1999). Analysis of total phenols and other oxidation substrates and antioxidants by means of Folin-Ciocalteu reagent. Oxidants and Antioxidants, Pt A, **299**: 152-178.

Slatkin, M. 1991. Inbreeding coefficients and coalescence times. Genetics Research **58**:167-175.

Smale, D. A. 2020. Impacts of ocean warming on kelp forest ecosystems. New Phytologist **225**:1447-1454.

Smale, D. A., and T. Wernberg. 2013. Extreme climatic event drives range contraction of a habitat-forming species. Proceedings of the Royal Society B: Biological Sciences **280**.

Somero, G. N. 2012. The Physiology of global change: Linking patterns to mechanisms. Annual Review of Marine Science **4**:39-61.

Sousa, M. C., A. Ribeiro, M. Des, M. Gomez-Gesteira, M. deCastro, and J. M. Dias. 2020. NW Iberian Peninsula coastal upwelling future weakening: Competition between wind intensification and surface heating. Sci Total Environ **703**:134808.

Steneck, R. S., and C. R. Johnson. 2013. Kelp forests: dynamic patterns, processes, and feedbacks. Pages 315-336 *in* M. Burtness, J. Bruno, B. Silliman, J. J. Stachowicz, M. Burtness, J. Bruno, B. Silliman, and J. J. Stachowicz, editors. Marine community ecology, Massachussets, USA.

Steneck, R. S., M. H. Graham, B. J. Bourque, D. Corbett, J. M. Erlandson, J. A. Estes, and M. J. Tegner. 2002. Kelp forest ecosystems: Biodiversity, stability, resilience and future. Environmental Conservation **29**:436-459.

Stipcich P, Resaikos V, Ceccherelli G. (2023). Experimental thermocline deepening highlights the resilience of the seagrass *Posidonia oceanica* : An opportunity to investigate shoot adaptability. Marine Pollution Bulletin **189**: 114824.

Stipcich, P., E. T. Apostolaki, N. Chartosia, P. T. Efthymiadis, C. E. Jimenez, G. La Manna, A. Pansini, E. Principato, V. Resaikos, and G. Ceccherelli. 2022. Assessment of *Posidonia oceanica* traits along a temperature gradient in the Mediterranean Sea shows impacts of marine warming and heat waves. Frontiers in Marine Science **9**.

Stuart-Smith, R. D., G. J. Edgar, N. S. Barrett, S. J. Kininmonth, and A. E. Bates. 2015. Thermal biases and vulnerability to warming in the world's marine fauna. Nature **528**:88-92.

Sunday JM, Fabricius KE, Kroeker KJ, Anderson KM, Brown NE, Barry JP, Connell SD, Dupont S, Gaylord B, Hall-Spencer JM. 2017. Ocean acidification can mediate biodiversity shifts by changing biogenic habitat. Nature Climate Change **7**: 81–85.

Sunday, J. M., A. E. Bates, and N. K. Dulvy. 2011. Global analysis of thermal tolerance and latitude in ectotherms. Proc Biol Sci **278**:1823-1830.

Sunday, J. M., A. E. Bates, and N. K. Dulvy. 2012. Thermal tolerance and the global redistribution of animals. Nature Climate Change **2**:686-690.

Sunday, J. M., K. E. Fabricius, K. J. Kroeker, K. M. Anderson, N. E. Brown, J. P. Barry, S. D. Connell, S. Dupont, B. Gaylord, J. M. Hall-Spencer, T. Klinger, M. Milazzo, P. L. Munday, B. D. Russell, E. Sanford, V. Thiyagarajan, M. L. H. Vaughan, S. Widdicombe,

and C. D. G. Harley. 2017. Ocean acidification can mediate biodiversity shifts by changing biogenic habitat. Nature Climate Change **7**:81-85.

Sunday, J. M., K. E. Fabricius, K. J. Kroeker, K. M. Anderson, N. E. Brown, J. P. Barry, S. D. Connell, S. Dupont, B. Gaylord, and J. M. Hall-Spencer. 2017. Ocean acidification can mediate biodiversity shifts by changing biogenic habitat. Nature Climate Change **7**:81-85.

Sydeman, W. J. 2014. Climate change and wind intensification in coastal upwelling ecosystems. Science **345**: 77-80.

Takahashi M, Noonan SHC, Fabricius KE, Collier CJ. 2016. The effects of long-term in situ CO2 enrichment on tropical seagrass communities at volcanic vents. ICES Journal of Marine Science **73**: 876–886.

Tanaka, K., S. Taino, H. Haraguchi, G. Prendergast, and M. Hiraoka. 2012. Warming off southwestern Japan linked to distributional shifts of subtidal canopy-forming seaweeds. Ecology and Evolution **2**:2854-2865.

Telesca, L., Belluscio, A., Criscoli, A., Ardizzone, G., Apostolaki, E.T., Fraschetti, S. et al. (2015). Seagrass meadows (*Posidonia oceanica*) distribution and trajectories of change. Scientific Reports, **5**: 12505.

Therneau, T. M. 2020. A Package for Survival Analysis in R.

Thibaut, T., A. Blanfuné, C. F. Boudouresque, and M. Verlaque. 2015. Decline and local extinction of Fucales in the French Riviera: The harbinger of future extinctions? Mediterranean Marine Science **16**:206-224.

Thibaut, T., S. Pinedo, X. Torras, and E. Ballesteros. 2005. Long-term decline of the populations of Fucales (*Cystoseira* spp. and *Sargassum* spp.) in the Albères coast (France, North-western Mediterranean). Mar Pollut Bull **50**:1472-1489.

Traboni C, Mammola SD, Ruocco M, Ontoria Y, Ruiz JM, Procaccini G, Marín-Guirao L. 2018. Investigating cellular stress response to heat stress in the seagrass *Posidonia oceanica* in a global change scenario. Marine Environmental Research **141**: 12–23.

Unsworth RKF, Collier CJ, Henderson GM, McKenzie LJ. 2012. Tropical seagrass meadows modify seawater carbon chemistry: implications for coral reefs impacted by ocean acidification. Environmental Research Letters **7**: 24026.

Valladares, F., S. Matesanz, F. Guilhaumon, M. B. Araújo, L. Balaguer, M. Benito-Garzón, W. Cornwell, E. Gianoli, M. Kleunen, D. E. Naya, A. B. Nicotra, H. Poorter, and M. A. Zavala. 2014. The effects of phenotypic plasticity and local adaptation on forecasts of species range shifts under climate change. Ecol Lett **17**:1351-1364.

Van den Hoek, C. 1982. The distribution of benthic marine algae in relation to the temperature regulation of their life histories. Biological Journal of the Linnean Society **18**:81-144.

Van den Hoek, C., A. M. Breeman, and W. T. Stam. 1990. The geographic distribution of seaweed species in relation to temperature: present and past. Pages 55-67 *in* J. J. Beukema, W. J. Wolff, J. J. W. M. Brouns, J. J. Beukema, W. J. Wolff, and J. J. W. M. Brouns, editors. Expected effects of climate change on marine coastal ecosystems, Dordrecht.

Vera, M., J. Carlsson, J. E. L. Carlsson, T. Cross, S. Lynch, P. Kamermans, A. Villalba, S. Culloty, and P. Martinez. 2016. Current genetic status, temporal stability and structure of the remnant wild European flat oyster populations: conservation and restoring implications. Marine Biology **163**: 239.

Verdura, J., J. Santamaría, E. Ballesteros, D. Smale, M. E. Cefalì, R. Golo, d. S. Caralt, A. Vergés, and E. Cebrian. 2021. Local-scale climatic refugia offer sanctuary for a habitat-forming species during a marine heatwave. Journal of Ecology **109**: 1758– 1773

Vergés A, Pérez M, Alcoverro T, Romero J. 2008. Compensation and resistance to herbivory in seagrasses: Induced responses to simulated consumption by fish. Oecologia **155**: 751-760.

Verlaque, M. 1987. Contribution à l'étude du phytobenthos d'un ecosystème photophile thermophile marin en Méditerranée Occidentale: étude structural et dynamique du photobenthos et analyse des relations faune - flore.

Wahid A. 2007. Physiological implications of metabolite biosynthesis for net assimilation and heat-stress tolerance of sugarcane (*Saccharum officinarum)* sprouts. Journal of Plant Research **120**: 219–228.

Wang, W., Xu, N., Zhang, L., Andersen, K.H., Klaminder, J., 2021. Anthropogenic forcing of fish boldness and its impacts on ecosystem structure. Global Change Biology, **27(6),** 1239–1249. https://doi.org/10.1111/gcb.15473

Wernberg, T. 2021. Marine heatwave drives collapse of kelp forests in Western Australia. Pages 325-343 *in* J. G. Canadell, R. B. Jackson, J. G. Canadell, and R. B. Jackson, editors. Ecosystem Collapse and Climate Change, Cham.

Wernberg, T., and K. Filbee-Dexter. 2019. Missing the marine forest for the trees. Marine Ecology Progress Series **612**:209-215.

Wernberg, T., B. D. Russell, M. S. Thomsen, C. F. D. Gurgel, C. J. A. Bradshaw, E. S. Poloczanska, and S. D. Connell. 2011. Seaweed communities in retreat from ocean warming. Current Biology **21**: 1828-1832.

Wernberg, T., D. A. Smale, F. Tuya, M. S. Thomsen, T. J. Langlois, T. De Bettignies, S. Bennett, and C. S. Rousseaux. 2013. An extreme climatic event alters marine ecosystem structure in a global biodiversity hotspot. Nature Climate Change **3**:78-82.

Wernberg, T., F. Arenas, C. Olabarria, M. S. Thomsen, and M. Mohring. 2016. Threats to ecosystem engineering macrophytes: climate change. Pages 201-225 *in* Ó. E, editor. Marine macrophytes as foundation species. Science Publisher/CRC Press, Boca Raton, USA.

Wernberg, T., S. Bennett, R. C. Babcock, D. T. Bettignies, K. Cure, M. Depczynski, F. Dufois, J. Fromont, C. J. Fulton, R. K. Hovey, E. S. Harvey, T. H. Holmes, G. a. Kendrick, B. Radford, J. Santana-garcon, B. J. Saunders, D. a. Smale, M. S. Thomsen, C. a. Tuckett, and F. Tuya. 2016. Climate-driven regime shift of a temperate marine ecosystem. Science **353**:169-172.

Wernberg, T., Smale, D.A., Tuya, F., Thomsen, M.S., Langlois, T.J., de Bettignies, T. et al. (2013). An extreme climatic event alters marine ecosystem structure in a global biodiversity hotspot. Nature Climate Change **3**: 78-82.

Wiens, J. J. 2016. Climate-related local extinctions are already widespread among plant and animal species. PLoS Biol **14**:1-18.

Willis, S. G., W. Foden, D. J. Baker, E. Belle, N. D. Burgess, J. A. Carr, N. Doswald, R. A. Garcia, A. Hartley, C. Hof, T. Newbold, C. Rahbek, R. J. Smith, P. Visconti, B. E. Young, and S. H. M. Butchart. 2015. Integrating climate change vulnerability assessments from species distribution models and trait-based approaches. Biological Conservation **190**:167-178.

Yarish, C., A. M. Breeman, and C. van den Hoek. 1986. Survival strategies and temperature responses of seaweeds belonging to different biogeographic distribution groups. Botanica Marina **29**:215-230.

Zayas-Santiago CC, Rivas-Ubach A, Kuo L-J, Ward ND, Zimmerman RC. 2020. Metabolic Profiling Reveals Biochemical Pathways Responsible for Eelgrass Response to Elevated CO2 and Temperature. Scientific Reports **10**: 4693.

Zieman JC. 1974. Methods for the study of the growth and production of turtle grass*, Thalassia testudinum* König. Aquaculture **4**: 139–143.

Zimmerman RC. 2021. Scaling up: Predicting the impacts of climate change on seagrass ecosystems. Estuaries and Coasts **44**: 558–576.

Zimmerman, VJ H, Jinuntuya M, Celebi B, Ruble D, Smith M, Cedeno T, M SW. 2017. Experimental impacts of climate warming and ocean carbonation on eelgrass Zostera marina. Marine Ecology Progress Series **566**: 1–15.